PART I: THEORETICAL CALCULATIONS OF EQUILIBRIUM INFRARED GAS EMISSIVITIES FROM SPECTROSCOPIC DATA

PART II: REPRESENTATIVE RADIATIVE ENERGY TRANSFER CALCULATIONS FOR TRANSPARENT AND OPTICALLY DENSE MEDIA

Thesis by

Louise D. Gray

In Partial Fulfillment of the Requirements

For the Degree of

Doctor of Philosophy

California Institute of Technology

Pasadena, California

1963

ACKNOWLEDGMENTS

The author wishes to express her gratitude to Professor S. S. Penner for suggesting the research presented here and for many helpful and stimulating discussions.

The author is indebted to Zonta International for an Amelia Earhart Scholarship for the academic years 1959-60 and 1961-62. The Office of Naval Research contributed financial support to the research under Contracts Nonr-220(03), NR 015 401 and Nonr-220(45), NR 015 401 with the California Institute of Technology.

The assistance of Mr. Bruce Gray in preparing the IBM 7090 program is gratefully acknowledged. Expressions of gratitude go also to Mrs. Barbara Mullican and Mrs. Roberta Duffy for their patience in the preparation of this manuscript.

ABSTRACT FOR PART I

Measured data for carbon dioxide emissivities at temperatures up to 1800°K have been correlated by postulating (a) that the effective spectral region widths, in which significant contributions are made to the total emission of radiant energy, increase with temperature and optical depth, and (b) that unknown combination and harmonic bands make contributions to the integrated intensities of selected spectral regions in such a way that the absolute values of the integrated intensities (cm^{-2} atm^{-1}) remain invariant with temperature.

Spectral emissivities have been calculated in the infrared for hydrogen chloride to the rigid-rotator harmonic oscillator approximation using the "smeared-out" rotational line model for temperatures of 600 and 2400°K. In the weak-line approximation, this model gives reasonable agreement with numerical calculations. In the strong-line approximation, there is quite a large discrepancy, particularly in the P-branch, at 2400°K; much better agreement is obtained if vibration-rotation interaction and anharmonicity terms are included in the calculation.

Equilibrium spectral emissivities have been computed for water vapor by using available low-temperature spectroscopic data. Satisfactory agreement with experimental results at 1111°K is obtained if the nearly symmetric top expressions for integrated intensities are used in conjunction with the just-overlapping line model.

ABSTRACT FOR PART II

The general equations of radiative energy transfer are presented. When the absorption coefficients and/or the gas volume are sufficiently large, the general transport equation can be approximated by the "diffusion approximation". This approximation is applied to a two-phase system consisting of carbon particles dispersed in a gas. The Rosseland mean absorption coefficients are calculated for spherical carbon particles of 200 and 987 A radius at temperatures of 1000 and 2000°K, and a comparison is made of the relative magnitudes of conductive and radiative heat transfer for this system.

In the special case when scattering may be neglected, and the temperature and pressure of the gas are constant, the transport equation can be integrated for a particular direction. The total radiant energy transfer to any given element of area depends upon geometrical interchange factors. These interchange factors have been evaluated for centrally located areas in cylindrical and conical chambers; simple relations are given for a transparent gas and an optically dense gas. A representative calculation has been carried out for the radiant energy transfer to a centrally-located area element at the plane of intersection of two truncated cones.

TABLE OF CONTENTS

Part	Title	Page
	PART I: Theoretical Calculations of Equilibrium Infrared Gas Emissivities from Spectroscopic Data	
I.	INTRODUCTION	2
A.	Emissivity	3
B.	Absorption Bands of Molecules	6
C.	Models of Spectral Bands	11
	1. Just-overlapping line model	12
	2. Box model	12
	3. Non-overlapping line model	12
	4. Statistical line model	13
	(a) "Weak-line" and "strong-line" approximations for non-overlapping lines	16
	5. Elsasser model	17
	6. Random Elsasser model	18
	7. Statistical band model	18
F.	Molecular Spectra	22
	1. Wave equation for a molecule	22
	2. Vibrations of polyatomic molecules	24
	(a) Normal Vibrations	24
	(b) Small oscillations	27
	(c) Applications of group theory to molecular vibrations	31
	(i) Symmetry of molecules	32
	(ii) Groups of symmetry operations	32
	(iii) Characters	34

Part	Title	Page
	(iv) Quantum mechanical applications	35
	(v) Normal modes of vibration for H_2O	41
	(vi) Linear molecules	50
	(d) Harmonic oscillator approximation	52
	(e) Fermi resonance	55
	(f) Anharmonicity	59
	(g) Infrared vibration spectra and selection rules	60
	3. Rotation of polyatomic molecules	62
	4. Vibration-rotation interaction	66
II.	CRUDE EMISSIVITY CALCULATIONS EMPLOYING STATISTICAL MODELS	69
	A. Approximate Total Emissivity Calculations for CO_2 Using the Statistical Band Model	69
	1. Introduction	69
	2. Emissivity calculations of randomly distributed weak bands and strong fundamental bands	70
	(a) Rotational structure of the vibration-rotation bands	70
	3. Values of integrated intensities and region widths assumed for empirical correlation of data	73
	4. Outline of calculations	74
	B. Approximate Calculations for Spectral Emissivities in the Infrared for HCℓ	80
	1. Introduction	80
	2. Outline of theoretical considerations	81
	(a) Calculation of spectral absorption coefficients and of spectral emissivities for fundamental vibration-rotation bands	81
	(b) Approximate spectral emissivity calculations for HCℓ	86

Part	Title	Page
	(c) Approximate calculations of spectral emissivities in the infrared for HCl in the strong-line approximation	86
III.	APPROXIMATE SPECTRAL EMISSIVITY CALCULATIONS FOR WATER VAPOR AT ELEVATED TEMPERATURES	95
	A. Introduction	95
	B. The Infrared Spectrum of Water Vapor	98
	C. Approximate Spectral Emissivity Calculations for Water Vapor	100
	APPENDIX A: Radiation from Isolated Spectral Lines	117
	REFERENCES FOR PART I	122

PART II: Representative Radiative Energy Transfer Calculations for Transparent and Optically Dense Media

I.	INTRODUCTION	148
II.	GENERAL EQUATIONS OF RADIATIVE ENERGY TRANSPORT	149
	A. Fundamental Quantities and Definitions	149
	B. Continuity Equation for Radiant Energy	152
	C. The Source Function S_ν	153
	1. Local thermodynamic equilibrium	153
	2. Pure scattering	153
	3. Both absorption and scattering occur	154
III.	THE DIFFUSION APPROXIMATION	155
	A. Equation of Transfer for Plane Geometries	156
	B. The Spherical Harmonic Method	157
	C. Boundary Conditions	160

Part	Title	Page
IV.	RADIATIVE ENERGY TRANSFER TO CENTRALLY LOCATED AREAS IN CYLINDRICAL AND CONICAL CHAMBERS CONTAINING ISOTHERMAL, GREY EMITTERS	163
V.	ROSSELAND MEAN ABSORPTION COEFFICIENTS IN TWO-PHASE SYSTEMS	172
A.	Definition of Rosseland Mean Absorption Coefficient	172
B.	Mean Absorption Coefficients for Dispersed Carbon Particles	173
C.	A Comparison of Radiative and Conductive Heat Transfer	176
REFERENCES TO PART II		182

PART I: THEORETICAL CALCULATIONS OF EQUILIBRIUM INFRARED GAS EMISSIVITIES FROM SPECTROSCOPIC DATA

I. INTRODUCTION

When a body of gas is heated, it radiates energy at frequencies characteristic of the gas. This radiation is the result of electronic, vibrational, and rotational transitions from excited energy levels to lower energy levels of the molecules.[1] The emitted radiant energy corresponding to these transitions is distributed over a well-defined wavelength region. For temperatures up to 2500°K, which occur in normal engineering applications, the bulk of the radiation is connected with changes in vibrational or rotational energy of the molecule. The radiation corresponding to these transitions lies in the near infrared, i.e., in the wavelength region from 1 to 30 microns.

The magnitude and spectral character of the radiant energy depends upon the temperature, pressure, and molecular composition of the gas. It is termed "thermal radiation" when the gas is in thermal equilibrium. In principle, it should be possible to calculate theoretically the radiation emitted by a heated gas if sufficient information is available on the spectroscopic constants of the molecules involved. However, in many cases, the required constants are imperfectly known, and most gases have been investigated experimentally only at relatively low temperatures. High-temperature measurements of gas emissivities under equilibrium conditions are possible, but the experiments are difficult to perform. The problem, then, is one of extrapolating low temperature laboratory data to high temperature conditions. Thus the ultimate objective of any theory of gas emissivities is to calculate the radiation emitted by a heated gas, at various temperatures, pressures, and geometrical path lengths, from spectroscopic parameters measured

at room temperature.

A. EMISSIVITY

The spectral emissivity, ϵ_ω, of a distributed gaseous radiator is defined as the ratio of the radiation emitted by the gas, in the wavenumber range between ω and $\omega + d\omega$, to that of a blackbody at the same temperature, viz.,

$$\epsilon_\omega = \frac{R_\omega d\omega}{R^\circ_\omega d\omega} = [1 - \exp(-P_\omega X)] \qquad (1)$$

where P_ω is the spectral absorption coefficient, X is the optical depth

$$X = ps \qquad (2)$$

(here p is the pressure of the radiating gas and s is the geometric length), and $R^\circ_\omega d\omega$ is the spectral blackbody radiancy in the wavenumber range between ω and $\omega + d\omega$ at the temperature T, and is given by the expression

$$R^\circ_\omega d\omega = 2\pi hc^2\omega^3[\exp(hc\omega/kT)-1]^{-1}d\omega \qquad (3)$$

where h is Planck's constant, c is the velocity of light, ω is the wavenumber, and k is Boltzmann's constant.

The total emissivity ϵ of the gas is obtained by integrating equation (1). Thus

$$\epsilon = \frac{1}{\sigma T^4}\int_0^\infty R^\circ_\omega[1 - \exp(-P_\omega X)]d\omega \qquad (4)$$

where σ is the Stefan-Boltzmann constant. In practice, the range of integration in equation (4) is only extended over the wavenumber range in which $P_\omega X$ is sensibly different from zero. In actual calculations,

it is often convenient to use the normalized blackbody radiancy, ρ_ω, where

$$\rho_\omega \equiv \frac{R^o_\omega}{R^o_{\omega_{max}}} = 2.097 \left(\frac{\omega}{T}\right)^3 \left[\exp\left(\frac{hc\omega}{kT}\right) - 1\right]^{-1} . \qquad (5)$$

The ratio of the maximum blackbody radiancy $R^o_{\omega_{max}}$ to the total blackbody radiancy σT^4 is given by

$$\frac{R^o_{\omega_{max}}}{\sigma T^4} = \frac{0.3148}{T} . \qquad (6)$$

Using equations (5) and (6), equation (4) can be rewritten as

$$\epsilon = \frac{0.3148}{T} \int_0^\infty \rho_\omega \, \epsilon_\omega \, d\omega . \qquad (7)$$

In Figure 1 the normalized blackbody function ρ_ω is plotted as a function of wavenumber for various temperatures.

For the limit of very small optical depths, the exponential in equation (1) may be expanded and

$$\epsilon_\omega \simeq P_\omega X . \qquad (8)$$

When equation (8) applies, the gas is termed "transparent" and is said to radiate "in the linear region of the curve of growth", i.e., self-absorption may be neglected.

In the case of a mixture of two gases, with spectral absorption coefficients P_{ω_1} and P_{ω_2}, and partial pressures p_1 and p_2, respectively, the spectral emissivity of the mixture is

$$\epsilon_\omega = 1 - \exp\left[-(P_{\omega_1} p_1 + P_{\omega_2} p_2) s\right]. \qquad (9)$$

Equation (9) may be rewritten in terms of the spectral emissivities of the two constituents as

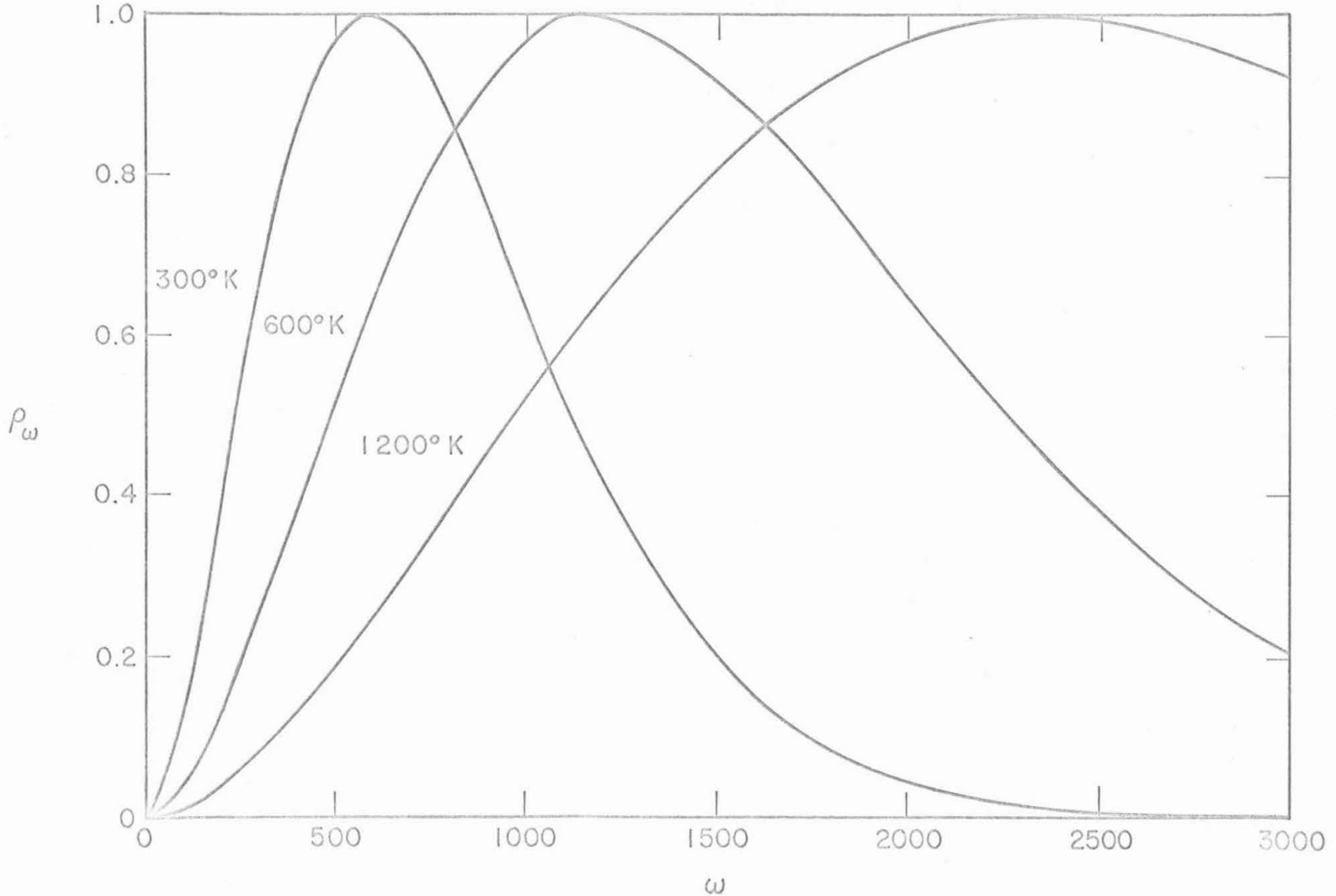

Figure 1. Variation of the Normalized Blackbody Function ρ_ω with Wavenumber ω at 300, 600, and 1200°K.

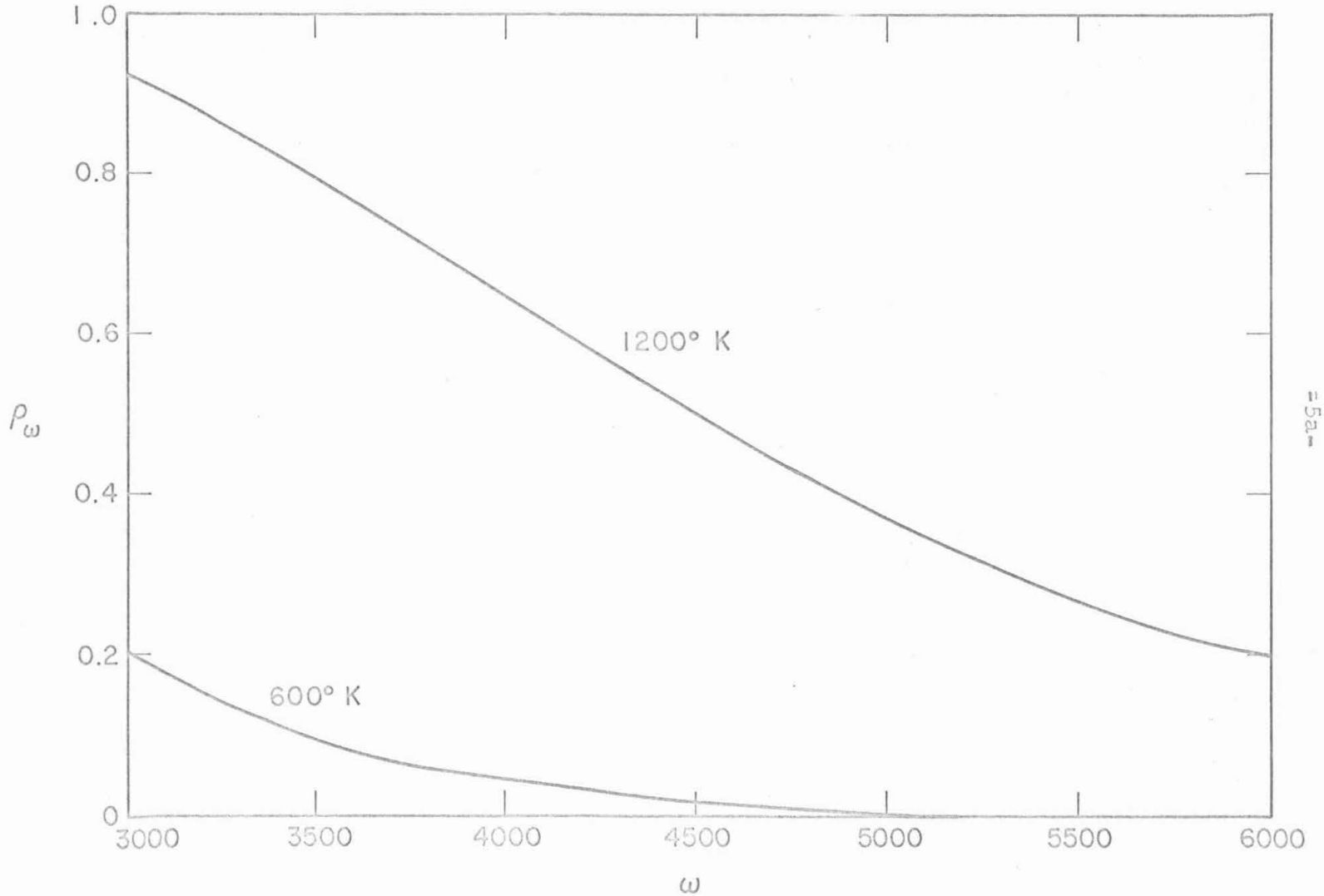

Figure 1 (continued). Variation of the Normalized Blackbody Function ρ_ω' with Wavenumber at 600 and at 1200°K.

$$\varepsilon_{\omega} = \varepsilon_{\omega_1} + \varepsilon_{\omega_2} - \varepsilon_{\omega_1}\varepsilon_{\omega_2} \qquad (10)$$

where $\varepsilon_{\omega_1} = (1 - \exp[-P_{\omega_i} p_i s])$. Thus, while the spectral absorption coefficients are additive, spectral emissivities are not additive unless the gases are transparent.

B. ABSORPTION BANDS OF MOLECULES

A vibration-rotation band consists of allowed rotational lines associated with a given vibrational transition. Each of these spectral lines produces a non-zero absorption coefficient in the neighborhood of the band center. The wavenumber ω of a particular line is given by the difference in the sum of the vibrational and rotational energies of the final and initial states. The width of an individual line is characteristic of the molecule and varies with temperature and pressure. At sufficiently low pressures, the spectral lines may be considered to be completely separated; at sufficiently high pressures, they merge to form a more or less continuous region of absorption.

The resolving power of the spectrometer used in an experimental transmission measurement of an absorption band affects the resulting data. With very low resolution, the band seems without structure. With somewhat higher resolution, it may be observed to consist of several adjoining maxima which form the envelope of the band. Figure 2 shows this contour for HCℓ. With spectrometers of sufficiently high resolution, the measured bands in the near infrared show the rotational line structure, which is either regularly or irregularly spaced (see Figure 3). The area under the curve of spectral absorptivity plotted as a function of wavenumber is independent of the spectrometer slit width (see Figure

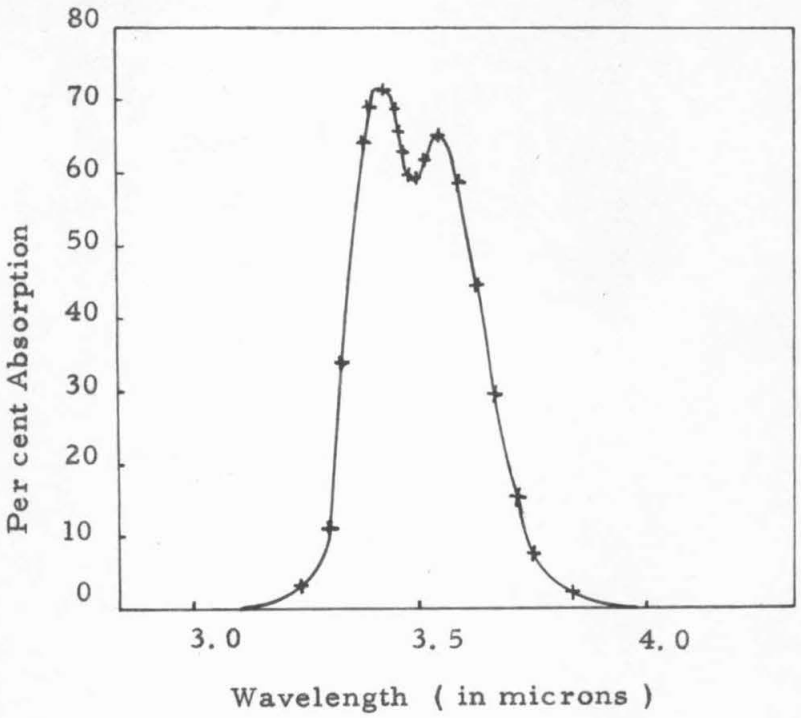

Figure 2. Fundamental absorption band of HCℓ in the near infrared. [From W. Burmeister, "Untersuchungen über die ultraroten Absorptionsspektra einiger Gase," Ber. deutsch. phys. Ges., 15, 595 (1913).]

Figure 3. Fine structure of the fundamental absorption band of HCℓ in the near infrared [from E. S. Imes, "Measurements on the Near Infrared Absorption of Some Diatomic Gases," Astrophys. J. 50, 260 (1919)].

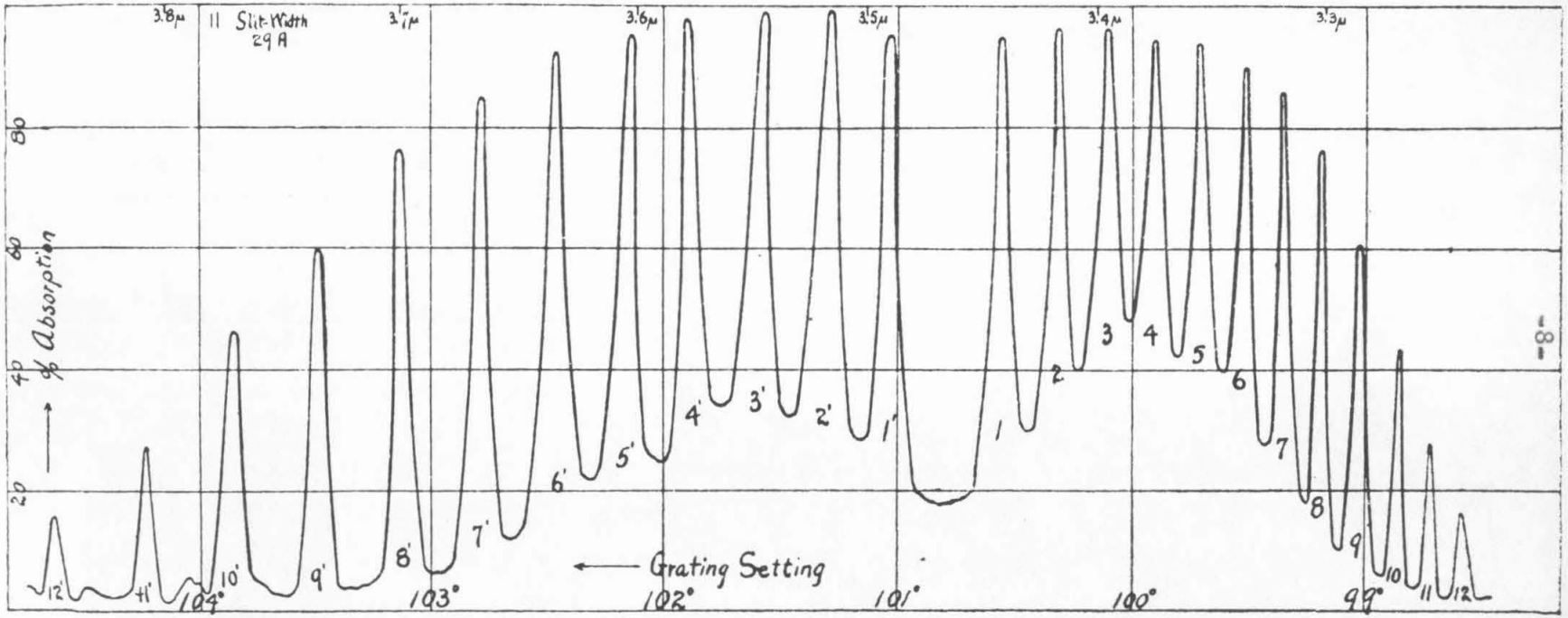
3.8μ
11 Slit-Width
29 A
3.7μ
3.6μ
3.5μ
3.4μ
3.3μ
80
60
40
20
% Absorption
12'
11'
10'
9'
8'
7'
6'
5'
4'
3'
2'
1'
1
2
3
4
5
6
7
8
9
10
11
12
104°
103°
102°
101°
100°
99°
Grating Setting

Figure 4. Effect of spectrometer slit width on the observed absorption spectrum of carbon dioxide and water vapor in the 2.7 micron region. The data are plotted as per cent absorption as a function of wavenumber (from ref. 3).

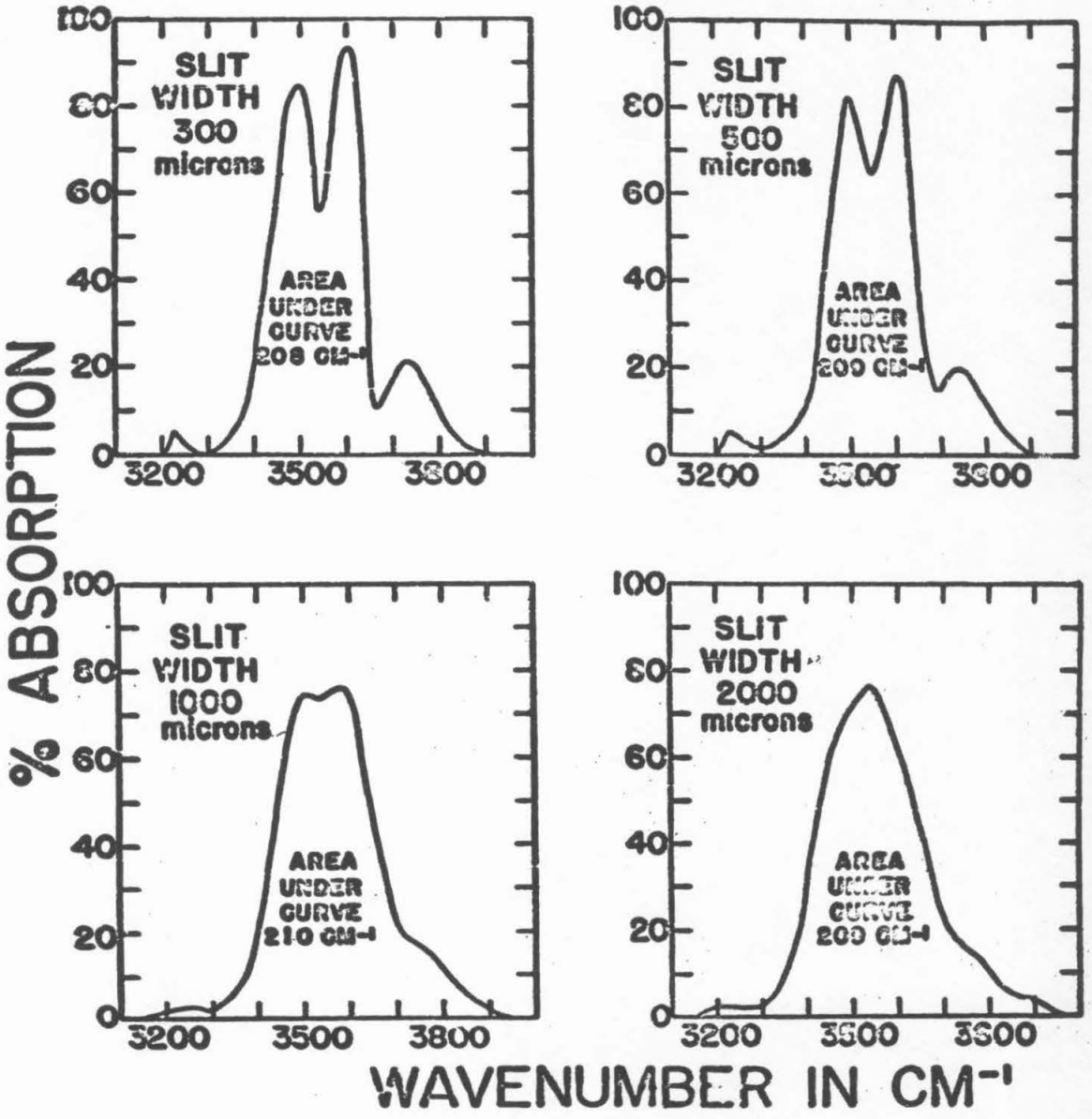
% ABSORPTION
SLIT WIDTH 300 microns
AREA UNDER CURVE 208 CM-1
SLIT WIDTH 500 microns
AREA UNDER CURVE 200 CM-1
SLIT WIDTH 1000 microns
AREA UNDER CURVE 210 CM-1
SLIT WIDTH 2000 microns
AREA UNDER CURVE 200 CM-1
100
80
60
40
20
0
3200
3500
3800
WAVENUMBER IN CM-1

4)[2]. This area is termed the band absorption A_B and is defined by the relation

$$A_B \equiv \int_{\text{band}} [1 - \exp(-P_\omega X)]\, d\omega \quad . \tag{11}$$

A more useful quantity, however, for theoretical calculations is the integrated intensity $\underline{\alpha}$ of the band. This is defined as the integral of the absorption coefficient over the region of the band

$$\alpha \equiv \int_{\text{band}} P_\omega \, d\omega \quad . \tag{12}$$

Similarly, the integrated intensity of an individual spectral line S is defined by the relation

$$S \equiv \int_{\text{line}} P_\omega \, d\omega \quad . \tag{13}$$

Unfortunately, it is difficult to determine experimentally the integrated intensity of a band. With a spectrometer of moderate resolution, it is found that the true spectral quantities are not measured because the individual lines, which constitute the band, have a width much narrower than the resolution attained with the spectrometer. Three methods may be used to resolve this difficulty: measurements may be made with high resolution, at small optical depths where equation (8) applies, or the fine structure may be broadened by examining the gas under high pressure*. When one of the specified conditions is not

---

* The area under the absorption-coefficient vs. wavenumber curve ($\alpha = \int P_\omega d\omega$) does not change significantly with moderate changes in pressure. Hence the effect of high pressure is primarily that of minimizing the variations of P_ω with ω. However, for polar molecules, such as H_2O, the integrated intensity may change appreciably with total pressure.[4]

met, an apparent absorption coefficient and an apparent integrated intensity may be found formally, but the true value of $\underline{\alpha}$ may then be as much as ten times as great as the apparent integrated intensity. Errors introduced by comparing the integrated intensities of two bands in the same spectrum are not as large, but they still exist and strong bands will appear to be less strong than they actually are.[5]

C. MODELS OF SPECTRAL BANDS

It may be seen from equation (13) that the absorption coefficient at the wavenumber $\underline{\omega}$ and associated with the j^{th} spectral line, which is centered at ω_j, may be represented by the relation[6-8]

$$P_{\omega} = S_j F(\omega - \omega_j; b) \tag{14}$$

where b is the half-width of the line, and $F(\omega-\omega_j;b)$ is the line shape factor which is normalized so that

$$\int_{-\infty}^{\infty} F(\omega - \omega_j; b)d\omega = 1 \quad . \tag{15}$$

Hence, the energy emitted by a gas at the wavenumber ω can be written as

$$R_{\omega} = R_{\omega}^{o}\{1 - \exp[-ps\sum_j S_j F(\omega-\omega_j;b)]\} \quad . \tag{16}$$

Equation (16) is true, of course, only if the gas is at a uniform temperature and pressure. The problem of radiative energy transport is discussed in Part II.

The emitted radiation is usually desired over a finite frequency interval containing a number of spectral lines, but when the spectral lines are irregularly spaced or partially overlap each other, then the integral of equation (16) becomes difficult to evaluate. However,

various models have been proposed that lead to reasonably simple mathematical expressions for the emitted radiant energy. The most appropriate model for a given application depends upon the spectrum of the molecule under consideration.

1. Just-Overlapping Line Model.[6, 9-11] This model does not require any knowledge of spectral linewidth since the lines are assumed to be just overlapping. The absorption coefficient for a given line is found by dividing the integrated intensity S of that line by the mean line spacing δ^*.

$$P_a = S/\delta^* \tag{17}$$

This smeared-out, average absorption coefficient will obviously show no pressure dependence.

2. Box Model.[6, 12, 13] The entire vibration-rotation band is represented by a (constant) average absorption coefficient over an effective bandwidth, i.e., $A_i = 1 - \exp[-P_i X]$ where P_i is the average absorption coefficient for the i^{th} band. The box model is useful in making crude calculations of total emissivity, the results being slightly lower than those predicted by the just-overlapping line model.[6, 9, 10]

3. Non-Overlapping Line Model.[6] The contributions of individual lines are added in the non-overlapping line model. For a band containing n identical non-overlapping lines, the total band absorption is

$$A_B = \sum_{j=1}^{n} A_{L_j} = nA_L \tag{18}$$

where A_L is the absorption of an individual line

$$A_L = \int_{\text{line}} \left(1 - e^{-P_\omega X}\right) d\omega \quad . \tag{19}$$

This procedure is applicable only for small optical depths or at very low pressures. At moderate optical depths, overlapping between spectral lines causes the sum of the separate line contributions to yield excessively large emissivities.

The radiation from an isolated spectral line is discussed in Appendix A.

4. Statistical Line Model.[6, 14-16] This model assumes random line spacing and strength, but constant line width. The position and intensity of a given spectral line is specified only by probability functions.

Let $N(\omega_1, \ldots, \omega_n)d\omega_1 \ldots d\omega_n$ be the probability that the center of the first line is in the wavenumber interval $d\omega_1$, when the center of the second line is in the interval $d\omega_2$, etc., up to line n. We take the origin for frequency at the center of a band of width $n\delta^*$ where δ^* is the mean spacing between spectral lines. Let $P(S_j)dS_j$ be the probability of the j^{th} line having an intensity between S_j and $S_j + dS_j$. Then the average absorption over the wavenumber interval $n\delta^*$ is

$$\bar{A}_{S.M.} = 1 - \frac{\int_{\frac{-n\delta^*}{2}}^{\frac{+n\delta^*}{2}} \cdots \int_{\frac{-n\delta^*}{2}}^{\frac{+n\delta^*}{2}} N(\omega_1, \ldots, \omega_n) d^n\omega \int_0^\infty \cdots \int_0^\infty \prod_j P(S_j) \exp[-S_j F X] dS_j}{\int_{\frac{-n\delta^*}{2}}^{\frac{+n\delta^*}{2}} \cdots \int_{\frac{-n\delta^*}{2}}^{\frac{+n\delta^*}{2}} N(\omega_1, \ldots, \omega_n) d^n\omega \int_0^\infty \cdots \int_0^\infty \prod_j P(S_j) dS_j} \tag{20}$$

where F is the line shape parameter of equation (14). Since $\int_0^\infty P(S_j)dS_j = 1$ and $N(\omega_1, \ldots, \omega_n)$ is a constant,

$$\bar{A}_{S.M.} = 1 - \left\{ \frac{1}{n\delta^*} \int_{\frac{-n\delta^*}{2}}^{\frac{+n\delta^*}{2}} d\omega \int_0^\infty [P(S)\, e^{-SFX}]dS \right\}^n$$

because the integral over each line is equal to the integral over any other line. This expression may be written

$$\bar{A}_{S.M.} = 1 - \left\{ 1 - \frac{1}{n\delta^*} \int_{\frac{-n\delta^*}{2}}^{\frac{+n\delta^*}{2}} d\omega \int_0^\infty [P(S)(1 - e^{-SFX})]dS \right\}^n . \qquad (21)$$

Interchanging the order of integration, equation (21) becomes

$$\bar{A}_{S.M.} = 1 - \left\{ 1 - \frac{1}{n\delta^*} \int_0^\infty P(S)dS \int_{\frac{-n\delta^*}{2}}^{\frac{+n\delta^*}{2}} [1 - e^{-SFX}]d\omega \right\}^n$$

or

$$\bar{A}_{S.M.} = 1 - \left\{ 1 - \frac{1}{n\delta^*} \int_0^\infty P(S)dS\, A_L \right\}^n . \qquad (22)$$

But the average line radiancy is just

$$\bar{A}_L = \int_0^\infty A_L\, P(S)\, dS \qquad (23)$$

and, therefore, the average absorption becomes

$$\bar{A}_{S.M.} = 1 - \left[1 - \frac{1}{n\delta^*} \bar{A}_L \right]^n . \qquad (24)$$

If the number of lines in a band is allowed to become infinite (the result-

ing expression is known to be useful when at least 5 lines are involved), then equation (24) becomes

$$\bar{A}_{S.M.} = 1 - \exp\left[-\frac{1}{\delta^*}\bar{A}_L\right] . \qquad (25)$$

If the distribution function for intensity is $P(S) = \delta(S-\bar{S})$, where δ is the Dirac delta function, the mean absorption is given by

$$\bar{A}_{S.M.} = 1 - \exp\left\{-\frac{1}{\delta^*}\int_0^\infty [1 - \exp(-SFX)]d\omega\right\} . \qquad (26)$$

The average absorption does not depend very strongly on the particular intensity distribution function chosen[6,15], and calculations are simplified if the lines are chosen to be of equal intensity, as was done in arriving at equation (26).

If the Lorentz line shape is assumed for the individual lines (see Appendix A), equation (26) reduces to

$$\bar{A}_{S.M.} = 1 - \exp\left[\frac{-2\pi b}{\delta^*} f(x)\right] . \qquad (27)$$

Regions of the spectrum for which no line is completely absorbing at the line center (i.e., for a particular value of X, $P_\omega \ll 1$ at all frequencies) are regions of weak heat transfer. Here the "weak line approximation" is applicable for the band absorption. This method involves substitution of equation (a-7) for the absorption of a spectral line into equation (25), viz.,

$$\bar{A}_{S.M.} = 1 - \exp[-\bar{S}X/\delta^*] . \qquad (28)$$

Regions of the spectrum where the majority of the strongest lines are black at the line centers (i.e., for a given optical depth X, a line absorbs virtually all radiation at frequencies within the half-width), are called regions of strong heat transfer. Here the "strong

line approximation" is used to determine the band absorption. In this case, equation (a-11) is used for the line absorption in equation (25) with the result

$$\bar{A}_{S.M.} = 1 - \exp\left[-(2/\delta^*)(\overline{Sb}X)^{\frac{1}{2}}\right] . \qquad (29)$$

The purpose of the preceding approximations is evidently that of simplifying the numerical calculations. The errors involved in using the simplifications in the exponents are given by equations (a-8) and (a-12). Because of the nature of the statistical line model, equation (27) is valid regardless of the degree of overlapping for equally intense spectral lines having a dispersion contour.

(a) "Weak Line" and "Strong Line" Approximations for Non-Overlapping Lines. - It is of interest to compare the weak-line and strong-line approximations with the linear and square-root approximations. The average absorption for a band consisting of n identical non-overlapping lines is, from equation (18),

$$\bar{A}_{N.O.} = \frac{nA_L}{\Delta\omega} = \frac{A_L}{\delta^*} \qquad (30)$$

where the band width $\Delta\omega = n\delta^*$. If the individual lines have a dispersion contour, then the aberage absorption becomes

$$\bar{A}_{N.O.} = (2\pi b/\delta^*) f(x) . \qquad (31)$$

When the lines are weak, then the average band absorption is

$$(\bar{A}_{N.O.})_L = (\overline{SX})/\delta^* . \qquad (32)$$

Alternatively, if the lines are strong, then the band absorption becomes

$$(\bar{A}_{N.O.})_{S.R.} = (2/\delta^*)(\overline{Sb}X)^{\frac{1}{2}} . \qquad (33)$$

Comparing equations (32) and (33), which are valid only for non-overlapping lines, with equations (28) and (29), which are valid for randomly

distributed lines, the distinction between the weak-line and strong-line approximation and the linear and square-root approximation is readily apparent.

5. Elsasser Model.[7, 17-20] If a band is assumed to consist of an infinte number of spectral lines, each with the same intensity S and half-width b, with all the lines equally spaced at intervals of δ^*, then Elsasser[18, 20] showed that the spectral absorption coefficient at the wavenumber ω is given by

$$P_{(\omega)} = \sum_{n=-\infty}^{+\infty} \frac{S}{\pi} \frac{b}{(\omega - n\delta^*)^2 + b^2} \quad , \tag{34}$$

for lines with dispersion contour. Letting

$$z = (2\pi\omega/\delta^*) \quad , \qquad x = (SX/2\pi b) \, , \tag{35}$$

and

$$\beta = (2\pi b/\delta^*) \, ,$$

it is found that the fractional absorption $\bar{A}$ integrated over a frequency range δ^* for an Elsasser band can be written in the form

$$\bar{A}_{E.M.} = 1 - (1/2\pi) \int_{-\pi}^{\pi} \exp \left[\frac{-\beta x \sinh \beta}{\cosh \beta - \cos z} \right] dz \, . \tag{36}$$

Although the integral in equation (36) cannot be evaluated in terms of elementary functions, a number of approximate expressions have been developed. For example, when $\beta > 3$, or $b/\delta^* > 1$,

$$\bar{A}_{E.M.} = 1 - \exp(-SX/\delta^*) \tag{37}$$

which is the weak line approximation; when $\beta < 0.3$ and $x > 1.63$, the strong line approximation applies, viz.,

$$\bar{A}_{E.M.} = \operatorname{erf} \left[(1/\delta^*)(\pi SbX)^{\frac{1}{2}} \right] \tag{38}$$

for the Elsasser model. It should be noted that these limiting forms were derived by Elsasser. Plass[7, 8] has found the error made in using these approximations and defined their regions of validity.

6. Random Elsasser Model.[7, 8, 16, 21-23] This model is used when several groups of lines are superposed and the lines are equidistant within each group. This model represents a case intermediate between the statistical model and the Elsasser model and can be shown[7] to approach the statistical model as the number of superposed bands becomes large.

In the weak line approximation, the absorption is again

$$\bar{A}_{R.E.M.} = 1 - \exp(-SX/\delta^*) \quad , \tag{39}$$

while, in the strong line approximation, it becomes

$$\bar{A}_{R.E.M.} = 1 - \prod_{i=1}^{N} \{1 - \mathrm{erf}[(1/\delta^*)(\pi S_i b_i X)^{\frac{1}{2}}]\} \tag{40}$$

where N is the number of superposed Elsasser bands, each with a half-width b_i and line intensity S_i.

7. Statistical Band Model.[10, 24, 25] Application of the Mayer-Goody procedure to randomly distributed bands shows that the mean value of the spectral emissivity (or the fractional absorption) at the wavenumber ω_k is given by the relation

$$\bar{\epsilon}_{\omega_k} = 1 - \exp[-(\bar{A}_k/\delta_B^*)] \tag{41}$$

where δ_B^* is the mean band spacing and $\bar{A}_k$ represents the mean absorption of the bands within the region k. If there are N_k bands in this region and the i^{th} band has an absorption A_i, defined by equation (11), then

$$\bar{A}_k = (1/N_k) \sum_{\substack{k^{th} \\ \text{region}}} A_i \quad . \tag{42}$$

Equations (41) and (42) are applicable at ω_k if a large number of bands (here, more than three) with mean spacing δ_B^* contribute to $\bar{\epsilon}_{\omega_k}$ and no contributions are made to $\bar{\epsilon}_{\omega_k}$ by bands located outside the interval $\omega_k \pm (N_k \delta_B^*/2)$.

The total region width $\Delta\omega_k$ is defined by the expression

$$\Delta\omega_k \equiv N_k \delta_B^* \quad . \tag{43}$$

In terms of $\Delta\omega_k$, equation (41) may be rewritten as

$$\bar{\epsilon}_{\omega_k} = 1 - \exp\left[-(1/\Delta\omega_k) \sum_{\substack{k^{th} \\ \text{region}}} A_i \right] . \tag{44}$$

In actual emissivity calculations, it is convenient to divide the entire spectrum into k localized regions in which a number of bands are grouped together. In order to obtain a reasonable approximation to the total emissivity ϵ_k for the k^{th} spectral region, an average blackbody radiancy $R^o_{\omega_k}$ is employed over the effective region width $\Delta\omega_k$, whence

$$\epsilon_k = \left[R^o_{\omega_k} \Big/ (\sigma T^4) \right] \epsilon_{\omega_k} \Delta\omega_k \tag{45}$$

where $R^o_{\omega_k}$ is the blackbody radiancy for region k evaluated at the average wavenumber $\bar{\omega}_k$. For a given region, $R^o_{\omega_k}$ is the weighted mean value

$$R^o_{\omega_k} = \left[\sum_{\substack{k^{th} \\ \text{region}}} R^o_{\omega_i} A_i \right] \Big/ \left[\sum_{\substack{k^{th} \\ \text{region}}} A_i \right] \tag{46}$$

where $R^o_{\omega_i}$ is the blackbody radiancy evaluated at a mean wavenumber $\bar{\omega}_i$ for the i^{th} band (usually the band center). From equations (44) and

(45) the total emissivity of the k^{th} region is seen to be

$$\epsilon_k = [R^{o}_{\omega_k}/(\sigma T^4)]\Delta\omega_k\left[1 - \exp\left[-(1/\Delta\omega_k)\sum_{\substack{k^{th}\\ \text{region}}} A_i\right]\right] \qquad (47)$$

or using equation (46),

$$\epsilon_k = \frac{\left[\sum_{\substack{k^{th}\\ \text{region}}} R^{o}_{\omega_i} A_i/(\sigma T^4)\right]\left\{1 - \exp\left[-(1/\Delta\omega_k)\sum_{\substack{k^{th}\\ \text{region}}} A_i\right]\right\}}{(1/\Delta\omega_k)\sum_{\substack{k^{th}\\ \text{region}}} A_i} \quad . \qquad (48)$$

Since the emissivity of the i^{th} band is approximately given by

$$\epsilon_i \simeq R^{o}_{\omega_i}/(\sigma T^4)\int_{\substack{i^{th}\\ \text{band}}}[1 - \exp(-P_{\omega_i} X)]d\omega = R^{o}_{\omega_i} A_i/(\sigma T^4) \quad , \qquad (49)$$

equation (48) may be written

$$\epsilon_k = \frac{\sum_{\substack{k^{th}\\ \text{region}}} \epsilon_i\left\{1 - \exp\left[-(1/\Delta\omega_k)\sum_{\substack{k^{th}\\ \text{region}}} A_i\right]\right\}}{(1/\Delta\omega_k)\sum_{\substack{k^{th}\\ \text{region}}} A_i} \quad . \qquad (50)$$

Equation (50) shows that the emissivity of the k^{th} region is equal to the sum of the emissivities of the individual bands within that region, each multiplied by an appropriate weighting factor. This weighting factor is shown in Figure 5. The total emissivity, ϵ, is equal to the sum of the emissivities of the k regions,

$$\epsilon = \sum_k \epsilon_k \quad . \qquad (51)$$

Any calculation of the emissivity of a gas requires knowledge of the spectral absorption coefficient P_ω. This can be obtained theoreti-

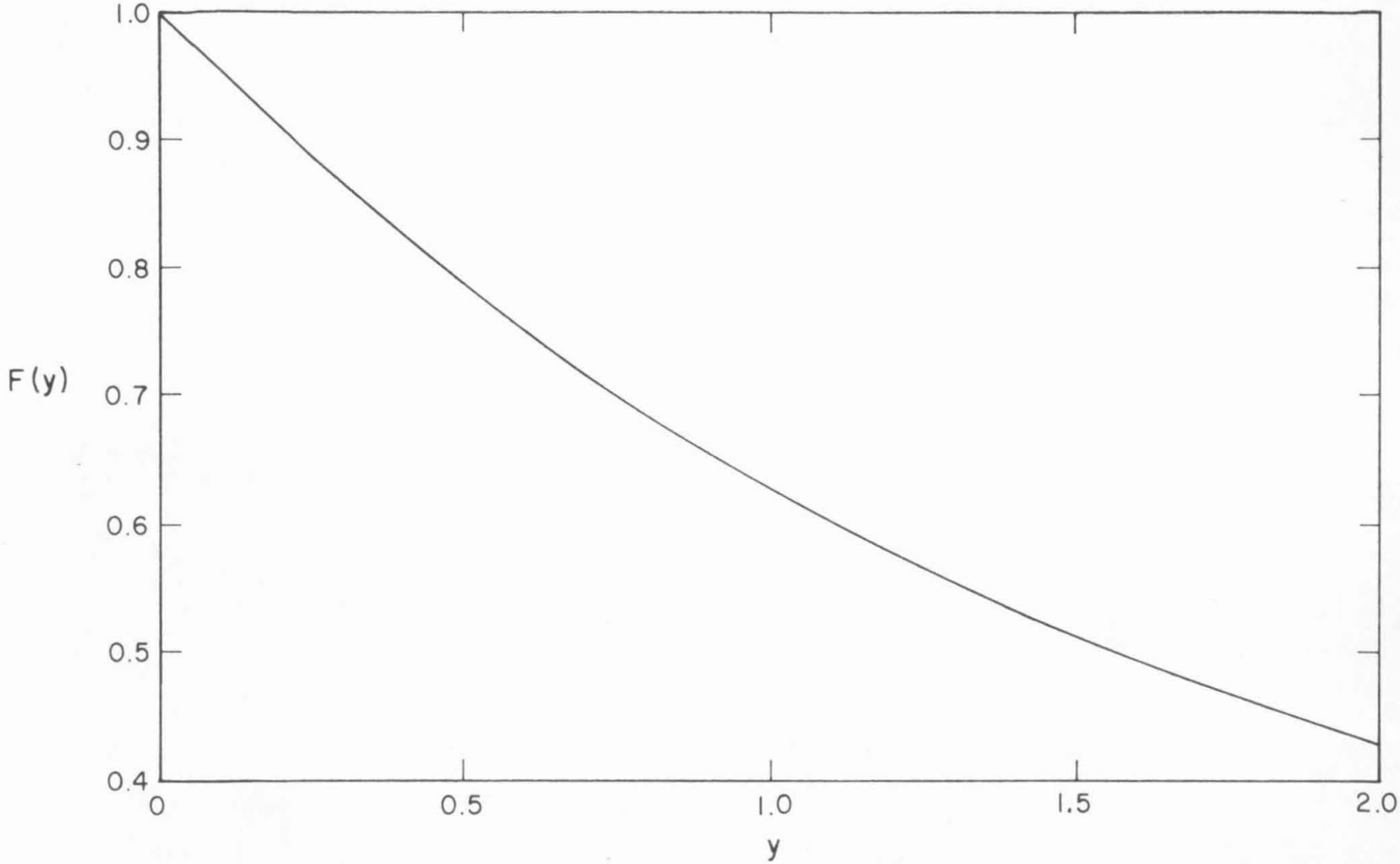

Figure 5. Weighting factor $F(y) = (1/y)[1 - \exp(-y)]$ for the statistical band model plotted as a function of y.

cally from molecular parameters in certain approximations. If the emitters have non-overlapping spectral lines, then detailed information concerning the spectral line profiles is also required.

D. MOLECULAR SPECTRA

1. Wave Equation for a Molecule.[26] - The complete wave equation for a molecule consisting of r nuclei and s electrons is

$$\sum_{j=1}^{r} \frac{\hbar^2}{2M_j} \nabla_j^2 \psi + \sum_{i=1}^{s} \frac{\hbar^2}{2m} \nabla_i^2 \psi + (E-V)\psi = 0 \qquad (52)$$

where

$$V = \sum_{i,i'} \frac{e^2}{r_{ii'}} + \sum_{j,j'} \frac{Z_j Z_{j'} e^2}{r_{jj'}} - \sum_{i,j} \frac{Z_j e^2}{r_{ij}} . \qquad (53)$$

Here M_j is the mass of the j^{th} nucleus of atomic number Z_j, m the mass of an electron, ∇_j^2 the Laplacian operator in terms of the coordinates of the j^{th} nucleus, ∇_i^2 the Laplacian operator in terms of the coordinates of the i^{th} electron. The sums in equation (53) include each pair of particles only once.

Born and Oppenheimer[27] were able to derive an approximate solution of the complete wave equation for a molecule by writing the wave function for the molecule as the product of an electronic wave function and a nuclear wave function.

Let ξ represent the 3r coordinates of the r nuclei, relative to fixed axes in space, and let x represent the 3s coordinates of the s electrons relative to axes determined by the coordinates of the nuclei. The quantum numbers associated with motion of the nuclei will be denoted by ν and those associated with motion of the electrons by n.

Then, in the Born-Oppenheimer approximation,

$$\psi_{n,\nu}(x,\xi) = \psi_n(x,\xi)\psi_{n,\nu}(\xi) \tag{54}$$

where $\psi_n(x,\xi)$ represents the electronic wave functions, corresponding to different values of the electronic quantum number n only, and independent of the nuclear quantum number ν. The $\psi_n(x,\xi)$ are functions of both the nuclear coordinates ξ and the electronic coordinates, x. The electronic wave functions are found by solving a wave equation for the electrons alone, the nuclei being restricted to a fixed configuration. The electronic wave equation is

$$\sum_{i=1}^{s} \frac{\hbar^2}{2m} \nabla_i^2 \psi_n(x,\xi) + [U_n(\xi) - V(x,\xi)]\psi_n(x,\xi) = 0 \tag{55}$$

where $V(x,\xi)$ is given by equation (53). For any fixed value of ξ, equation (55) is an ordinary wave equation for the s electrons, with $V(x,\xi)$ depending on the value of ξ chosen for the nuclear coordinates. As a result, the electronic energy eigenvalues, U_n, are also functions of ξ. Once $U_n(\xi)$ is evaluated, the nuclear wave functions, $\psi_{n,\nu}(\xi)$ may be found by solving the nuclear wave equation

$$\sum_{j=1}^{r} \frac{\hbar^2}{2M_j} \nabla_j^2 \psi_{n,\nu}(\xi) + [E_{n,\nu} - U_n(\xi)]\psi_{n,\nu}(\xi) = 0 \ . \tag{56}$$

For each set of values of the electronic quantum number, n, equation (56) must be solved for the set of solutions corresponding to the allowed values of the nuclear quantum numbers, ν. The values of $E_{n,\nu}$ are the energy eigenvalues for the molecule.

The Born-Oppenheimer approximation can be justified[27] by a procedure involving an expansion of the quantities involved in the complete wave equation for the molecule, equation (52), in a power series

in $(m/M)^{1/4}$ in which M is an average nuclear mass.

2. Vibration of Polyatomic Molecules. - The solution of equation (56), found by introducing for the electronic energy eigenvalues $U_n(\xi)$ either an expression obtained by solving the electronic wave equation, equation (55), or some empirical expression (e. g., a Morse potential), gives the rotational and vibrational motion of a polyatomic molecule. This treatment is so difficult that it is customary, as a first approximation, to neglect all interaction between the rotational motion and vibrational motion of the molecule.

The nuclear wave equation can then be separated into a rotational wave equation, representing the rotational motion of a rigid body, and a vibrational wave equation, representing vibrational motion of a non-rotating molecule. Thus, while it is theoretically possible to start with a model consisting of electrons and nuclei interacting coulombically and obeying the laws of quantum mechanics, in practice it is necessary to assume the nature of the equilibrium configuration and of the forces between the nuclei.

(a) Normal Vibrations.[5] The general properties of the vibrational spectra of diatomic molecules will be briefly reviewed since they may be carried over directly to apply to the polyatomic case. Consider a molecule consisting of two nuclei, A and B , which have a position of stable equilibrium at $\underline{r} = r_e$, where $\underline{r}$ is the distance between the two nuclei. A typical curve representing the electronic energy function, $U_n(r)$ is shown in Figure 6. The horizontal lines represent the possible energy states, which are discrete below D the dissociation energy of the molecule, and are continuous above D . It is found experimentally

Figure 6. Electronic potential energy curve of the H_2 ground state with vibrational levels and continuous term spectrum. The broken curve is a Morse potential (from ref. 1).

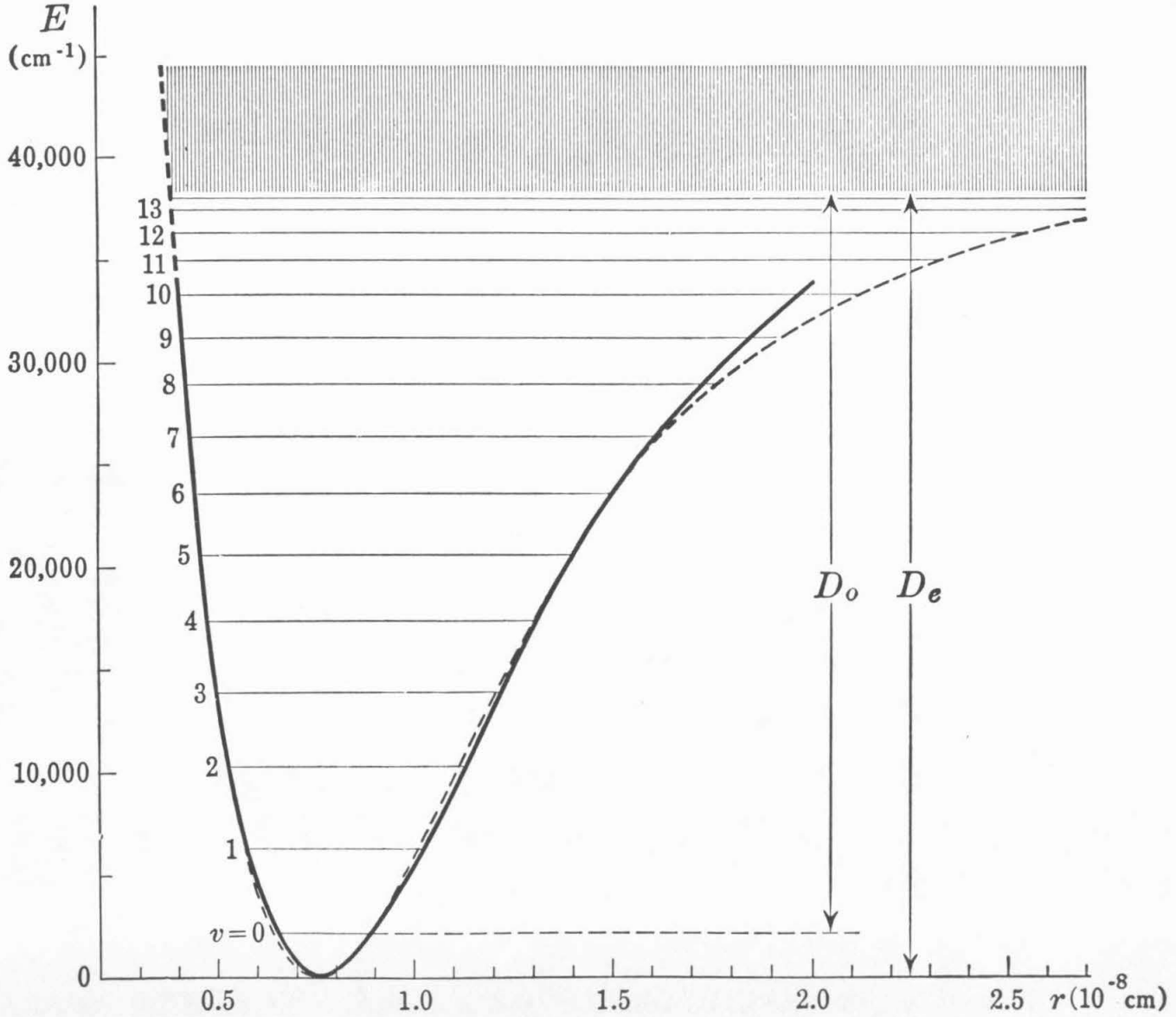
E
(cm⁻¹)
40,000
30,000
20,000
10,000
0
13
12
11
10
9
8
7
6
5
4
3
2
1
v=0
D_o
D_e
0.5
1.0
1.5
2.0
2.5
r(10⁻⁸cm)

that the distance between the lower vibrational energy levels is nearly constant and much smaller than D, $h\nu_o/D \ll 1$. Near room temperature, infrared absorption bands arise from transitions from the lowest vibrational energy states to those states immediately above. Under these conditions, the force between the two nuclei is approximately a linear function of their separation distance.

For transitions between the lowest states, it is found experimentally that 1) the frequency of radiation absorbed or emitted is very nearly the mechanical frequency of motion of a simple harmonic oscillator as computed by classical mechanics; 2) the intensity of radiation is nearly that computed by classical electrodynamics, i.e., it depends on the square of the amplitude of the electric moment; 3) the wave function differs from zero only in the neighborhood of $\underline{r} = r_e$, corresponding to a classical amplitude of motion small compared with the equilibrium distance between the nuclei, i.e., the classical theory of small oscillations is applicable.

These general properties are also true for polyatomic molecules. In this case, there are $\underline{r}$ atomic nuclei, which are assumed to have an equilibrium position. The system as a whole has $3\underline{r}$ degrees of freedom. Of these, three correspond to uniform translation of the center of mass. For a non-linear molecule, there are three rotational degrees of freedom, and $3\underline{r} - 6$ vibrational degrees of freedom; for a linear molecule, there are only two rotational degrees of freedom* and $3\underline{r} - 5$ vibrational degrees of freedom.

---

* Since it is meaningless to speak of the rotation of a linear molecule about its axis.

(b) Small Oscillations.[28-30] Consider the motion of a molecule about its configuration of stable equilibrium. The departures from equilibrium are assumed to be small, so that all functions may be expanded in a Taylor series about the equilibrium position, and only the lowest order terms retained. Let the generalized coordinates* of the nuclei be denoted by $\xi_1 \cdots \xi_{3r}$, and the deviations of the generalized coordinates from their equilibrium position be denoted by $q_1 \cdots q_{3r}$. From the relation

$$\xi_j = \xi_{je} + q_j \tag{57}$$

it is apparent that the q_j may be taken as new generalized coordinates of motion. Expanding the potential energy about the equilibrium position gives

---

* A system of r particles, free from constraints, has 3r independent coordinates or degrees of freedom. Frequently, it is more convenient to use a set of coordinates other than the cartesian coordinates $x_1, y_1, z_1, \ldots, x_r, y_r, z_r$. If a set of new independent variables $q_1, \ldots, q_{3r}$ is introduced, the old cartesian coordinates of the i^{th} particle x_i, y_i, z_i are related to the new coordinates by the equations of transformation,

$$x_i = x_i(q_1, q_2, \ldots, q_{3r})$$
$$y_i = y_i(q_1, q_2, \ldots, q_{3r})$$
$$z_i = z_i(q_1, q_2, \ldots, q_{3r}) .$$

These is such a set of three equations for each particle i.

Generalized coordinates must not be thought of in terms of conventional orthogonal position coordinates, and it may be convenient to use quantities with the dimensions of energy or angular momentum as coordinates. The generalized momentum conjugate to a generalized coordinate $p_i \equiv \partial L/(\partial \dot{q}_i)$ will not necessarily have the dimensions of momentum, but the product $p_i q_i$ will always have the dimensions of action (e.g., erg-sec.).

$$U(\xi) = U(\xi_e) + \sum_{j=1}^{3r} \left(\frac{\partial U}{\partial \xi_j}\right)_e q_j + \frac{1}{2} \sum_{i=1}^{3r} \sum_{j=1}^{3r} \left(\frac{\partial^2 U}{\partial \xi_i \partial \xi_j}\right)_e q_i q_j + \cdots \quad (58)$$

The linear term in q_j vanishes automatically, from the definition of equilibrium, i.e., when the generalized forces acting on the system vanish: $F_j = \left(\frac{\partial U}{\partial \xi_j}\right)_e = 0$. The first term in the series is the potential energy of the equilibrium position and by shifting the arbitrary zero of potential to coincide with the equilibrium potential, this term may also be made to vanish. Thus, a first approximation of U is given by

$$U = \frac{1}{2} \sum_{j=1}^{3r} \sum_{i=1}^{3r} \left(\frac{\partial^2 U}{\partial \xi_i \partial \xi_j}\right)_e q_i q_j = \frac{1}{2} \sum_{i=1}^{3r} \sum_{j=1}^{3r} b_{ij} q_i q_j \quad (59)$$

where the second derivatives of U have been designated by the constants b_{ij} depending only on the equilibrium values of the ξ_j's. From their definition, the b_{ij}'s are obviously symmetrical, i.e., $b_{ij} = b_{ji}$. Equation (59) can be rewritten in the form of an inner product

$$U = \frac{1}{2} < q, Bq > \quad (60)$$

where B is a matrix with components b_{ij} and q is a vector with components $(q_1, q_2, \ldots, q_{3r})$.

A similar series expansion can be obtained for the kinetic energy. Since the generalized coordinates do not involve the time explicitly, the kinetic energy T is a homogeneous quadratic function of the velocities:

$$T = \frac{1}{2} \sum_{i=1}^{3r} \sum_{j=1}^{3r} \tilde{a}_{ij} \dot{\xi}_i \dot{\xi}_j = \frac{1}{2} \sum_{i=1}^{3r} \sum_{j=1}^{3r} \tilde{a}_{ij} \dot{q}_i \dot{q}_j \, . \quad (61)$$

The coefficients a_{ij} are in general functions of the coordinates, ξ_i, but they may be expanded in a Taylor series about the equilibrium position

$$\tilde{a}_{ij}(\xi) = \tilde{a}_{ij}(\xi)_e + \sum_{k=1}^{3r} \left(\frac{\partial a_{ij}}{\partial \xi_k}\right)_e q_k + \dots \quad .$$

Retaining only the first term in the expansion of $\tilde{a}_{ij}$, henceforth to be denoted by a_{ij}, the kinetic energy can be written as

$$T = \frac{1}{2} \sum_{i=1}^{3r} \sum_{j=1}^{3r} a_{ij} \dot{q}_i \dot{q}_j \quad . \tag{62}$$

Since the a_{ij}'s are symmetric, equation (62) can be rewritten in a form similar to that of equation (60), i. e.,

$$T = \frac{1}{2} < \dot{q}, A\dot{q} > \quad . \tag{63}$$

The two quadratic forms, equations (60) and (63) can simultaneously be diagonalized by means of a linear transformation to the so-called normal coordinates[31] $Q_1, Q_2, \dots, Q_{3r}$. In terms of the normal coordinates, the kinetic energy would have the form

$$2T = \dot{Q}_1^2 + \dots + \dot{Q}_{3r}^2 \quad . \tag{64}$$

Similarly, the potential energy could be written as

$$2V = \lambda_1 Q_1^2 + \dots + \lambda_{3r} Q_{3r}^2 \quad . \tag{65}$$

The equations of motion of the system reduce to the equation of a simple harmonic oscillator for each of the normal coordinates:

$$\ddot{Q}_k + \lambda_k Q_k = 0 \quad , \qquad k = 1, 2, \dots, 3r \quad . \tag{66}$$

In order to determine the linear transformation from the gener-

alized coordinates to the normalized coordinates, the following eigenvalue problem must be solved. Find the eigenvalues λ for which the equation

$$(B - \lambda A)y = 0 \tag{67}$$

has a non-trivial solution. Here y is an eigenvector with $3r$ components. When equation (67) is considered as a set of $3r$ linear equations for the components of y, it is clear that λ is an eigenvalue if and only if

$$\det | B - \lambda A | = 0 . \tag{68}$$

Since this determinental equation is of degree $3r$, it will give $3r$ values for λ, and the eigenvector corresponding to the k^{th} eigenvalue λ_k will be denoted by y_k.

The eigenvectors form an orthogonal set with respect to A, which can be normalized such that

$$< y_k , Ay_j > = \delta_{jk} \tag{69}$$

where $\delta_{jk} = 0$ for $j \neq k$ and $\delta_{jj} = 1$. From equation (67) it follows that

$$<y_k, By_j> = <y_k, \lambda_j Ay_j> = \lambda_j \delta_{jk} . \tag{70}$$

Hence, the matrix C, whose columns are the eigenvectors $y_1, y_2, \ldots, y_{3r}$, is the desired linear transformation from the generalized coordinates to the normal coordinates.

$$q = C\Omega \tag{71}$$

From equation (71), equation (60) becomes

$$U = \tfrac{1}{2}<q, Bq> = \tfrac{1}{2}< C\Omega, BC\Omega > = \tfrac{1}{2}<\Omega, C^{*}BC\Omega > \tag{72}$$

where C^{*} is the transpose of C. From equation (70) it follows that

$$C^{*}BC = \Lambda \tag{73}$$

where Λ is a diagonal matrix of the eigenvalues λ_i. Hence

$$U = \tfrac{1}{2}\langle Q, \Lambda Q\rangle = \frac{1}{2}\sum_{i=1}^{3r} \lambda_i Q_i^2 \ . \qquad (74)$$

Similarly, equation (63) becomes

$$T = \tfrac{1}{2}\langle \dot{q}, A\dot{q}\rangle = \tfrac{1}{2}\langle \dot{Q}, C^* AC\dot{Q}\rangle = \tfrac{1}{2}\langle \dot{Q}, \dot{Q}\rangle$$

or

$$T = \frac{1}{2}\sum_{i=1}^{3r} \dot{Q}_i^2 \qquad (75)$$

since it follows from equation (69) that

$$C^* AC = I \qquad (76)$$

where I is the identity matrix. From equations (74) and (75), the total energy of a system of particles executing small oscillations can be written as

$$E = \tfrac{1}{2}\sum_{\alpha}\sum_{i} \dot{Q}_{\alpha_i}^2 + \tfrac{1}{2}\sum_{\alpha} \tilde{\omega}_\alpha^2 \sum_{i} Q_{\alpha i}^2 \qquad (77)$$

where the $\tilde{\omega}_\alpha$ are the frequencies of the corresponding independent vibrations ($\tilde{\omega}_\alpha^2 = \lambda_\alpha$). The subscript α denotes the frequencies and the subscript $i = 1, 2, \ldots, f_\alpha$ numbers the coordinates belonging to a given frequency (f_α being the multiplicity of the frequency $\tilde{\omega}_\alpha$).

(c) Applications of group theory to molecular vibrations.[32-36] The difficulty of solving the secular equation [equation (68)] which is an algebraic equation of degree 3r for the eigenfrequencies can be reduced in many cases by the use of group theory. Molecules generally possess some symmetry. This is determined by the position and type of nuclei, and molecules of different symmetry have qualitatively different spectra[37]. With the aid of group theory, the symmetry and geometry of a molecular model can be used to determine the number of fundamental frequencies, their degeneracies, the selection rules for the infrared and Raman spectra, the possibility of perturbations due to resonance, etc.

(i) Symmetry of molecules.[34, 36, 37] - It is necessary to have a definite method of classifying and describing the symmetry of a given molecule. This can be done by considering all the possible rearrangements of the nuclei which leave the molecule in an equivalent configuration, i. e., a configuration that is indistinguishable from the original configuration when nuclei of the same kind are considered to be indistinguishable. These rearrangements of the nuclei are called symmetry operations and can be represented as a combination of one or more of the fundamental types of operation: rotation of the molecule through a definite plane about some axis and reflection of it in some plane.

A molecule may have one or several symmetry elements such as a plane of symmetry, a center of symmetry, or an axis of symmetry. To each symmetry element, there corresponds a symmetry operation, i. e., a reflection or rotation of the coordinates that will produce a configuration of nuclei indistinguishable from the original one.

Thus, corresponding to a plane of symmetry σ is the operation of reflection in that plane (also designated σ); for a center of symmetry i the corresponding operation is inversion or reflection at the center (also called i); for a p-fold axis of symmetry C_p, the corresponding operation (also denoted C_p) is rotation through an angle of $2\pi/p$ about that axis; for a p-fold rotation-reflection axis S_p, the corresponding operation S_p is a rotation through an angle of $2\pi/p$ about this axis followed by reflection in a plane perpendicular to the rotation axis. There is also the identity operation E which leaves the molecule unchanged.

(ii) Groups of symmetry operations.[32-36, 38, 39] - When a molecule is subjected to two symmetry operations in succession, it

reaches a point that could have been obtained by the use of one symmetry operation. The set of all symmetry operations for a given molecule is called its symmetry group.

If A_i is an element of the group G, and it is possible to associate a square matrix $\Gamma(A_i)$ with each member of the group in such a way that if

$$A_i A_j = A_k \tag{78}$$

and

$$\Gamma(A_i)\Gamma(A_j) = \Gamma(A_k), \tag{79}$$

then such matrices are said to form a representation of the group and the order of the matrices is called the dimension of the representation.* Every group has the identity representation in which every element of the group is represented by the identity matrix of order one; this is referred to as the completely symmetrical representation.

Suppose that a representation of a group has been found consisting of the elements $\Gamma(A_1), \Gamma(A_2), \ldots, \Gamma(A_g)$ where g is the order of the group G, i.e., the number of elements of the group. Then it is often possible to find a transformation of the type $P^{-1}\Gamma(A_k)P = \Gamma'(A_k)$ such that every matrix Γ of the representation is brought into the form

$$\Gamma = \begin{bmatrix} \Gamma^{(1)} & & & \\ & \Gamma^{(2)} & & \\ & & \ddots & \\ & & & \Gamma^{(s)} \end{bmatrix} \tag{80}$$

with smaller matrices $\Gamma^{(i)}(A_k)$ along the diagonal and zeros elsewhere. Equation (80) is written

$$\Gamma = \Gamma^{(1)} + \Gamma^{(2)} + \ldots + \Gamma^{(s)} \tag{80a}$$

---

* Examples are given in ref. 40.

and Γ is said to contain the representations $\Gamma^{(i)}$. If there are g elements of the group there will be g equations like the above, one for each element of the group. Equation (80) is called the "direct sum" and shows that the matrix Γ has been reduced. A representation that cannot be reduced is termed irreducible.

(iii) Characters[32,33,38] - If $\Gamma(A_k)$ is any representation of a group of transformations A_k, then the sum of the diagonal elements, or the trace of the matrix, is called the character χ of A_k in this representation, i.e.,

$$\chi(A_k) = \sum_i \Gamma_{ii}(A_k) \tag{81}$$

Elements of the group which can be obtained from one another by a similarity transformation are said to be in the same class, and the character of every element in a class will be the same since the character of a matrix is unchanged by a similarity transformation. Clearly the identity element E always forms a class of its own, and $\chi(E)$ is the dimension of the representation.

The characters of the irreducible representations satisfy the following orthogonality relation;*

$$\sum_{\text{elements}} \chi^i(A_k)\ \chi^j(A_k) = g\delta_{ij} \tag{82}$$

---

* The proof of this relation may be found in books on group theory such as refs. 41-43.

Equation (82) could also be written as

$$\sum_{\text{classes}} r(A_k)\chi^i(A_k)\chi^j(A_k) = g\delta_{ij} \qquad (83)$$

where $r(A_k)$ is the number of elements in the class of A_k.

From equation (80), the character of a reducible representation $\Gamma(A_k)$ is seen to be

$$\chi(A_k) = \sum_{i=1}^{s} n_i \chi^i(A_k) \qquad (84)$$

where n_i is the number of times the irreducible component $\Gamma^{(i)}$ occurs in the reduction of Γ. From equations (83) and (84), the number of times an irreducible representation $\Gamma^{(i)}$ appears in reducing a representation Γ can be found from

$$n_i = \frac{1}{g} \sum_{\text{classes}} r(A_k)\chi(A_k)\chi^i(A_k) \qquad (85)$$

where $\chi^i(A_k)$ is obtained from a character table, and $\chi(A_k)$, the character of a particular symmetry operation, is found by methods to be discussed later.

Tables of characters have been given by many authors[32-38, 44-48] and for convenience Tables I and II reproduce the character tables of the point groups C_{2v} (to which H_2O belongs) and $D_{\infty h}$ (CO_2).

(iv) Quantum mechanical applications. - The quantum mechanical applications of group theory are based on the fact that Schroedinger's equation for a physical system is invariant with respect to symmetry transformations of the system. In other words, under a symmetry transformation the wave functions of the stationary states of the system belonging to a given energy level transform into linear combinations of one another. These wave functions give some representation

Table I. Character Table for the Point Group C_{2v}

C_{2v}				E	C_2	$\sigma_{v_{xz}}$	$\sigma'_{v_{yz}}$
u_z	x^2, y^2, z^2	z	A_1	1	1	1	1
	xy	R_z	A_2	1	1	-1	-1
u_x	xz	R_y, x	B_1	1	-1	1	-1
u_y	yz	R_x, y	B_2	1	-1	-1	1

Table II. Character Table for the Symmetry Group $D_{\infty h}$

$D_{\infty h}$				E	$2C_\phi$	C'_2	i	$2iC_\phi$	iC'_2
x^2+y^2, z^2		Σ_g^+	A_{1g}	1	1	1	1	1	1
		Σ_u^-	A_{1u}	1	1	1	-1	-1	-1
		Σ_g^-	A_{2g}	1	1	-1	1	1	-1
	z	Σ_u^+	A_{2u}	1	1	-1	-1	-1	1
(xz, yz)	(R_x, R_y)	π_g	E_{1g}	2	$2\cos\phi$	0	2	$2\cos\phi$	0
	(x, y)	π_u	E_{1u}	2	$2\cos\phi$	0	-2	$-2\cos\phi$	0
(x^2-y^2, xy)		Δ_g	E_{2g}	2	$2\cos 2\phi$	0	2	$2\cos 2\phi$	0
		Δ_u	E_{2u}	2	$2\cos 2\phi$	0	-2	$-2\cos 2\phi$	0
		..		.....	.....	.....	.....	.....	.....

of the group, and this is an irreducible representation. The dimension of this representation determines the degree of degeneracy of the level concerned, or, the number of different states with the same energy. The fixing of the irreducible representation determines all the symmetry properties of the given state, i.e., its behavior with respect to the various symmetry transformations.

Group theoretical methods are extremely useful in the investigation of molecular vibrations[49]. Equation (77) for the vibrational energy of a molecule must be invariant with respect to symmetry transformations. This means that, under any transformation belonging to the symmetry point group of the molecule, the normal coordinates, $Q_{\alpha i}$, are transformed into linear combinations of themselves, in such a way that the sum of the squares $\sum_i Q_{\alpha i}^2$ remains unchanged. In other words, the normal coordinates belonging to any particular eigenfrequency of the vibrations of the molecule give some irreducible representation of its symmetry group; the multiplicity of the frequency determines the dimension of the representation. The normal coordinates and normal modes of vibration of symmetrical molecules have certain special symmetry properties. Nondegenerate normal modes of vibration are always either symmetrical (unaltered) or antisymmetrical (changed in sign) with respect to a given symmetry operation of the point group of the undistorted molecule.

These considerations enable the eigenvibrations of a molecule to be classified without actually solving for its normal coordinates. To do so, the representation given by all the vibrational coordinates together must first be found. This representation is called the total

representation, and is reducible. Upon decomposing it into irreducible parts, the multiplicities of the eigenfrequencies and the symmetry properties of the corresponding vibration modes are determined. If the same irreducible representation appears several times in the total representation, it means that there are several different frequencies of the same multiplicity and with oscillations of the same symmetry.

The total representation may be found by using the fact that the characters of a representation are invariant with respect to a linear transformation of the base functions. As a result, the normal coordinates need not be chosen as base functions , but the generalized coordinates or simply the cartesian components of the displacements of the nuclei from their equilibrium positions can be used. As a result, the number of normal coordinates with given symmetry properties can be obtained when the characters of the transformations of the displacement coordinates are known. These could be obtained directly by writing out the transformations, but much easier methods can be used.

Consider some operation A_k which moves nucleus 1 to a new position previously occupied by nucleus 2. Then the representation of this operation $\Gamma(A_k)$ will have its matrix elements Γ_{12} and Γ_{21} equal to some numbers, but Γ_{11} and Γ_{22} will be equal to zero, and $\chi(A_k)$ will therefore be zero. Hence, to calculate the character of some element A_k of a point group, only those nuclei need be considered whose equilibrium position remains fixed under the given symmetry operation.

Consider a rotation C_ϕ through an angle ϕ about some symmetry axis. Each nucleus lying on the axis of symmetry will contribute $(1 + 2\cos\phi)$ to the character.

$$\chi(C_\phi) = N_c (1 + 2\cos\phi) \tag{86}$$

where N_c is the total number of nuclei lying on the axis of symmetry.

For a rotary reflection S_ϕ each nucleus contributes $(-1 + 2\cos\phi)$ to the character.

$$\chi(S_\phi) = N_s (-1 + 2\cos\phi) \tag{87}$$

where N_s is the number of nuclei left unmoved by the operation S_ϕ. (This number is either zero or one depending on whether there is a nucleus at the center of inversion or not.) It follows from equation (87) that the contribution to the character of reflection in a plane $\sigma = S_1^1$ is

$$\chi(\sigma) = N_\sigma \tag{88}$$

and that of inversion $i = S_2^1$ is

$$\chi(i) = -3N_i \ . \tag{89}$$

Except for cases of accidental degeneracy, the representation formed by the normal coordinates is a completely reduced one. Consequently, equation (85) can be applied to find the number of normal coordinates of each symmetry species, i.e., in each irreducible representation.

As an illustration, consider the water molecule, H_2O. The character table for its point group, C_{2v}, is given in Table I.

There are four elements in the group: E, C_{2v}, $\sigma_v(xz)$, and $\sigma_v(yz)$. The character for E is $3N = 9$, the number of coordinates. The character for C_2 is -1 (see equation (86)), while that for $\sigma_v(xz)$ is 1 and for $\sigma_v(yz)$ is 3. Therefore, $\chi(E) = 9$, $\chi(C_2) = -1$, $\chi(\sigma_v(xz)) = 1$, and $\chi(\sigma_v(yz)) = 3$. Substituting these values into equation (85) gives

$$n(A_1) = (1/4)\{(1)(1)(9) + (1)(1)(-1) + (1)(1)(1) + (1)(1)(3)\} = 3$$

$$n(A_2) = (1/4)\{(1)(1)(9) + (1)(1)(-1) + (1)(-1)(1) + (1)(-1)(3)\} = 1$$

$$n(B_1) = (1/4)\,[(1)(1)(9) + (1)(-1)(-1) + (1)(1)(1) + (1)(-1)(3)] = 2$$

$$n(B_2) = (1/4)\,[(1)(1)(9) + (1)(-1)(-1) + (1)(-1)(1) + (1)(1)(3)] = 3$$

There are three totally symmetric coordinates, A_1, one coordinate with symmetry species A_2, two coordinates with symmetry species B_1, and three with symmetry species B_2. The representation formed by the cartesian coordinates (including translation and rotation) of water is

$$\Gamma = 3A_1 + A_2 + 2B_1 + 3B_2 \quad . \tag{90}$$

Since it is desired to find the number of vibrational normal coordinates with each symmetry, the symmetry of the translational and rotational coordinates must be obtained and the proper numbers subtracted from the total values of $n(A_k)$. From Table I it is apparent that

$$\Gamma_{trans} = A_1 + B_1 + B_2 \tag{91}$$

and

$$\Gamma_{rot} = A_2 + B_1 + B_2 \quad . \tag{92}$$

Hence,

$$\Gamma_{vib} = 2A_1 + B_2 \quad . \tag{93}$$

The two vibrations of A_1 are non-degenerate unless they accidentally coincide. Consequently, the group-theoretical treatment predicts that H_2O will have three normal frequencies, none of which are degenerate.

A brief discussion of infra-red spectra will be given later and the situation is as follows[33], if all overtones and combination frequencies are neglected. A normal vibration Q_β gives an absorption line in the infra-red spectrum if Q_β transforms in the same way as one of the dipole moment components, μ_x, μ_y, μ_z. Further, Q_β gives a line in the Raman spectrum if it transforms in the same way

as one of the polarizability tensor components, α_{ij} (or linear combination thereof). The dipole moment is an ordinary vector, and the components μ_x, μ_y, μ_z transform like x, y, z. In the case of water this is according to $A_1 + B_1 + B_2$. The polarizability α_{ij} is a symmetric tensor and hence the components transform in the same way as x^2, y^2, z^2, xz, yz, xy.

The transformation properties of these quantities are summarized in Table III. From this table, together with the group character tables, the symmetry species of the vibrational normal coordinates of any molecule can easily be derived by the methods described above, and the infra-red and Raman active ones among them immediately written down.

Table III. Transformation Properties of Some Often Used Quantities

Quantity	Transforms like
translation of center of mass X_{cm}, Y_{cm}, Z_{cm}	x, y, z (vector)
rotational displacements R_x, R_y, R_z	I_x, I_y, I_z (pseudo-vector)
dipole moment μ_x, μ_y, μ_z	x, y, z
polarizability tensor α_{ij}	x^2, y^2, z^2, xy, xz, yz

(v) Normal Modes of Vibration for H_2O. - If the coordinate system is taken with its origin at the center of gravity of the molecule as shown in Fig. 7, the z axis as usual being the symmetry axis, and

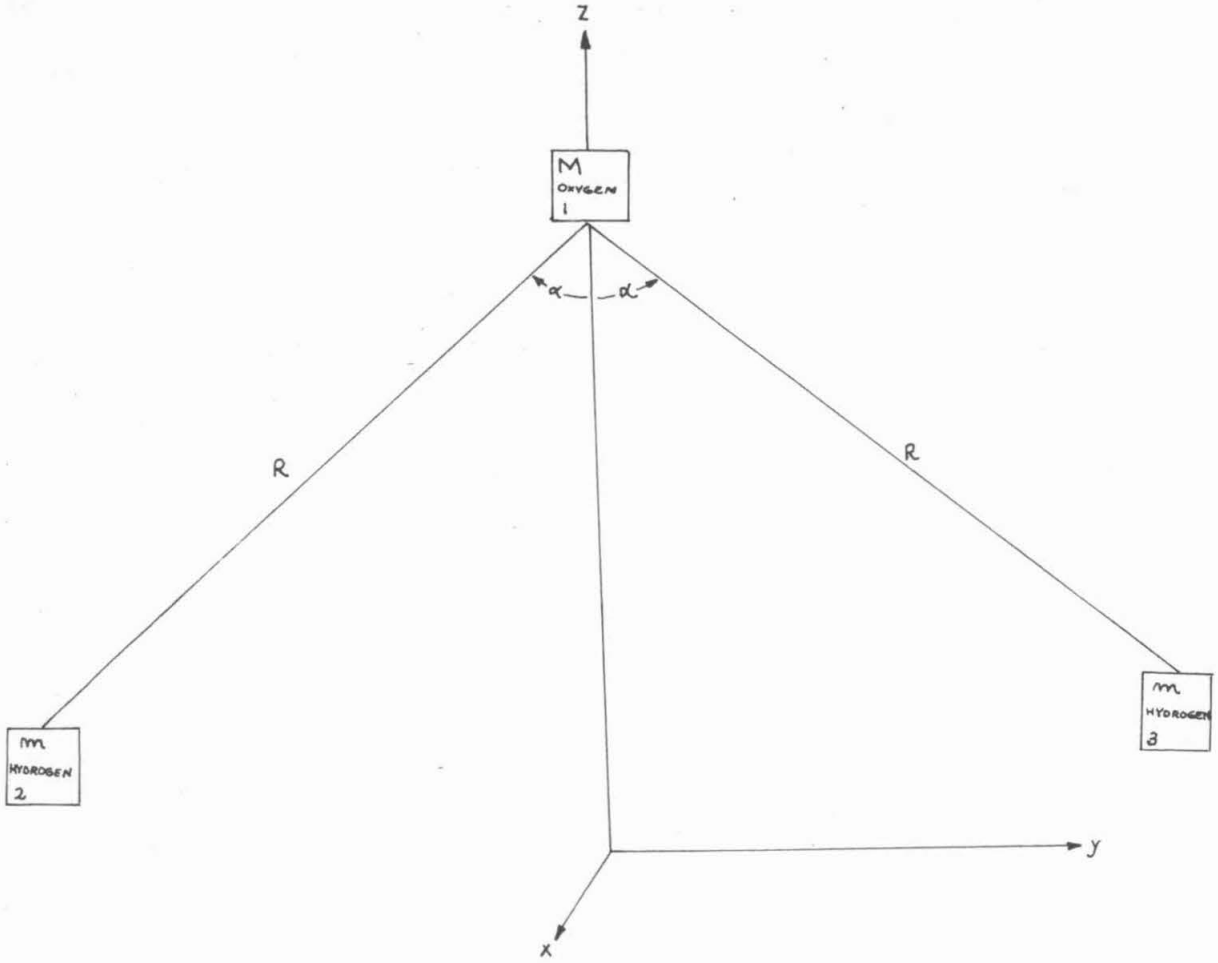

Figure 7. Coordinate axes used in determining the normal modes of vibration of the H_2O molecule.

the x axis chosen normal to the plane of the molecule, then the effect of the various symmetry operations of the group C_{2v} may be summarized as follows:

E	C_2	σ_{xz}	σ_{yz}
$x_1 \rightarrow x_1$	$x_1 \rightarrow -x_1$	$x_1 \rightarrow x_1$	$x_1 \rightarrow -x_1$
$x_2 \rightarrow x_2$	$x_2 \rightarrow -x_3$	$x_2 \rightarrow x_3$	$x_2 \rightarrow -x_2$
$x_3 \rightarrow x_3$	$x_3 \rightarrow -x_2$	$x_3 \rightarrow x_2$	$x_3 \rightarrow -x_3$
$y_1 \rightarrow y_1$	$y_1 \rightarrow -y_1$	$y_1 \rightarrow -y_1$	$y_1 \rightarrow y_1$
$y_2 \rightarrow y_2$	$y_2 \rightarrow -y_3$	$y_2 \rightarrow -y_3$	$y_2 \rightarrow y_2$
$y_3 \rightarrow y_3$	$y_3 \rightarrow -y_2$	$y_3 \rightarrow -y_2$	$y_3 \rightarrow y_3$
$z_1 \rightarrow z_1$	$z_1 \rightarrow z_1$	$z_1 \rightarrow z_1$	$z_1 \rightarrow z_1$
$z_2 \rightarrow z_2$	$z_2 \rightarrow z_3$	$z_2 \rightarrow z_3$	$z_2 \rightarrow z_2$
$z_3 \rightarrow z_3$	$z_3 \rightarrow z_2$	$z_3 \rightarrow z_2$	$z_3 \rightarrow z_3$

These give the characters $\chi(E)=9$, $\chi(C_2)= -1$, $\chi(\sigma_{xz}) = 1$, and $\chi(\sigma_{yz}) = 3$ as stated earlier.

The normal coordinates corresponding to translation are:

$$Q_1 = (x_1 + x_2 + x_3) = T_x \tag{94}$$

$$Q_2 = (y_1 + y_2 + y_3) = T_y \tag{95}$$

$$Q_3 = (z_1 + z_2 + z_3) = T_z \tag{96}$$

which belong to the irreducible representations denoted B_1, B_2 and A_1 respectively (see Table I). The normal coordinates for rotation are:

$$Q_4 = -y_1 + (M/2m)(y_2 + y_3) + (z_3 - z_2)\{(2m + M)/2m\} \tan\alpha = R_x \quad (97)$$

$$Q_5 = x_1 - (M/2m)(x_2 + x_3) = R_y \quad (98)$$

$$Q_6 = x_2 - x_3 = R_z \quad (99)$$

belonging to the irreducible representations B_2, B_1 and A_2 respectively. These may be obtained by inspection if the nuclei are imagined to have velocities $\dot{x}_1$, $\dot{y}_1$, $\dot{z}_1$, etc. and one asks how the velocities must be related in order that the angular momentum about the axis in question shall be a maximum. Here, M is the mass of the oxygen nucleus, m is the mass of a hydrogen nucleus and 2α is the angle between the OH bonds.

The two normal coordinates for vibration coming under A_1 may be obtained from the general expression

$$Q = a_1x_1 + a_2x_2 + a_3x_3 + b_1y_1 + b_2y_2 + b_3y_3 + c_1z_1 + c_2z_2 + c_3z_3 \ . \quad (100)$$

The character for C_2 in A_1 is 1 (see Table I) and $C_2Q = 1 \times Q$. But

$$C_2Q = -a_1x_1 - a_2x_3 - a_3x_2 - b_1y_1 - b_2y_3 - b_3y_2 + c_1z_1 + c_2z_3 + c_3z_2. \quad (101)$$

From the equation $C_2Q = Q$, the following relations must hold:

$$a_2 = -a_3; \quad b_2 = -b_3; \quad c_2 = +c_3 \text{ and } b_1 = a_1 = 0.$$

Similarly, from the equation $\sigma_{yz}Q = Q$, the further relations $a_2=0$; $a_3=0$ are obtained. The equation $\sigma_{xz}Q = Q$ yields no new relations. So a normal coordinate coming under the irreducible representation A_1 must be of the form

$$b_2(y_2 - y_3) + c_1 z_1 + c_2(z_2 + z_3)$$

The symmetry coordinates coming under A_1 may be taken as any three orthogonal combinations of S_1, S_2, S_3 where

$$S_1 = z_1; \quad S_2 = z_2 + z_3; \quad S_3 = y_2 - y_3. \tag{102}$$

But it has already been shown that T_z belongs to this representation: $T_z = S_1 + S_2$. Taking one of the symmetry coordinates as T_z, two linear functions of S_1, S_2, S_3 can be formed which, along with T_z, form an orthogonal set of symmetry coordinates coming under A_1. One such choice is as follows:

$$Q_3 = S_1 + S_2 = T_z = z_1 + z_2 + z_3 \tag{103}$$

$$Q_7 = S_1 - (M/2m)\, S_2 = z_1 - (M/2m)(z_2 + z_3) \tag{104}$$

$$Q_8 = S_3 = y_2 - y_3 \tag{105}$$

Out of the three normal coordinates that should be expected from the representation B_2, two have been already written down, namely T_y and R_x. Proceeding as before, the symmetry coordinates are $S_4 = y_1$; $S_5 = (y_2 + y_3)$; $S_6 = (z_2 - z_3)$ and the third normal coordinate, which is unique in this case, is obtained as

$$Q_9 = -(2m/M)\, y_1 \tan\alpha + (z_2 - z_3) + (y_2 + y_3) \tan\alpha \tag{106}$$

The symmetry modes for H_2O are schematically illustrated in Figure 8.

Instead of having to solve a 9 x 9 secular determinant for the frequencies, we have reduced the problem to solving one 2 x 2 and one 1 x 1 (since we know that the frequencies corresponding to translation

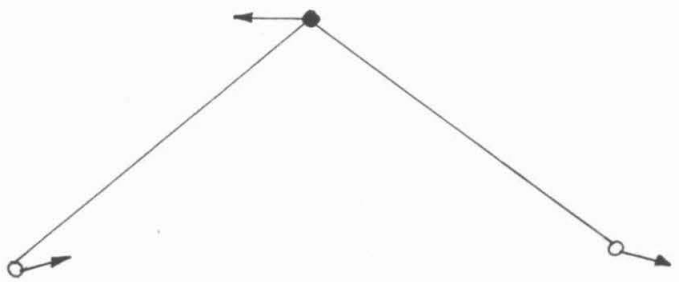

Q_9

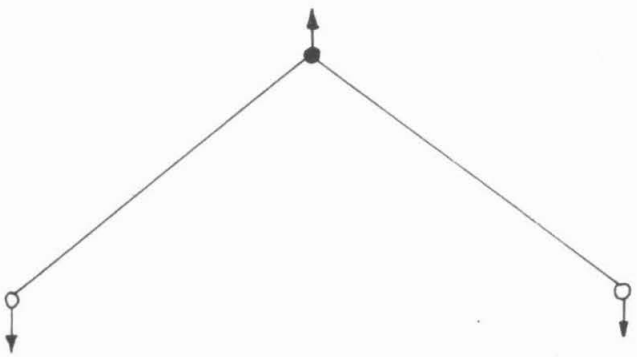

Q_7

Q_8

Figure 8. Normal Modes of Vibration of H_2O.

and rotation of the molecule as a whole will turn out to be zero). By the proper choice of normal coordinates, i.e., those of only one symmetry type rather than some mixture of types, the matrices A and B [c.f. equation (67)] have already been partially diagonalized as shown below.

$$A = \begin{bmatrix} a_{11} & a_{12} & 0 \\ a_{21} & a_{22} & 0 \\ 0 & 0 & a_{33} \end{bmatrix} \qquad B = \begin{bmatrix} b_{11} & b_{12} & 0 \\ b_{21} & b_{22} & 0 \\ 0 & 0 & b_{33} \end{bmatrix}$$

This is due to the fact that the matrix elements vanish which correspond to different symmetry types. For the example chosen, H_2O, it is easier to find the normal modes of vibration by classical methods but the advantage of using group theory for more complicated molecules (e.g. benzene) is apparent.[50-52]

Let us first look at the normal modes having the symmetry type A_1. If Q_7 and Q_8 are assumed to have amplitudes δ for the displacement of nucleus 1 and γ for the displacements of nucleus 2 and nucleus 3, respectively, and these are simultaneously excited, then the variations in the lengths and angles are:

$$\Delta R_{12} = \Delta R_{13} = \delta[(2m+M)/2m] \cos\alpha - \gamma \sin\alpha \tag{107}$$

$$\Delta R_{23} = -2\gamma \tag{108}$$

$$\tfrac{1}{2}\Delta\phi_{213} = \Delta\phi_{123} = \Delta\phi_{132} = \{(\delta/R)[(2m+M)/2m]\sin\alpha + (\gamma/R)\cos\alpha\} \tag{109}$$

where R is the (constant) equilibrium length of $R_{12} = R_{13}$. If it is

assumed that a change in the length of R_{12} or R_{13} gives rise to a Hooke's law restoring force with proportionality constant equal to K_1, then each will contribute a term

$$2V_{12} = K_1 \{\delta[(2m+M)/2m] \cos\alpha - \gamma \sin\alpha\}^2$$

to the potential energy of vibration of the molecule. Similarly, if the force constants K_2, K_3, and K_4 refer to the changes in R_{23}, $R\phi_{213}$, and $R\phi_{123}$ or $R\phi_{132}$, respectively, the total potential energy is

$$2V = \Big(2K_1 \{\delta[(2m+M)/2m] \cos\alpha - \gamma \sin\alpha\}^2 + K_2 [-2\gamma]^2 \\ [2K_4 + 4K_3] \{\delta[(2m+M)/2m] \sin\alpha + \gamma \cos\alpha\}^2\Big) \qquad (110)$$

The total kinetic energy is

$$2T = M\left[\frac{2m+M}{2m}\right] (\dot{\delta})^2 + 2m(\dot{\gamma})^2 . \qquad (111)$$

Hence the matrix elements of A and B are

$$a_{11} = M[(2m+M)/2m]; \quad a_{12} = a_{21} = 0; \quad a_{22} = 2m;$$

$$b_{11} = \{[(2m+M)/2m]^2 [2K_1 \cos^2\alpha + (2K_4 + 4K_3) \sin^2\alpha]\};$$

$$b_{12} = b_{21} = \{[(2m+M)/2m] \sin\alpha \cos\alpha [2K_4 + 4K_3 - 2K_1]\};$$

$$b_{22} = [2K_1 \sin^2\alpha + 4K_2 + (2K_4 + 4K_3) \cos^2\alpha] .$$

The roots of the secular equation are λ_1 and λ_2, where[53-59]

$$\lambda_1 + \lambda_2 = \frac{a_{11}b_{22} + a_{22}b_{11}}{a_{11}a_{22}}.$$

or

$$\lambda_1 + \lambda_2 = \left\{ \frac{K_1}{m} \left[1 + \frac{2m}{M} \cos^2\alpha\right] + \frac{2K_2}{m} + \left[\frac{K_4 + 2K_3}{m}\right] \left[1 + \frac{2m}{M} \sin^2\alpha\right] \right\} \tag{112}$$

and

$$\lambda_1 \lambda_2 = \frac{b_{11}b_{22} - b_{12}^2}{a_{11}a_{22}}$$

or

$$\lambda_1 \lambda_2 = \left[\frac{2m+M}{M}\right] \left\{ \left(\frac{K_1}{m}\right)\left(\frac{2K_2}{m}\right) \cos^2\alpha + \frac{K_1}{M}\left[\frac{K_4 + 2K_3}{m}\right] + \frac{2K_2}{m}\left[\frac{K_4 + 2K_3}{m}\right] \sin^2\alpha \right\}. \tag{113}$$

By a similar procedure for the case of symmetry mode Q_9, with δ the amplitude of vibration of nucleus 1, the variations in lengths and angles are found to be

$$\Delta R_{12} = \Delta R_{13} = (\delta / \sin\alpha)\{ (M/2m) + \sin^2\alpha\} , \tag{114}$$

$$\Delta R_{23} = 0 , \tag{115}$$

$$\Delta\phi_{123} = -\Delta\phi_{132} = (\delta / R) \left(\frac{\cot\alpha}{\sin\alpha}\right) \{ (M/2m) + \sin^2\alpha\} , \tag{116}$$

$$\Delta\phi_{213} = 0 . \tag{117}$$

The kinetic energy is

$$2T = M[1 + (M/2m)(1/\sin^2\alpha)](\dot{\delta})^2 , \tag{118}$$

and the potential energy is

$$2V = \Big(2K_1 \left[\left(\delta / \sin\alpha \right) \left[(M/2m) + \sin^2\alpha \right] \right]^2 + 2K_4 \left[\left(\delta \frac{\cot\alpha}{\sin\alpha} \right) \left\{ (M/2m) + \sin^2\alpha \right\} \right]^2 \Big) \quad . \tag{119}$$

Hence, the eigenfrequency for this case is

$$\lambda_3 = \frac{b_{33}}{a_{33}} = \left[\frac{2K_1}{M} + \frac{2K_4}{M} \cot^2\alpha \right] \left[(M/2m) + \sin^2\alpha \right] \quad . \tag{120}$$

If $K_2 = 0$ and $K_4 = 0$, then the values of λ_1, λ_2 and λ_3 correspond to a valence force system[56] while for $K_3=0$ and $K_4=0$, values of λ_1, λ_2 and λ_3 appropriate to the central force system are obtained. Expressions relating to the frequencies in other special cases, such as a linear symmetrical molecule (e.g., CO_2) or an equilateral triangular structure, etc., with specific types of forces can readily be derived from the above equations by making suitable substitutions. By the application of the selection rules already given, it is possible to determine if combinations or overtones of the normal frequencies of a molecule are active in infrared absorption (or Raman scattering). For example, combinations of the fundamentals Q_7, Q_8 and Q_9 can combine in pairs to give lines which are active both in Raman scattering and infrared absorption. Similarly, first overtones of Q_7, Q_8 and Q_9 are all active in both spectra.

(vi) Linear molecules.[33] – The procedure for obtaining the normal vibrations of a linear molecule is essentially the same as that illustrated for water. There is one minor difference. If the axis of

the molecule is chosen as the z-axis, then a rotation about 0z for the molecule in its equilibrium position will not result in any change of position. As a result, there are only two rotational coordinates.

The symmetry group of a linear molecule is either $D_{\infty h}$ or $C_{\infty v}$ depending upon whether the molecule has a center of inversion symmetry or not. As an example, consider carbon dioxide which has symmetry $D_{\infty h}$.

Application of the rules for the characters [equations (86)-(89)] yields for the total representation (including translation and rotation of the molecules as a whole)

$$\chi(E) = 9$$

$$\chi(i) = -3$$

$$\chi(C_\phi) = 3(1+2\cos\phi)$$

$$\chi(iC_\phi) = \chi(S_{\phi+\pi}) = -2\cos\phi - 1$$

$$\chi(C_2') = -1$$

$$\chi(iC_2') = 3$$

whence from the character table for $D_{\infty h}$ (Table II),

$$\Gamma_{tot} = A_{1g} + 2A_{2u} + E_{1g} + 2E_{1u} \tag{121}$$

The representations of the three translational components are given in the character table:

$$\Gamma_{trans} = A_{2u} + E_{1u}. \tag{122}$$

Here the symmetry species A_{2u} corresponds to z and the doubly degenerate E_{1u} and x and y. The two rotational coordinates belong to

the representation

$$\Gamma_{rot} = E_{1g} \cdot \tag{123}$$

Subtracting equations (122) and (123) from equation (121) we obtain

$$\Gamma_{vib} = A_{1g} + A_{2u} + E_{1u}. \tag{124}$$

There are two non-degenerate modes (A_{1g} and A_{2u}) and a pair of degenerate ones (E_{1u}). Of these A_{1g} is Raman but not infrared active, and the others are infrared but not Raman active. The normal modes are pictured in Fig. 9.

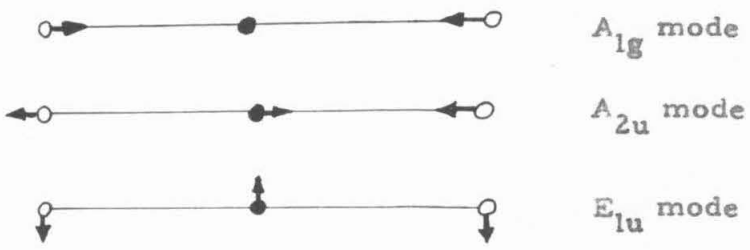

Fig. 9. Vibrational normal modes of the CO_2 molecule. The second E_{1u} mode is the same as the one shown above, but in the plane perpendicular to the page.

(d) Harmonic Oscillator Approximation[26,34,37,60]. Having obtained the classical expressions for the potential and kinetic energy of vibration for a molecule in terms of the normal coordinates [equations (64) and (65)], the nuclear wave equation [equation (56)] may now be written in terms of these coordinates as:

$$\sum_{i=1}^{3r} \frac{\partial^2 \psi}{\partial Q_i^2} + \frac{2}{\hbar^2}\left(E^{(v)} - \frac{1}{2}\sum_{i=1}^{3r} \lambda_i Q_i^2\right)\psi = 0 \qquad (125)$$

Equation (125) is immediately separable into $3r$ one-dimensional harmonic oscillator equations. If we write

$$\psi = \prod_{k=1}^{3r} \psi_k(Q_k) \quad , \qquad (126)$$

each of the ψ_k satisfies the equation

$$\frac{d^2 \psi_k}{dQ_k^2} + \frac{2}{\hbar^2}\left[E_k - \frac{1}{2}\lambda_k Q_k^2\right]\psi_k = 0 \qquad (127)$$

and the total vibrational energy $E^{(v)}$ is the sum of the energies associated with each normal coordinate.

$$E^{(v)} = \sum_{k=1}^{3r} E_k^{(v)} = \sum_{k=1}^{3r} (v_k + \tfrac{1}{2})\, h\nu_k \qquad (128)$$

Here v_k is the vibrational quantum number ($v_k = 0, 1, 2, \ldots$) associated the kth classical normal mode of vibration with frequency ν_k.

In general if the molecule has some degree of symmetry, not all the $3r$ frequencies ν_k will have different numerical values, but there may be several of the normal coordinates for which the frequencies will be necessarily identical. If f_α is the multiplicity of the frequency ν_α, then equation (128) may be written as

$$E^{(v)} = \sum_{\alpha} \left[v_{\alpha} + (1/2) f_{\alpha} \right] h \nu_{\alpha} \qquad (129)$$

where $v_{\alpha} = \sum_{k=1}^{f_{\alpha}} v_{k\alpha}$. If there are multiple frequencies among the ν_{α} , the vibrational energy levels are in general degenerate since the vibrational energy depends only upon the sums $v_{\alpha} = \Sigma\, v_{k\alpha}$. This degeneracy is usually removed when terms of higher order in the normal coordinates are taken into account in the Hamiltonian (anharmonic vibrations).

The numerical values of the frequencies are always obtained from an analysis of the spectrum of the molecule. If all $(3\underline{r}-6)$ [or $(3r-5)$ for a linear molecule] different frequencies are actually observed, no mechanical analysis of the motion of the molecule is necessary. For a symmetrical molecule, even if all the different frequencies ν_{α} are actually observed in the spectrum of the gas, their total number will often be less than $(3\underline{r}-6)$ owing to the essential degeneracies present.

To a surprisingly good first approximation, a potential function composed only of quadratic terms in the displacements of the nuclei form their equilibrium positions may be made to fit the vibration spectrum of most molecules.[61] That the forces between atoms in molecules are not strictly Hooke's law forces is evident from the fact that overtone frequencies of the fundamentals, and sum and difference frequencies occur. The existence and intensity of such frequencies is

indicative of the amount of anharmonicity. The appropriate potential should therefore include cubic and quartic terms. The inclusion of such terms in V for polyatomic molecules enormously complicates the problem of obtaining the harmonic frequencies as the number of nuclei and hence the number of frequencies required is increased. For CO_2 (see Fig. 9) one would expect to find two strong infra-red frequencies and one strong line in the Raman spectrum, the frequency of which should be between those of the two infra-red-active vibrations. The lower of the two infra-red-active frequencies is the degenerate one.

The actual situation in CO_2 is complicated by the occurrence of what is called an accidental degeneracy. The frequency of the bending motion is almost exactly half of that of the frequency of the Raman active vibration so that the two quantum levels, one in which there are two quanta in the bending degrees of freedom and one in which there is one quantum in the stretching degree of freedom, have the same energy. These two levels combine, that is, they form two new levels, one of lower, and one of higher energy, each of which has some of the mechanical properties of both of the original levels.[62] This is called Fermi resonance.

(e) Fermi Resonance[37] If two vibrational levels of the same electronic state which belong to different vibrations have nearly the same energy, i.e., E_a and E_b are degenerate, then first order perturbation theory[26,34] predicts the perturbed energy levels to be given by

$$E = \frac{1}{2}\left[E_a + E_b \pm \sqrt{(E_a - E_b)^2 + 4 \langle a | W | b \rangle^2} \right] \qquad (130)$$

where W is, in general, a small correction to the unperturbed Hamiltonian operator H. For a harmonic oscillator, W is essentially given by the anharmonic (cubic, quartic, ...) terms in the potential energy. From equation (130) Fermi resonance can occur only between vibrational levels of the same symmetry species, i.e., belonging to the same irreducible representation, since H (and hence W) belongs to the totally symmetric representation. This follows from the general theorem of group theory[34] which states: If Φ is a function belonging to some reducible representation of a group, the integral $\int \Phi \, d\tau$ will be zero except when this representation contains the totally symmetric representation. Hence,

$$\langle a | W | b \rangle = \int \psi_{a,\alpha}^{o*} \, W \, \psi_{b,\beta}^{o} \, d\tau \qquad (131)$$

where ψ_a^o and ψ_b^o are the eigenfunctions of the unperturbed operator H, will be zero unless the representation $\Gamma^{(\alpha)} \times \Gamma^{(\beta)}$ contains the totally symmetric representation. The direct product of two different irreducible representations does not contain the totally symmetric representation, while the direct product of an irreducible representation with itself always contains the totally symmetric representation, and only once. Thus the matrix element $\langle a | W | b \rangle$ will be zero unless the vibrational levels a and b belong to the same representation.

As mentioned above, for CO_2 there is a very close resonance between the levels (1, 0, 0) and (0, 2, 0) since $2\nu_2$ happens to be very nearly equal to ν_1. The level (0, 2, 0) consists of two sublevels $(0, 2^0, 0)$ and $(0, 2^2, 0)$ with $\ell_2 = 0$ and 2,* and which have the symmetry species Σ_g^+ and Δ_g. Since the $(1, 0^0, 0)$ level has the species Σ_g^+, only the $(0, 2^0, 0)$ sublevel can perturb it. This is shown in Fig. 10. The separation of the two levels $(1, 0^0, 0)$ (= 1388.3 cm^{-1}) and $(0, 2^0, 0)$ (= 1285.5 cm^{-1}) is much larger than would have been expected on the basis of the value for ν_2 (= 667.3 cm^{-1}). In consequence of the strong perturbation, a strong mixing of the eigenfunctions of the levels $(1, 0^0, 0)$ and $(0, 2^0, 0)$ occurs. Each actual level is a mixture of the two; this is exhibited experimentally by the presence of two strong Raman lines rather than one.

As a consequence of the Fermi resonance between the levels $(1, 0^0, 0)$ and $(0, 2^0, 0)$ of CO_2, there are also perturbations between certain higher levels. This has been discussed in detail by Adel and Dennison [63] [see also references 37 and 64].

A somewhat different perturbation has been found to occur in H_2O by Darling and Dennison.[59] The two vibrations $\nu_1 = 3652$ cm^{-1} and $\nu_3 = 3756$ cm^{-1} have a similar magnitude but cannot perturb each other since they have different species. The two overtones $2\nu_1$ and $2\nu_3$, however, have the same species (A_1) and can perturb each other

---

* The ℓ_i are integral numbers[37] which assume the values $\ell_i = v_i$, $v_i - 2$, $v_i - 4$, ..., 1 or 0; for non-degenerate vibrations $\ell_i = 0$.

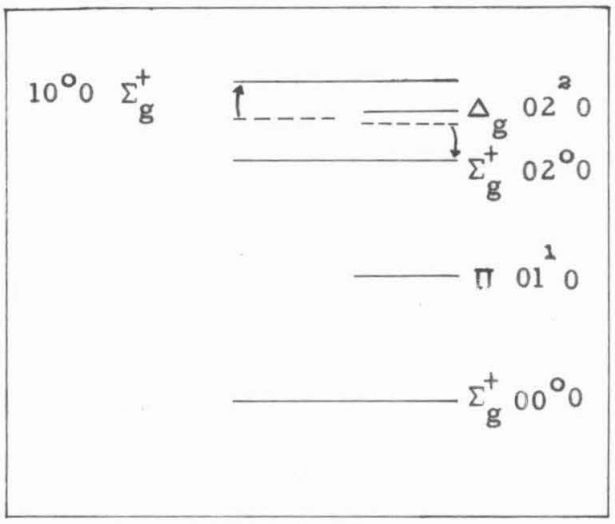

Figure 10. Schematic energy level diagram for carbon dioxide. The broken lines represent the unperturbed levels which go over, on account of Fermi resonance, into the two levels to which the arrows point (from ref. 37).

and, in general, any state (v_1, v_2, v_3) with $v_1 > 2$ is perturbed by a state $(v_1-2,\ v_2,\ v_3+2)$.

(f) Anharmonicity[37] The concept of normal vibrations rests upon the assumption of "small" amplitudes of oscillation, when only quadratic terms in the potential energy need to be considered. However, the amplitudes of the quantized oscillations are not infinitesimal, and higher terms must be included in the potential energy, i.e., the oscillations are anharmonic. If the potential energy of a polyatomic molecule contains terms of degree higher than quadratic, then it is no longer rigorously possible to resolve the vibrational motion into a number of normal vibrations.

The vibrational energy is no longer a sum of independent terms corresponding to the different normal vibrations, but it contains cross-terms containing the vibrational quantum numbers of two or more normal vibrations [see equation (128)]. Thus for a nonlinear triatomic molecule (e.g., H_2O) the energy is given by[57,59,64]

$$E(v_1, v_2, v_3) = hc \{\omega_1(v_1+\tfrac{1}{2}) + \omega_2(v_2+\tfrac{1}{2}) + \omega_3(v_3+\tfrac{1}{2}) + x_{11}(v_1+\tfrac{1}{2})^2 + x_{22}(v_2+\tfrac{1}{2})^2 + x_{33}(v_3+\tfrac{1}{2})^2 + x_{12}(v_1+\tfrac{1}{2})(v_2+\tfrac{1}{2}) + x_{23}(v_2+\tfrac{1}{2})(v_3+\tfrac{1}{2}) + x_{13}(v_1+\tfrac{1}{2})(v_3+\tfrac{1}{2}) + \dots \}. \quad (132)$$

For a diatomic molecule, the energy is given by[1]

$$E^{(v)} = hc \{\omega_e(v+\tfrac{1}{2}) - \omega_e x_e(v+\tfrac{1}{2})^2 + \omega_e y_e(v+\tfrac{1}{2})^3 + \dots \}. \quad (133)$$

A comparison of equations (132) and (133) shows that the constants ω_1, ω_2, and ω_3 for a polyatomic molecule are analogous to ω_e for a diatomic molecule; similarly, the x_{ik} are analogous to $\omega_e x_e$.

In the harmonic oscillator approximation, the total vibrational eigenfunction is simply a product of oscillator eigenfunctions corresponding to the different normal coordinates [compare equation (126)]. If the anharmonicity is taken into account, this is no longer the case, but the symmetry species of vibrational levels remain the same whether the oscillations are harmonic or anharmonic.

(g) Infrared Vibration Spectra and Selection Rules[37,60] According to classical electrodynamics, any motion of an atomic system which leads to a change in the electric dipole moment of that system will cause the emission or absorption of radiation.* During the vibrational motion of a molecule, the charge distribution undergoes a periodic change and so, in general, the dipole moment will also vary periodically. In the harmonic oscillator approximation, any vibrational motion of the molecule can be resolved into a sum of normal vibrations with appropriate amplitudes. The normal frequencies are the only simple periodic motions and hence these are the frequencies emitted or absorbed by the molecule. They lie in the near infrared. Only the

---

* A change of the quadrupole moment or the magnetic dipole moment may also lead to the emission or absorption of radiation. The intensity of this is negligible, however, in the infrared.[1,60,65]

fundamentals, ν_i are active, in this approximation, since the vibrational motion does not contain the overtone frequencies $2\nu_i$, $3\nu_i, \cdots$ or combination frequencies $\nu_i + \nu_k, \cdots$. If anharmonicity is taken into account, the classical vibrational motion will contain combinations and overtones. Hence they may also occur in the infrared spectrum but will be much weaker than the fundamentals since anharmonicities are generally slight.

Apart from this mechanical anharmonicity, an electrical anharmonicity may also cause overtones and combination vibrations to occur. In fact, electrical anharmonicity must occur for homopolar bonds since the dipole moment vanishes both for zero and infinitely large internuclear distance.

In quantum mechanics, the electric dipole moment of a molecule $\vec{\mu}$ is represented by a matrix with matrix elements

$$\mathcal{R}_{nm} = \langle n | \vec{\mu} | m \rangle \tag{134}$$

where $\vec{\mu}$ is a vector. The diagonal matrix elements $\mathcal{R}_{mm} = \mu_o$ represent the permanent dipole moments of the states m. The off-diagonal matrix elements are related to the transitions from the state n to the state m. In fact, the vibrational transition probability is proportional to the square of

$$\mathcal{R}_{u\ell} = \langle u | \vec{\mu} | \ell \rangle \tag{135}$$

where u denotes the upper state and ℓ the lower state. The matrix element given in equation (135) will vanish unless at least one component of μ has the same symmetry species as the product

ψ_u, ψ_ℓ according to the general theorem of group theory stated earlier. This gives a simple method of finding the selection rules for vibrational transitions. In the harmonic oscillator approximation, one finds that $\mathcal{R}_{mn} = 0$ for $m \neq n \pm 1$, and hence for the infrared, we have the selection rule

$$\Delta v_i = \pm 1 \tag{136}$$

for <u>each</u> normal vibration, ν_i.

3. Rotation of Polyatomic Molecules[26,34,37,60]

The investigation of the rotational levels of a polyatomic molecule is complicated by the necessity of considering the rotation simultaneously with the vibrations. As a first approximation, it is customary to regard the nuclei as fixed and to consider the rotation of a molecule as a rigid body.*

Let ξ , η , ζ be a system of coordinates with axes along the principal axes of inertia of a rigid body, and rotating with it.** The quantum mechanical Hamiltonian is obtained from the classical one simply by replacing the components of the classical angular momentum J_ξ , J_η , J_ζ by their corresponding operators:

---

* See, however, references (66-70).

** Every body has three axes which allow the kinetic energy to be expressed in a particularly simple form. These are called the principal axes of inertia. The moment of inertia about a principal axis is defined by $I \equiv \int \rho r^2 d\tau$ where ρ is the density of matter in the volume element $d\tau$, r is the perpendicular distance of $d\tau$ from the axis in question, and the integration is over the volume of the solid [see references 28-30].

$$H = \frac{1}{2}\hbar^2 \left(\frac{J_\xi^2}{I_A} + \frac{J_\eta^2}{I_B} + \frac{J_\zeta^2}{I_C} \right) \tag{137}$$

where I_A, I_B and I_C are the principal moments of inertia of the body.

The commutation rules for the operators J_ξ, J_η, J_ζ of the angular momentum components in a rotating system of coordinates are not obvious, but they can be shown to be the complex conjugate of those for a fixed coordinate system.[34] Hence, all the results which can be deduced from the commutation rules, relating to eigenvalues and matrix elements, still hold with the difference that all expressions must be replaced by their complex conjugates. In particular, the eigenvalues of J_ζ are $K = -J, \cdots, J$.

The energy eigenvalues of a rotating body are easiest to find for the case of a spherical top, where all three principal moments of inertia of the body are equal: $I_A = I_B = I_C = I$. In this case equation (137) becomes

$$H = (\hbar^2/2I)\, J^2 \tag{138}$$

with the energy eigenvalues

$$E^{(r)} = (\hbar^2/2I)\, J\,(J+1) \tag{139}$$

As usual every energy level is (2J+1)-fold degenerate with respect to the (2J+1) orientations of the angular momentum in space, but in addition there is a (2J+1)-fold degeneracy with respect to the directions of the angular momentum relative to the body itself. Therefore the

total degeneracy g_J is*

$$g_J = (2J + 1)^2 . \tag{140}$$

A rigid body in which two of the three principal moments of inertia are equal ($I_A = I_B \neq I_C$) is called a symmetrical top. For this case, equation (137) becomes

$$H = (\hbar^2/2I_A)\, J^2 + (\hbar^2/2)(I_C^{-1} - I_A^{-1})\, J_\zeta^2 \tag{141}$$

and in a state with given J and K, the energy will be

$$E^{(r)} = (\hbar^2/2I_A)\, J(J+1) + (\hbar^2/2)(I_C^{-1} - I_A^{-1})\, K^2 . \tag{142}$$

The (2J+1)-fold degeneracy with respect to values of K which occurred for a symmetrical top is now partially removed, and values of the energy will be the same only for K values differing in sign. Hence the total degree of degeneracy for a symmetric top is

$$g_J = 2\,(2J+1) \qquad \text{for } K \neq 0$$

and

$$g_J = (2J+1) \qquad \text{for } K = 0. \tag{143}$$

An asymmetric top molecule (e.g., H_2O) has all three principal moments of inertia unequal: $I_A \neq I_B \neq I_C$. In this case it is impossible to calculate the energy eigenvalues in a general form. However, their degeneracy with respect to K is completely removed, so

$$g_J = (2J + 1) . \tag{144}$$

---

* This is the total degeneracy, apart from a constant factor corresponding to nuclear spin, only for a molecule that is accidentally a spherical top rather than by virtue of its symmetry. [See reference (37) for a more detailed discussion.]

Fairly elaborate calculations are necessary in order to obtain a representation of the energy levels by quantitative formulae.[5,71-83] It is convenient in practical calculations to use the simpler "nearly symmetric top" representation in the form:

$$E^{(r)} = (\hbar^2/2)(I_B I_C)^{-1/2} J(J+1) + (\hbar^2/2)\left[I_A^{-1} - (I_B I_C)^{-1/2}\right] K^2 \qquad (145)$$

where $I_A < I_B < I_C$. The degeneracies of the energy levels are given by equation (143).

A linear molecule, diatomic or polyatomic, has the energy levels of a "simple rotator" whose moment of inertia about the internuclear axis is identically zero:*

$$E^{(r)} = hc[\, B J(J+1) - D J^2 (J+1)^2 + \cdots] \qquad (146)$$

where B is the rotational constant

$$B = \hbar (4\pi c I_B)^{-1} \qquad (147)$$

and I_B is the moment of inertia about an axis perpendicular to the internuclear axis and going through the centre of mass. The term $DJ^2(J+1)^2$ in equation (146) arises from the non-rigidity of the molecule and is related to B and the vibrational frequency ω by

$$D = 4B^3 \omega^{-2}. \qquad (148)$$

The selection rule for the infrared spectrum

$$\Delta J = \pm 1 \qquad (149)$$

---

* This is true if the angular momentum of the electrons about the internuclear axis is zero, which is the case for the ground states of most linear molecules.

is valid whether the rotator is rigid or not.[37]

For a linear molecule of point group $C_{\infty v}$ (no centre of symmetry) the statistical weight of a rotational level in a totally symmetric electronic state ($^1\Sigma^+$) is

$$g_J = 2J + 1. \tag{150}$$

If the molecule belongs to the point group $D_{\infty h}$, alternate rotational levels have different statistical weights, as in the case of homonuclear diatomic molecules. If the spins of all the nuclei are zero (with the possible exception of the one at the centre of symmetry) the antisymmetric rotational levels are missing entirely, i.e., for Σ_g^+ electronic states the odd rotational levels are absent. This is the case for CO_2.

4. Vibration-Rotation Interaction[37]

In the zeroth approximation, the energy of a vibrating and rotating molecule is simply the sum of the vibrational energy [equations (129) or (132)] and the rotational energy [equations (139), (142), (145) or (146)]. In higher approximation, account must be taken of the fact the moments of inertia change periodically during the vibration.[26, 34, 84-91] As a first approximation, a formulae of the type

$$B_{[v]} = B_e - \sum_i \alpha_i^B (v_i + f_i/2) \tag{151}$$

might be expected to hold, where the α_i^B are small compared to B_e, which is the rotational constant for the equilibrium position, and f_i is the degree of degeneracy of the vibration ν_i. The variation α of the

rotational constant is due to several reasons: (1) the mean value of $(I_B)^{-1}$ is not equal to $(I_{B_e})^{-1}$ although the mean value of r is r_e; (2) due to anharmonicity of the vibrations the mean value of r is greater than r_e; (3) the Coriolis force acts to couple vibration and rotation.

If a linear molecule is in a degenerate vibrational state ($\Pi, \Delta, \ldots$) there is a vibrational angular momentum, $\ell\hbar$ ($\ell = 1, 2, \ldots$) about the internuclear axis and the symmetric-top energy formulae have to be applied. Apart from an additive constant, the rotational energy is given by

$$E_{[v]}^{(r)} = hc \{ B_{[v]} [J(J+1) - \ell^2] - D_{[v]} [J(J+1) - \ell^2]^2 \} . \qquad (152)$$

For the degenerate vibrational levels J must be larger than or at least equal to ℓ :

$$J = \ell , \ell + 1, \ell + 2, \ldots \qquad (153)$$

The total energy of vibration and rotation of a linear molecule is given by

$$[E^{(v)} + E^{(r)}] = hc \Big[\sum_i \omega_i (v_i + f_i/2) + \sum_i \sum_k x_{ik} (v_i + f_i/2)(v_k + f_k/2)$$

$$+ \sum_i g_{ii} \ell_i^2 + B_{[v]} J(J+1) - D_{[v]} J^2 (J+1)^2 \Big] \qquad (154)$$

where the terms in ℓ^2 have been taken into the term $\sum g_{ii} \ell_i^2$.

To a good approximation, selection rules for the pure vibration spectrum and the pure rotation spectrum are not changed by the interaction of vibration and rotation.[37] The selection rules for several types of rotors are summarized in Table IV.

Table IV. Infrared Rotational Selection Rules

Rotor type	Band type	Selection rules
Linear	$\parallel (\mu_z)$	$\Delta J = \pm 1$
	$\perp (\mu_x, \mu_y)$	$\Delta J = 0, \pm 1$
Spherical	(μ_x, μ_y, μ_z)	$\Delta J = 0, \pm 1$
Symmetric	$\parallel (\mu_z)$	$\Delta J = 0, \pm 1$; $\Delta K = 0$ if $K \neq 0$
		$\Delta J = \pm 1$; $\Delta K = 0$ if $K = 0$
	$\perp (\mu_x, \mu_y)$	$\Delta J = 0, \pm 1$; $\Delta K = \pm 1$
Asymmetric *	$\parallel_x (\mu_x)$	$\Delta J = 0, \pm 1$
	$\parallel_y (\mu_y)$	"
	$\parallel_z (\mu_z)$	"

* G. Herzberg, Infrared and Raman Spectra of Polyatomic Molecules, pp. 468-491, Van Nostrand, New York (1945).

II. CRUDE EMISSIVITY CALCULATIONS EMPLOYING STATISTICAL MODELS

A. APPROXIMATE TOTAL EMISSIVITY CALCULATIONS FOR CO_2 USING THE STATISTICAL BAND MODEL[10, 25]

1. Introduction. It has been shown previously[13] that the measured equilibrium emissivities for carbon dioxide at room temperature are consistent with the results derived from approximate computations using a "box approximation" for the vibration-rotation bands and the best available spectroscopic data for the fundamental vibration-rotation bands[6, 13]. More recently, Plass has performed machine calculations[21] for the spectral equilibrium emissivities of carbon dioxide and has obtained numerical data that are in good accord with direct experimental measurements at temperatures up to about 600°K.

The calculated emissivities become relatively too small as the temperature is raised, and significant discrepancies (of about a factor of two to four) have been noted at temperatures between 1200°K and 2000°K[92, 93]. These discrepancies are probably produced by the appearance of new bands which are not observed at 300°K and which make significant contributions to the total emissivity at higher temperatures. To account for the contributions of unobserved bands at elevated temperatures, some sort of intensity multiplication scheme may be used. Since the location of the new bands, the effective bandwidths, line shapes, and line widths[94] are unknown, a statistical treatment is indicated. A proper analysis should lead to the same emissivity estimates as those of Penner[13] and Plass[21] at 300°K, those of Plass[21] at 600°K, and

values in agreement with experimental data on spectral and total emissivities[92, 93, 95, 96] at elevated temperatures. *

A correlation of available emissivity data at temperatures up to 1800°K has been performed utilizing an intensity multiplication procedure at elevated temperatures. The effect of lack of knowledge concerning spectral line shapes and widths has been minimized by using the Mayer-Goody statistical model[6].

2. Emissivity Calculations for Superpositions of Randomly Distributed Weak Bands and of Strong Fundamental Bands. The derivation of formal expressions for the average spectral emissivities has been presented earlier in the discussion of the statistical band model. Since the numerical estimates depend upon the band structure, it will be necessary to examine, in some detail, the structure of individual vibration-rotation bands.

(a) Rotational structure of the vibration-rotation bands. - It is reasonable to use a box model or a just-overlapping line model for the stronger bands at moderate optical depths. For the weak bands, a non-overlapping line model may actually be more appropriate at very small optical depths. However, in view of the experimentally observed lack of sensitivity of total emissivity to pressure, the present analysis will use the simpler just-overlapping line model for all of the bands. In this model, the absorption coefficient for the J^{th} line is represented

---

* While numerous measurements have been made of the infrared spectra of carbon dioxide[97-220], the majority of these experiments were concerned with obtaining data pertaining to the structure of the molecule. Relatively few measurements or calculations have been made of the spectral or total emissivity at elevated temperatures for a wide range of carbon dioxide concentrations.

by the average value across the line: $\bar{P}_J = S_J/\delta'$ where S_J is the integrated intensity of the J^{th} line and δ^* is the line spacing, viz., $\delta^* \simeq 4B_e$ for large J for CO_2 (B_e = rotational constant). *

For a linear triatomic molecule[60],

$$\frac{S(n_1 n_2^{\ell} n_3; J \rightarrow n_1' n_2'^{\ell'} n_3'; J')}{\sum_{\ell'} \alpha(n_1 n_2^{\ell} n_3 \rightarrow n_1' n_2'^{\ell'} n_3')} \simeq \frac{w(n_1 n_2^{\ell} n_3; J \rightarrow n_1' n_2'^{\ell'} n_3'; J')}{w^* Q_R} \frac{g_{J'\ell'}}{g_\ell} \left| \mathcal{R}^{J'\ell'}_{J\ell} \right|^2 \times e^{-E_R(J)/kT},$$

where n_1, n_2, and n_3 are the vibrational quantum numbers corresponding to the three fundamental vibrational frequencies ν_1, ν_2, and ν_3, and ℓ is the quantum number that measures the angular momentum about the symmetry axis of the bending mode. The rotational transition is identified by the symbol $n_1 n_2^{\ell} n_3; J \rightarrow n_1' n_2'^{\ell'} n_3'; J'$; the quantum numbers of the initial state are unprimed, whereas the final state numbers are primed; w^* is the wave number for the $J = 0 \rightarrow J' = 0$ transition; $g_{J'\ell'}$ is the statistical weight of the upper state and is equal to $2J' + 1$ for $\ell' = 0$ or to $2(2J' + 1)$ for $\ell' \neq 0$; g_ℓ is the statistical weight of the lower state and is equal to 1 for $\ell = 0$ or 2 for $\ell \neq 0$; $\left| \mathcal{R}^{J'\ell'}_{J\ell} \right|^2$ represents tabulated [60] rotational amplitudes for the transition $J\ell \rightarrow J'\ell'$; $E_R(J) = hc\, B_e\, J(J+1)$ is the rotational energy for quantum number J ; $Q_R = \sum_J g_J \exp[-E_R(J)/kT]$ is the rotational partition function. Since we shall consider many rotational lines, we may use the following relation, valid only to the harmonic-oscillator rigid-rotator approximation,

---

* The line spacing is $4B_e$ since alternate rotational levels are missing.

$$S(J\rightarrow J-1) + S(J\rightarrow J+1) = (2J+1)\alpha\left(\frac{2hcB_e}{kT}\right)\exp\left[-\frac{hcB_eJ(J+1)}{kT}\right]. \qquad (155)$$

Derivation of equation (155) involves use of the following approximations:

$\omega^* \simeq \omega(n_1 n_2^{\ell} n_3; J\rightarrow n_1' n_2'^{\ell'} n_3'; J')$; $\alpha = \sum_{\ell'}\alpha(n_1 n_2^{\ell} n_3; J\rightarrow n_1' n_2'^{\ell'} n_3'; J')$;

$Q_R \simeq kT/2hcB_e$, and $\omega^* >> 2B_eJ$ for the important contributing lines. At elevated temperatures, a large number of rotational lines contribute to the emission. Hence we may make the further approximation that

$$S(J \rightarrow J-1) \simeq S(J \rightarrow J+1) \simeq S_J$$

and, for large values of J,

$$(2J+1)/2 \approx J \; ; \qquad J(J+1) \simeq J^2 .$$

Thus the average absorption coefficient for the just-overlapping line model becomes

$$\overline{P}_J = \frac{S_J}{4B_e}\left(\frac{\alpha hc}{2kT}\right) J \exp(-hcB_eJ^2/kT) . \qquad (156)$$

If we let $\gamma = hcB_e/kT$ and $\xi = \sqrt{\gamma}\,J$, then

$$\overline{P}_\omega = \frac{\alpha\sqrt{\gamma}}{2B_e}\,\xi \exp(-\xi^2) . \qquad (157)$$

But $\omega = \omega^* \pm 2B_eJ = \omega^* \pm 2B_e\xi/\sqrt{\gamma}$ whence $d\omega = \pm (2B_e/\sqrt{\gamma})d\xi$. Thus the band absorption becomes

$$A(\alpha) = \frac{4B_e}{\sqrt{\gamma}} \int_0^{\infty} \left[1 - \exp\left(-\frac{\alpha X\sqrt{\gamma}}{2B_e}\,\xi e^{-\xi^2}\right)\right] d\xi . \qquad (158)$$

If we let $K = \alpha X\sqrt{\gamma}/2B_e$ and

$$I(K) \equiv \int_0^{\infty} [1 - \exp(-K\,\xi_e^{-\xi^2})]d\xi , \qquad (159)$$

equation (158) reduces to $A = (4B_e/\sqrt{\gamma})I(K)$. Values of the integral $I(K)$ for K up to 120 have been obtained previously through use of a

digital computer[6]. For small K, which corresponds to the transparent gas regime, $I \simeq K/2$ (good to 2 per cent for $K = 0.05$); in the other extreme, $\lim_{K\to\infty} I = \sqrt{\ell n(CK/2)}$, where C is Euler's constant.* In order to find $I(K)$ for intermediate values of K, an extrapolation was performed subject to the restriction that $I(K)$ is of the form

$$(\text{constant}) \times \sqrt{\ell n(\text{constant}' \times K)} \ .$$

This expression was then fitted to the $I(K)$ versus K curve for large values of K and led to the expression $I \simeq 1.11\sqrt{\ell n(1.21K)}$.†

3. Values of Integrated Intensities and Region Widths Assumed for Empirical Correlation of Data.[10, 25] Experimentally determined values of the total emissivity of CO_2 may be correlated satisfactorily if the value of integrated intensity of the bands at all temperatures is set equal to the value at 300°K, i.e.,

$$\alpha(T) = \alpha(300^\circ K) \ . \tag{160}$$

Equation (160) implies that the actual ratio of the intensities $\alpha(T)/\alpha(300^\circ K)$ has been multiplied by the factor[60]

$$\left\{ \frac{N_T(300)}{N_T(T)} \frac{Q_V(T)}{Q_V(300)} \left[\exp \frac{E_V}{k} \left(\frac{1}{T} - \frac{1}{300} \right) \right] \left[\frac{1-\exp(-hc\omega^*/k\,300)}{1-\exp(-hc\omega^*/k\,T)} \right] \right\} \ ,$$

where N_T = total number of molecules per unit volume per unit pressure, Q_V = vibration partition function[6] = $\prod_{i=1}^{3n-5} \frac{\exp(-\frac{1}{2}hc\omega_i/kT)}{[1-\exp(-hc\omega_i/kT)]}$, and E_V = vibrational energy. Thus, the simple assumption of constant integrated intensity represents physically a very complicated temperature-dependent scheme of intensity multiplication. However, emissivity calculations using the correct values of $\alpha(T)$ rather than equation (160)

---

* $C = 0.57721\ldots$.

† Curves showing $I(K)$ as a function of K for $0.02 \leq K \leq 10,000$ are given in reference (24).

for optical depths of 1 and 2 ft-atmos, yield emissivities at 1200°K that are approximately half of the experimental values as may be seen from Fig. 11.

We assume that the region widths may be represented by a relation of the form $\Delta\omega = cX^a(T/300)^b$ where a, b, and c are constants. Variation of region width with optical depth and temperature appears intuitively plausible. In order to obtain reasonably good agreement with the experimentally measured values of Hottel, we use the relation

$$\Delta\omega = \left(\frac{\Delta\omega_o}{0.9}\right) X^{0.45} \left(\frac{T}{300}\right)^{0.25} . \qquad (161)$$

Here $\Delta\omega_o$ was found by taking the difference between the wavenumbers of the band centers of the extreme bands of a region and multiplying by the factor N/(N-1) where N is the number of bands in the region.

4. Outline of Calculations. In the present calculations, the spectrum has been divided into four regions, as indicated in Table V. Within each of these four regions, bands which have an integrated intensity at 300°K in excess of 10 cm^{-2} $atmos^{-1}$ have been treated separately, whereas the contributions of the weaker bands have been added together to form an effective integrated intensity, α_k^*, which was then distributed uniformly throughout the k^{th} region.

The emissivity of the k^{th} region is given by equation (50). We may illustrate the method of calculation by finding the emissivity at 1500°K and 0.1 ft-atmos. For region one, $\alpha_{667} = 240$ and $\alpha_1^* = 9.675$ cm^{-2}-$atmos^{-1}$ whence $K_{667} = 18.13$ and $K_1^* = 0.73$; $I(K_{667}) = 1.951$ and $I(K_1^*) = 0.325$. Thus $\sum_{1st\ region} \epsilon_k = .0080$, $\sum_{1st\ region} A_i = 183.70$, and $\sum_{1st\ region} A_i/\Delta\omega_1 = 0.625$; from Fig. 5 the weighting factor is 0.744 and, therefore, $\epsilon_1 = .0059$. Similar calculations for the

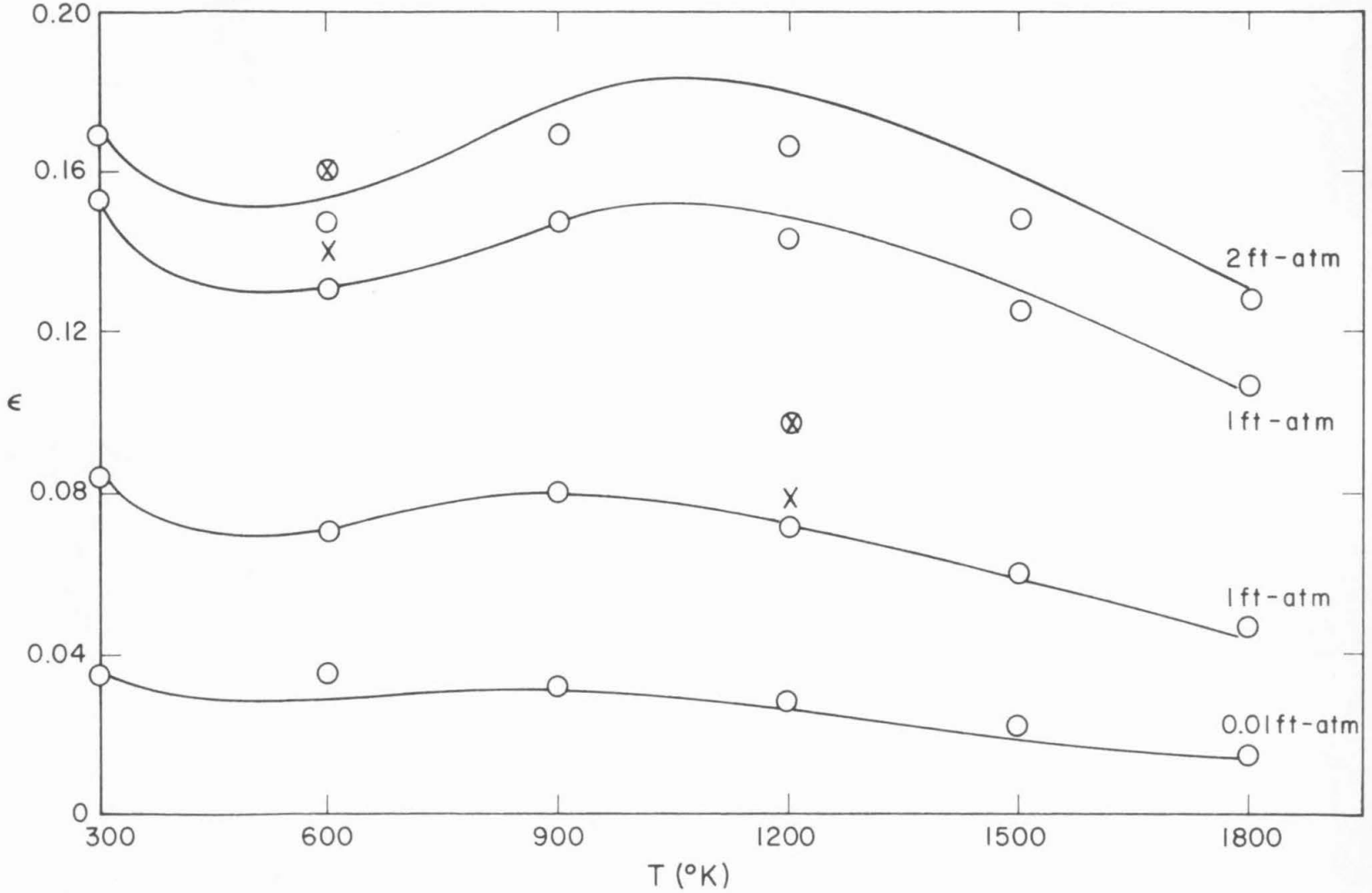

Figure 11. Comparison of calculated CO_2 emissivities (indicated by solid lines) with those measured by Hottel [denoted by O]. Emissivity values calculated theoretically from data obtained at room temperature are also shown for optical depths of 1 (x) and 2 (⊗) ft-atm and temperature of 600°K and 1200°K.

Table V. Integrated Intensities of the Stronger Vibration-Rotation Bands of CO_2 [6]

Band Center (cm^{-1})	Transition	$\alpha(300^{\circ}K)$ (cm^{-2}-atmos^{-1})	Region
648*	$01^10 \rightarrow 00^00$	1.88	
667.3	$01^10 \rightarrow 00^00$	240 **	1
720.5	$10^00 \rightarrow 01^10$	7.5	1
740.8	$11^10 \rightarrow 02^20$	.22	1
960.8	$00^01 \rightarrow 10^00$	.0219	1
1063.6	$00^01 \rightarrow 02^00$	.0532	1
1886	$04^00 \rightarrow 01^10$	.0415 **	
1932.5	$03^10 \rightarrow 00^00$	.0415 **	2
2076.5	$11^10 \rightarrow 00^00$	.12 **	2
2094	$12^20 \rightarrow 01^10$	.020 **	2
2137	$20^0 0 \rightarrow 01^10$	.005 **	2
2284.5*	$00^01 \rightarrow 00^00$	30.0	2
2394.3	$00^01 \rightarrow 00^00$	2676	
3609	$02^01 \rightarrow 00^00$	28.5	3
3716	$10^01 \rightarrow 00^00$	42.3	3
4860.5	$04^01 \rightarrow 00^00$	.272	4
4983.5	$12^01 \rightarrow 00^00$	1.01	4
5109	$20^01 \rightarrow 00^00$	.426	4

* Transitions of $C^{13}O_2^{16}$ ($C^{13}O_2^{16}$ is assumed to represent 1.1 per cent of the total CO_2.)

** These numerical values have been chosen to equal the listed band intensities (see reference 6, pp. 310, 314).

other three regions yield $\epsilon_2 = .0363$, $\epsilon_3 = .0169$, $\epsilon_4 = .0069$. Addition of these partial emissivities gives $\epsilon = .060$. Hottel's measured value[95] is $\epsilon_H = .057$. The results of all of our calculations are summarized in Fig. 11.

The semi-empirical calculations are seen to be quite successful (compare Fig. 11) for correlating emissivity data over a wide range of temperature and optical depths. Our approximate computation procedure is easily applied and the method yields values that differ from the experimentally observed data by less than 10 per cent at all optical depths and temperatures.

Bevans[200] has obtained a correlation using Hottel's total emissivity measurements of carbon dioxide by means of an empirical expression of the form

$$\epsilon = K_1 X + K_2 X^{\frac{1}{2}} + K_3 \log (K_4 X),$$

where K_1, K_2, K_3, and K_4 are functions of temperature. While Bevans has been able to fit the preceding expression to Hottel's data with an accuracy of 3 per cent, his method is unsuitable for extrapolating to the higher temperatures where emissivity measurements have not been made.

The experimental values of total emissivity given by Hottel and his co-workers[145, 146] were chosen in preference to data obtained by Eckert[147, 221] since Hottel covered a larger range of optical depths and temperatures. Hottel has estimated the experimental errors to be about 5 per cent; the discrepancies between Hottel's values and those of Eckert are of the order of 5 per cent[200].

Numerous measurements and calculations have been made of spectral emissivities and of the absorption by individual bands of carbon dioxide. These are summarized in Table VI.

Table VI. Measurements or Calculations of Spectral Emissivities or of the Absorption by Individual Bands of Carbon Dioxide

Spectral Region (cm^{-1})	Total Pressure (atm)*	Optical Depth (cm atm)	Temperature (°K)	Reference**
2150-2400	0.1 - 8.0 CO_2	.05 - 2.5	1200	(220) cell
2272	0.26 - 0.92 CO_2, O_2, N_2, CO, H_2O	0.1 - 1.0	1273	(219) cell
2272	1.0	0.07 - 0.30	1620, 1710	(219) burner
2000 - 2400 3250 - 3800	.0066 - 2.0 CO_2, N_2	.003 - 3.56	1200, 1500	(218) cell
500 - 10,000	.01 - 1.0	.001 - 50	300	(212)
2150 - 2500	1.0	.05 - 500 283	280, 217 2500	(206)
2272	0.26 - 0.92 N_2, He	0.1 - 3.0	1273	(203) cell

* The species used to broaden the spectral lines is indicated; CO_2 indicates self-broadening.

** The experimental apparatus is indicated after the number of the reference; no such indication appears in the case of theoretical calculations.

Spectral Region (cm^{-1})	Total Pressure (atm)	Optical Depth (cm atm)	Temperature (^{o}K)	Reference
500-9500	1, 10, 31	10^{5} - 2.34×10^{7}	300	(217)
2100 - 2400	0.58	0.40 - 0.70	1200-2400	(216) rocket exhaust
2000 - 2400	1.0	.40 - .83	300, 600, 1200, 1800, 2400	(22)
550 - 850	.026 - .98	1 - 863	295	(3) cell
2000 - 2500	.0013 - 1.0	4.7 - 1565		
3400 - 3900	.0013 - 1.0	4.74 - 1730		
4600 - 5400	.046 - 1.0	540 - 8630		
6000 - 7300	.013 - 1.0 N_2	108 - 8630		
2225 - 2405 3520 - 3820	.065 - 1.0 N_2	5 - 100	318	(173) cell
540 - 820	1.0	100	300	(177)
2100 - 2500	0.07 - .92 N_2, CO_2	0.84 - 11.7	298 - 1273	(210) cell
3400 - 3800	.92 N_2	1.67 - 10.0	1273	(204) cell
2200 - 2500 3400 - 3800	0.07 - .92 N_2	0.84 - 11.7	300 - 1273	(93) cell

Spectral Region (cm^{-1})	Total Pressure (atm)	Optical Depth (cm atm)	Temperature (^{o}K)	Reference
2000 - 2400	1.0	0.4 - 0.8	1200 - 2400	(211) rocket exhaust
400 - 9000	0.5 - 10 N_2, CO_2	3.05 - 305	300 - 1400	(208) cell
2174 - 2288	0.26 - 1.05 N_2	0.1 - 0.4	1200 - 2100	(209) shock tube
1800 - 2500	1.0	.01 - 100	300 - 2400	(21)
450 - 9000	0.5 - 10 N_2, CO_2	1.9 - 1290	300 - 1400	(96) cell

B. APPROXIMATE CALCULATIONS OF SPECTRAL EMISSIVITIES IN THE INFRA-RED FOR HCℓ (222)

1. Introduction. In a recent paper (16), Stull and Plass have presented the results of infrared emissivity calculations for HCℓ at elevated temperatures. The data were obtained through the use of machine computations by employing the best available spectroscopic data. Numerical values that are in good accord with their spectral absorption coefficients may be obtained, when the weak line approximation holds, by utilizing the results of a relatively simple analytical treatment to the harmonic oscillator approximation. This method is similar to an analysis first used by Kivel, Mayer, and Bethe (223) in emissivity calculations on the ultraviolet bands of NO. Their method of treatment for electronic band systems has been refined recently by Keck, Camm, Kivel, and Wentink (224) in order to account for the influence of vibrational

structure on emissivities. A derivation of the basic equations given by Keck, et al.[224] has recently been published by Patch, Shackleford, and Penner[225] who show, to the same order of approximation, that the equations of this "smeared out rotational line model" yield results identical with those of the "just-overlapping" line model. Golden[226] has shown that this is also true for pure rotational transitions.

2. Outline of Theoretical Considerations.[225, 227]

(a) Calculation of spectral absorption coefficients and of spectral emissivities for fundamental vibration-rotation bands. - Consider transitions between the ground state with vibrational quantum number v'' and rotational quantum number J'' and the upper state v', J'. Since both vibrational levels belong to the same electronic state of the HCℓ molecule, the respective rotational energies (E_J) may be written in the form

$$E_{J''} = J''(J'' + 1)\, hc\, B_e \qquad (162a)$$

and

$$E_{J'} = J'(J' + 1)\, hc\, B_e \; . \qquad (162b)$$

The selection rules allow $\Delta J = \pm 1$ for a rigid rotator.* Hence the energy of vibration-rotation transition $(v'', J'') \rightarrow (v', J')$ is

$$hc\omega = hc\omega_{v', v''} \pm 2J''\, hc\, B_e \qquad (163)$$

for molecules without Q-branch, where $\omega_{v', v''} \equiv (E_{v'} - E_{v''})/hc$ and we have assumed that $J + 1 \simeq J$ or $J'' \simeq J'$, which is true at sufficiently high temperatures. If the dominant contributions to the absorption are

---

* Observations of the infrared spectrum of HCℓ show no spectral line corresponding to a Q-branch (i.e., corresponding to $\Delta J = 0$ transitions).

made by the higher rotational energy levels, then, using equation (163), equation (162a) may be written as

$$E_{J''} \simeq (J'')^2 hc B_e = \left[\frac{\omega - \omega_{v'v''}}{2 B_e} \right]^2 hc B_e \quad . \tag{164}$$

The spectral absorption coefficient P_ω for the transition $(v'', J'') \rightarrow (v', J')$ is

$$P_{\omega_{v', v''}} \simeq \frac{\pi e^2}{mc^2} \frac{N_{v''}}{p} \frac{df_{v''-v'}}{d\omega} \left[1 - \exp\left(- \frac{hc\omega}{kT} \right) \right] \quad . \tag{165}$$

Equation (165) follows from the definition of the f-number, or oscillator strength for a vibrational transition:

$$\alpha_{v', v''} = \int_{\text{band}} P_{\omega_{v', v''}} d\omega = \frac{\pi e^2}{mc^2} \frac{N_{v''}}{p} f_{v''-v'} \left[1 - \exp\left(- \frac{hc\omega}{kT} \right) \right] \quad . \tag{166}$$

Here e and m denote, respectively, the charge (in esu) and mass (in gm) of an electron, and $N_{v''}/p$ is the total number of molecules in the lower vibrational state v'' per unit volume per unit pressure. The f-number may be thought of as a dimensionless integrated intensity; it is proportional to the square of the matrix element $|R_{\ell u}|^2$ for the transition.

For a non-degenerate rotational line, the integrated intensity is*

$$S_{(v'', J'', M_{J''}), (v', J', M_{J'})} = \left\{ \frac{8\pi^3}{3hc} \frac{N_{v'', J'', M_{J''}}}{p} \omega_{(v'', J'', M_{J''}), (v', J', M_{J'})} \right.$$

$$\left. \times \left[1 - \exp\left(-hc\omega_{(v'', J'', M_{J''}), (v', J', M_{J'})} / kT \right) \right] \left| R_{(v'', J'', M_{J''}), (v', J', M_{J'})} \right|^2 \right\} \tag{167}$$

For degenerate energy levels, equation (167) becomes

* See reference 60, equations (7-82) and (7-84).

$$S_{(v'', J''), (v', J')} = \left\{ \frac{8\pi^3}{3hc} \frac{N_{v'', J''}}{p} \omega_{(v'', J''), (v', J')} \right.$$

$$\times \left[1 - \exp(-hc\omega_{(v'', J''), (v', J')}/kT)\right]$$

$$\left. \times (2J''+1)^{-1} |\mathfrak{M}_{(v'', J''), (v', J')}|^2 [J''\delta_{J''-1, J'} + (J''+1)\delta_{J''+1, J'}] \right\} \qquad (168)$$

where the relations

$$|\mathfrak{R}_{(v'', J''), (v', J')}|^2 = \frac{1}{2J+1} \sum_{M_{J''}, M_{J''}} |\mathfrak{R}_{(v'', J'', M_{J''}), (v', J', M_{J'})}|^2$$

and

$$\sum_{M_{J''}, M_{J'}} |\mathfrak{R}_{(v'', J'', M_{J''}), (v', J', M_{J'})}|^2 = |\mathfrak{M}_{v'', v'}|^2$$

$$\times [J''\delta_{J''-1, J'} + (J''+1)\delta_{J''+1, J'}]$$

for the square of the matrix element of a diatomic molecule represented by the superposition of a (possibly) anharmonic oscillator and a rigid rotator have been used.

In order to obtain the integrated intensity of the band, equation (168) must be summed over all values of J. It may be shown, for example, that*

$$\alpha_{v'', v''+1} = \sum_{J', J''} S_{(v'', J''), (v''+1, J')}$$

$$\simeq \left(\frac{8\pi^3}{3hc}\right)\left(\frac{N_{v''}}{p}\right)\overline{\omega}_{v'', v''+1}\left[1-\exp\left(-\frac{hc\omega_{v'', v''+1}}{kT}\right)\right]|\mathfrak{M}_{v'', v''+1}|^2 \qquad (169)$$

where $\overline{\omega}_{v'', v''+1}$ is the effective wavenumber of the band and $\omega_{v'', v''+1}$

---

* See reference 60, equation (7-90).

corresponds to $\omega_{(v'', 0), (v''+1, 0)}$ in equation (168).

Comparing equations (168) and (169), the variation of $f_{v''\to v'}$ with wavenumber would be expected to be given by

$$\frac{df_{v''\to v'}}{d\omega} \simeq \text{constant} \times \frac{J''}{(2J''+1)} \frac{N_{v'', J''}}{N_{v''}} f_{v''\to v'}$$

$$\simeq \text{constant} \times J'' f_{v''\to v'} \frac{\exp(-E_{J''}/kT)}{Q_R} \qquad (170)$$

where Q_R is the rotational partition function. For the rigid rotator, $Q_R \simeq kT/hcB_e$. The constant in equation (170) is determined by the condition

$$f_{v''\to v'} = 2 \left| \int_{\omega = \frac{E_{v'} - E_{v''}}{hc}}^{\infty} \frac{df_{v''\to v'}}{d\omega} \, d\omega \right| . \qquad (171)$$

Substituting for $E_{J''}$ from equation (164) and carrying out the integration indicated by equation (171), we see the constant in equation (170) must be equal to $\frac{1}{2}B_e$. Hence equation (170) becomes

$$df_{v''\to v'} \simeq \tfrac{1}{2}B_e f_{v''\to v'} \left(\frac{\omega - \omega_{v'v''}}{2B_e}\right)\left(\frac{1}{Q_R}\right) \exp\left\{-\frac{(\omega - \omega_{v'v''})^2 hc}{4B_e kT}\right\} \qquad (172)$$

where we have used equations (163) and (164). Substituting equation (172) into equation (165) for the spectral absorption coefficient and using the relation $N_{v''}/N_T = \exp(-E_{v''}/kT)/Q_V$, where Q_V is the vibrational partition function, we obtain

$$P_{\omega_{v'v''}} \simeq \left\{\frac{\pi e^2}{mc^2} \frac{N_T}{p} \exp \frac{(-E_{v''}/kT)}{Q_V} \left\{ \frac{f_{v''\to v'}}{2B_e} \left(\frac{\omega - \omega_{v'v''}}{2B_e}\right) \right.\right.$$

$$\left.\left. \times \frac{1}{Q_R} \exp\left[-\frac{hc(\omega - \omega_{v'v''})^2}{4B_e kT}\right]\right\}\left[1 - \exp\left(-\frac{hc\omega}{kT}\right)\right]\right) \qquad (173)$$

where N_T is the total number of molecules per unit volume.

At elevated temperatures, many vibrational transitions occur in a given spectral region, and the total spectral absorption coefficient P_ω is obtained by summing over the $P_{\omega_{v'v''}}$ that fall within that region.

Before performing the summation, it is now convenient to write

$$f_{v''\to v'} = f_{0\to(v'-v'')}\chi^2_{v',v''} \tag{174}$$

where $f_{0\to(v'-v'')}$ is the f-number for the transition from the ground vibrational state that falls in the same spectral region as the transition $v''\to v'$, and $\chi_{v',v''}$ is proportional to the vibrational matrix element for the transition.

In the harmonic oscillator approximation, only the transitions $v''\to v''+1$ are allowed (in absorption), and

$$\chi^2_{v',v''} = v''+1 = v' \ . \tag{175}$$

Furthermore,

$$E_{v''} = (v'' + \tfrac{1}{2})\, hc\, \omega_o \ , \tag{176}$$

$$\omega_{v'v''} = \omega_o \ , \tag{177}$$

and equation (173) takes the particularly simple form

$$P^{h.o.}_{\omega_{v',v''}} = \left(\frac{1}{2B_e}\,\frac{\pi e^2}{mc^2}\, f_{0\to 1}\,\frac{N_T}{p\Omega_T}\,(v''+1)\exp\left[-\frac{hc\omega_o}{kT}\,(v''+\tfrac{1}{2})\right] \right.$$
$$\left. \times \left(\frac{\omega-\omega_o}{2B_e}\right)\exp\left[-\frac{hc(\omega-\omega_o)^2}{4B_e kT}\right]\left[1-\exp\left(-\frac{hc\omega}{kT}\right)\right]\right) \tag{178}$$

where $\Omega_T = \Omega_V\Omega_R$ is the total partition function. Summing equation (178) over v'', the absorption coefficient, to the harmonic oscillator

approximation, is*

$$P_{\omega}^{h.o.} = \frac{\pi e^2}{mc^2} \frac{f_{0\to1}}{2B_e} \frac{N_T}{pQ_T} [1-\exp(-hc\omega/kT)]\left(\frac{\omega-\omega_o}{2B_e}\right)$$

$$\exp\left[-\frac{hc(\omega-\omega_o)^2}{4B_e kT}\right] \exp\left[-\frac{hc\omega_o}{2kT}\right]\left[1-\exp\left(-\frac{hc\omega_o}{kT}\right)\right]^{-2} . \qquad (179)$$

The spectral emissivities for gases uniformly distributed throughout a length s at a partial pressure p_i may be computed readily from equation (179). Thus

$$\varepsilon_{\omega}^{h.o.} \simeq 1 - \exp\left(-P_{\omega}^{h.o.} p_i s\right) . \qquad (180)$$

(b) Approximate spectral emissivity calculations for HCℓ. - Calculations performed for the spectral emissivity of the 3.46 micron bands of HCℓ using equation (179) are compared with the numerical calculations of Stull and Plass[16] in Figs. 12 and 13. For purposes of comparison, we used a numerical estimate of $f_{1,0}$ equivalent to that employed by Stull and Plass for the sum of the isotopic species $HC\ell^{35}$ and $HC\ell^{37}$. This value is probably somewhat low.†

(c) Approximate calculations of spectral emissivities in the infrared for HCℓ in the strong line approximation.[231] - At the elevated temperatures for which equation (179) is applicable, a great number of rotational lines belonging to different vibrational transitions (e.g., 1→2, 2→3) will lie within the same spectral region as the fundamental band. Since a great many lines are distributed more or less at

---

* since

$$\sum_{n=0}^{\infty} n e^{-nx} = -\frac{d}{dx} \sum_{n=0}^{\infty} e^{-nx} = -\frac{d}{dx} [1-\exp(-x)]^{-1} = [1-\exp(-x)]^{-2} .$$

† Stull and Plass used the data of Benedict, et al.[228] for the integrated intensity of the HCℓ fundamental. Their value is 130 ± 7 cm^{-2} atm^{-1} compared with the values of 150 cm^{-2} atm^{-1} obtained by Penner and Weber[230] and 150 ± 5 cm^{-2} atm^{-1} obtained by Babrov, et al.[229]

Figure 12. Comparison of spectral emissivities in the weak-line approximation obtained by Stull and Plass (dashed curves), with the spectral emissivities calculated to the harmonic oscillator - rigid rotator approximation (solid curves) for various optical depths at 600°K.

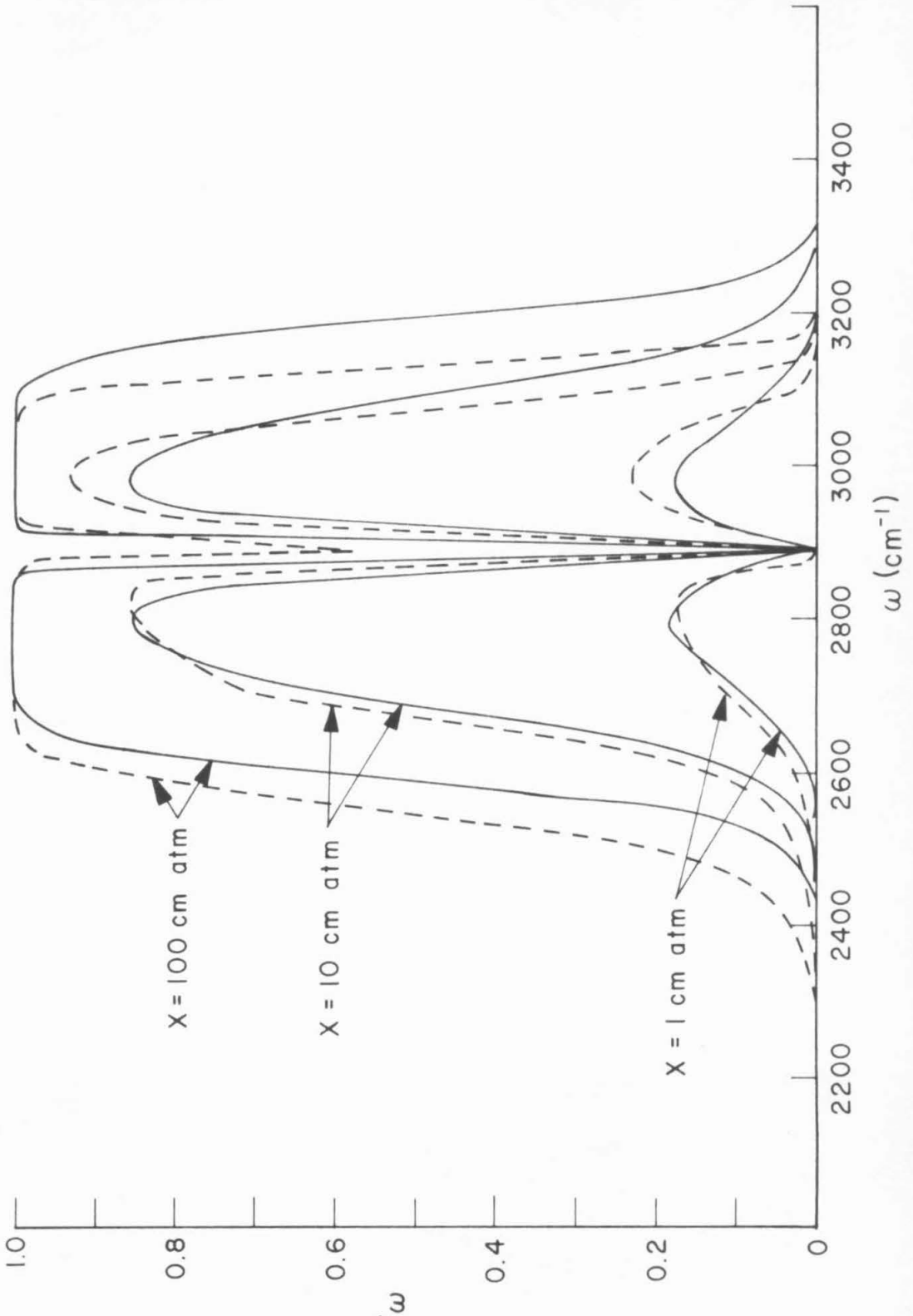
1.0
0.8
0.6
0.4
0.2
0
ϵ_ω
2200
2400
2600
2800
3000
3200
3400
ω (cm^{-1})
X = 100 cm atm
X = 10 cm atm
X = 1 cm atm

Figure 13. Comparison of spectral emissivities in the weak-line approximation obtained by Stull and Plass (dashed curves) with the spectral emissivities calculated to the harmonic oscillator - rigid rotator approximation (solid curves) for various optical depths at 2400°K. The spectral emissivity for an optical depth of 100 cm-atm as calculated by Malkmus and Thomson is also shown (dot-dash curves).

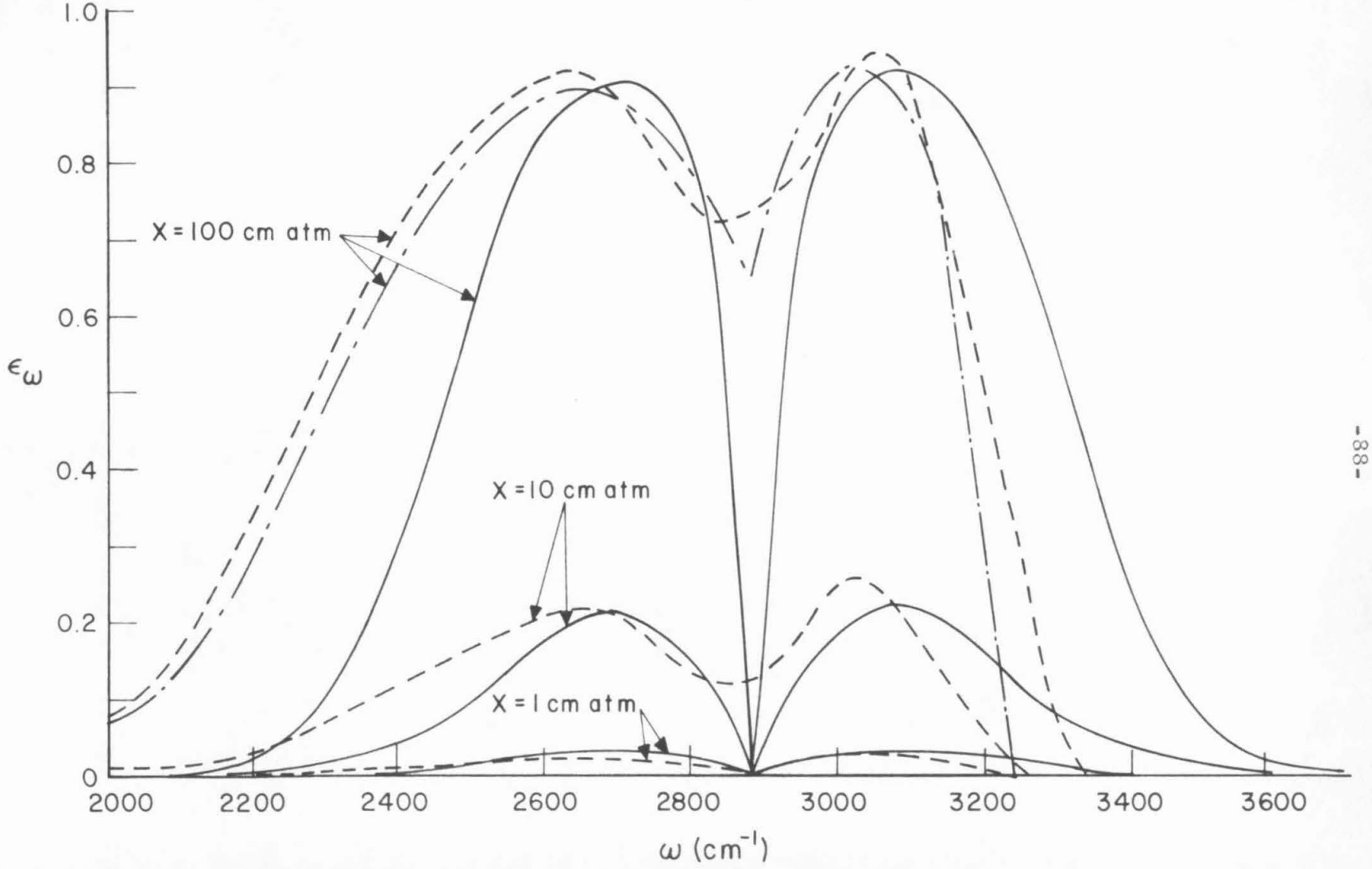
1.0
0.8
0.6
0.4
0.2
0
ϵ_ω
X = 100 cm atm
X = 10 cm atm
X = 1 cm atm
2000
2200
2400
2600
2800
3000
3200
3400
3600
ω (cm^{-1})

random within this region, the statistical line model should be applicable. From equation (28), the spectral emissivity in the weak-line approximation is

$$\epsilon = \left[1 - \exp\left(-\frac{\overline{S}X}{\delta^*}\right)\right] . \qquad (181)$$

However, $\overline{S}/\delta^* = P_\omega$ if the rotational lines are assumed to be just overlapping, and hence equation (181) is identical with equation (180).

In the strong line approximation, the spectral emissivity is given by [see equation (29)]

$$\epsilon = \left[1 - \exp\left(-\frac{2}{\delta^*}\sqrt{\overline{S}bX}\right)\right] . \qquad (182)$$

In order to include the pressure dependence of the collision half width b, equation (182) may be written as*

$$\epsilon = \left[1 - \exp\left(-\sqrt{4b_o(P_\omega/\delta^*)p^2 s}\right)\right] , \qquad (183)$$

where b_o is the half width at a pressure of one atmosphere. The values of b_o used by Stull and Plass are given in Table VII.

Table VII. Average Half Widths of HCℓ Rotational Lines at One Atmosphere Pressure[16]

T ($^\circ$K)	b_o (cm^{-1} atm^{-1})
300	0.184
600	0.109
1200	0.059
1800	0.039
2400	0.031

* Observations[228] at room temperature indicate that the rotational lines of HCℓ have a dispersion contour, except in the wings.

The mean line spacing δ^* will decrease as the temperature is raised and vibrational transitions from excited states (e. g., 2→3) become appreciable. Hence the number of lines contributing in any given spectral range is assumed to be proportional to the number of excited vibrational energy states. In this case

$$\frac{\delta^*(T)}{\delta^*(300^\circ K)} = \left[1 + \sum_{v''} (v''+1)\exp\{-(v''+\tfrac{1}{2})hc\omega/kT\} \right]^{-1} . \qquad (184)$$

The calculation of the spectral emissivity of hydrogen chloride was further refined to include the effects of the following isotopes: $HC\ell^{35}$ (75. 4 per cent); $HC\ell^{37}$ (24. 6 per cent); $DC\ell^{35}$ (0. 012 per cent); $DC\ell^{37}$ (0. 003 per cent). While the abundance of $DC\ell$ is relatively small in natural hydrogen chloride, it can have a significant effect on the spectral emissivity in the strong-line approximation. This is due to the fact that, for a diatomic molecule, the rotational and vibrational constants, B_e and ω_e, are inversely proportional to the reduced mass of the molecule and the square root of the reduced mass, respectively. The molecular constants for $HC\ell$ are given in Table VIII.

Table VIII. Molecular Constants for $HC\ell$ (16)

	ω_e (cm^{-1})	B_e (cm^{-1})
$HC\ell^{35}$	2989. 74	10. 5909
$HC\ell^{37}$	2987. 47	10. 5748
$DC\ell^{35}$	2144. 77	5. 449
$DC\ell^{37}$	2141. 82	5. 432

In order to make a quantitative comparison with the results obtained by Stull and Plass[16] by numerical calculations, their estimates for the integrated intensities of the bands will be used. These are given in Table IX.

Table IX. Estimates[16] for the Total Band Integrated Intensity $\alpha_{v''-v'}$

Molecular Species	Temperature (^{o}K)	Integrated Intensity (cm^{-2} atm^{-1})
$HC\ell^{35}$	300	$\alpha_{01} = 98.0$
$HC\ell^{37}$	300	$\alpha_{01} = 32.0$
$HC\ell^{35}$	600	$\alpha_{12} = 0.111$
$HC\ell^{37}$	600	$\alpha_{12} = 0.036$
$HC\ell^{35}$	1200	$\alpha_{23} = 0.078$
$HC\ell^{37}$	1200	$\alpha_{23} = 0.025$
$DC\ell^{35}$	300	$\alpha_{01} = 7.9 \times 10^{-3}$
$DC\ell^{37}$	300	$\alpha_{01} = 2.6 \times 10^{-3}$

A band head is formed in the R branch of each vibration - rotation band at approximately 3187 cm^{-1} for $HC\ell$ and at 2218 cm^{-1} for $DC\ell$. Emission in the wave number interval beyond the band head is produced by intense rotational lines near the band center and was calculated from the relation:[232]

$$P(\omega) = \sum_{j=0}^{\infty} \left[P_{j \to j-1}(\omega) + P_{j \to j+1}(\omega) \right] . \qquad (185)$$

Spectral emissivities computed by the use of equation (183) are compared with the data of Stull and Plass[16] in Figs. 14 and 15. At

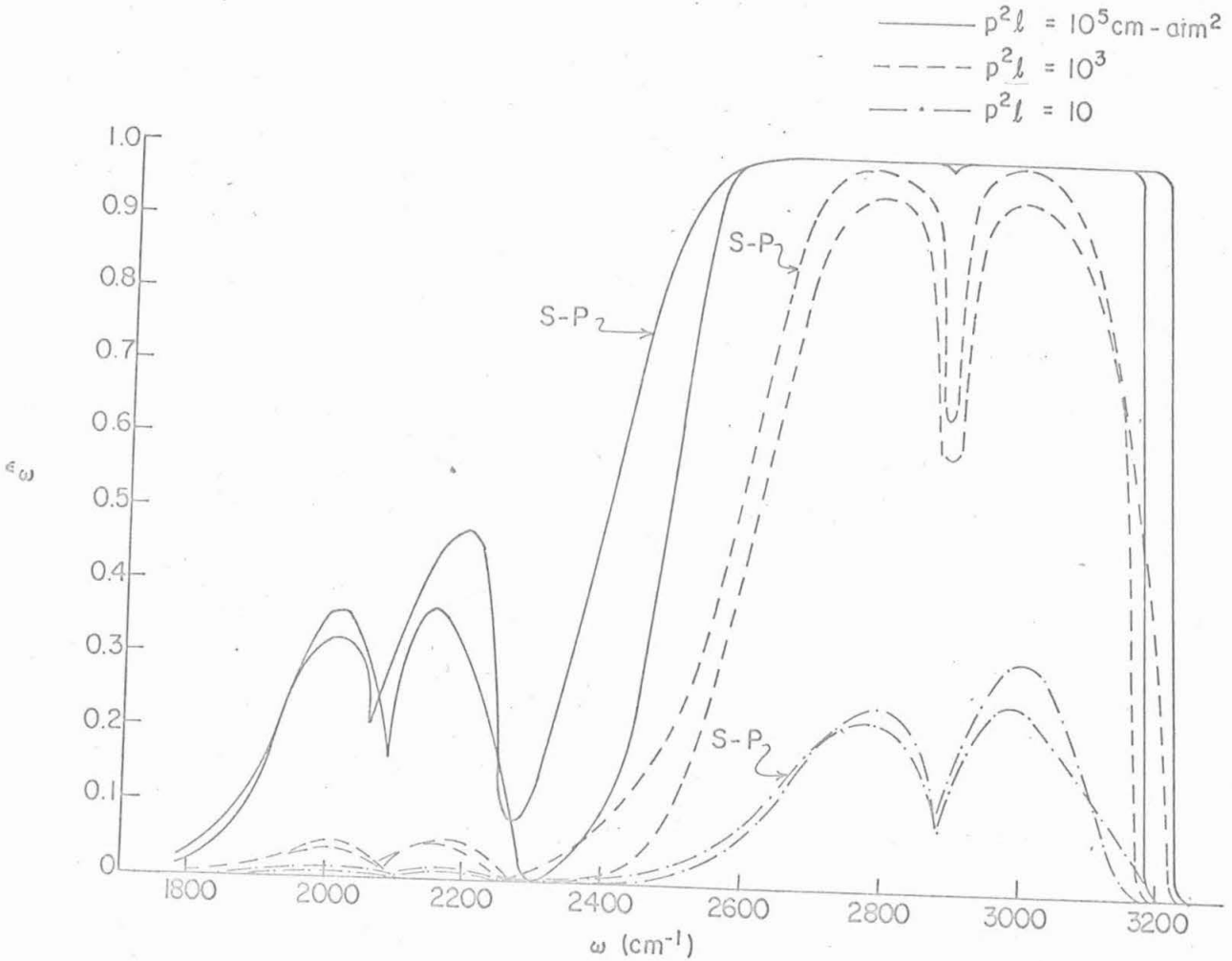

FIG.14. SPECTRAL EMISSIVITIES OF HCℓ AT 600°K, CALCULATED TO THE HARMONIC OSCILATOR-RIGID ROTATOR APPROXIMATION, COMPARED WITH THE RESULTS OBTAINED BY STULL AND PLASS. THE CURVES COMPUTED BY STULL AND PLASS ARE IDENTIFIED BY THE NOTATION S-P.

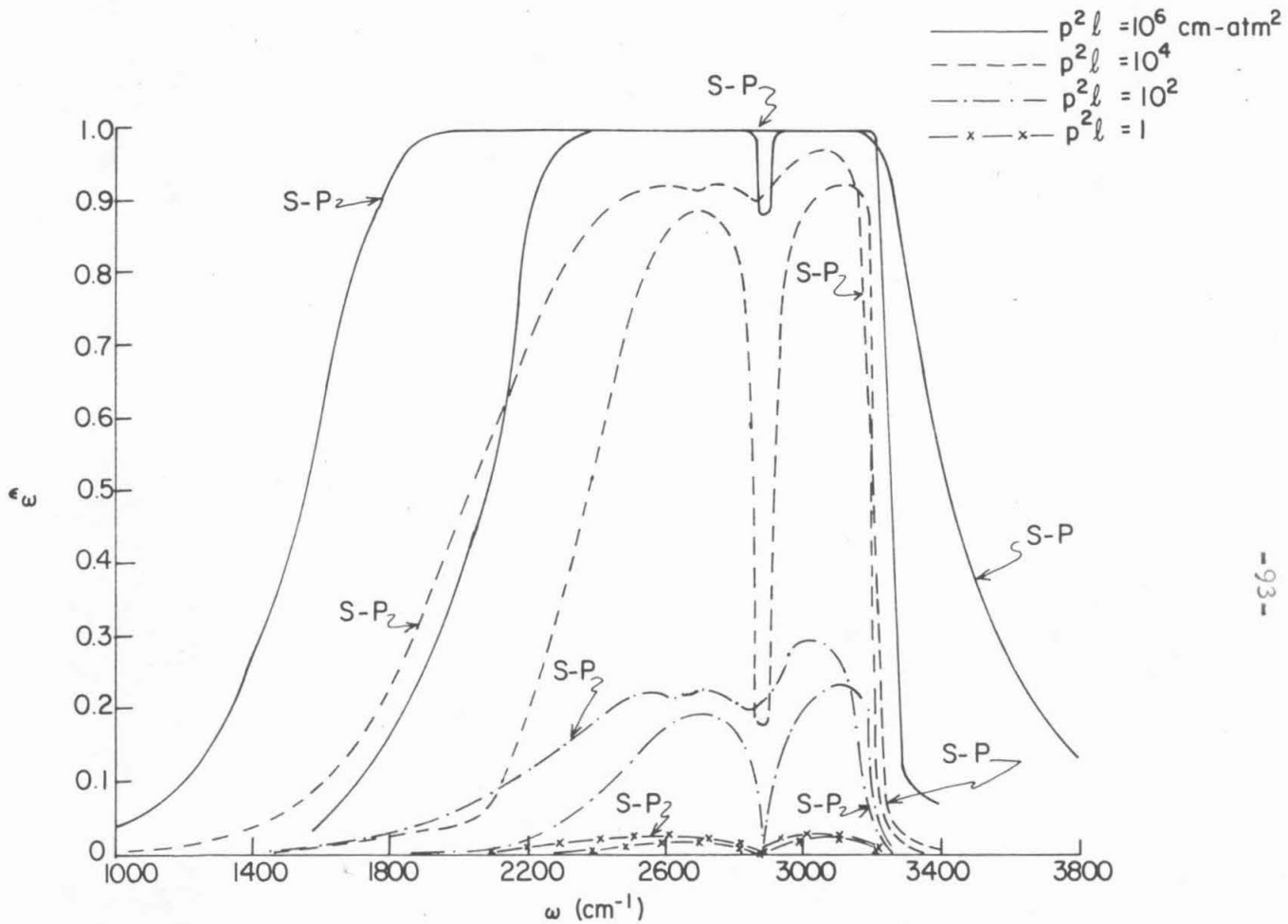

FIG. 15a. SPECTRAL EMISSIVITIES OF HCl AT 2400°K, CALCULATED TO THE HARMONIC OSCILLATOR-RIGID ROTATOR APPROXIMATION, COMPARED WITH THE RESULTS OBTAINED BY STULL AND PLASS. THE CURVES COMPUTED BY STULL AND PLASS ARE IDENTIFIED BY THE NOTATION S-P.

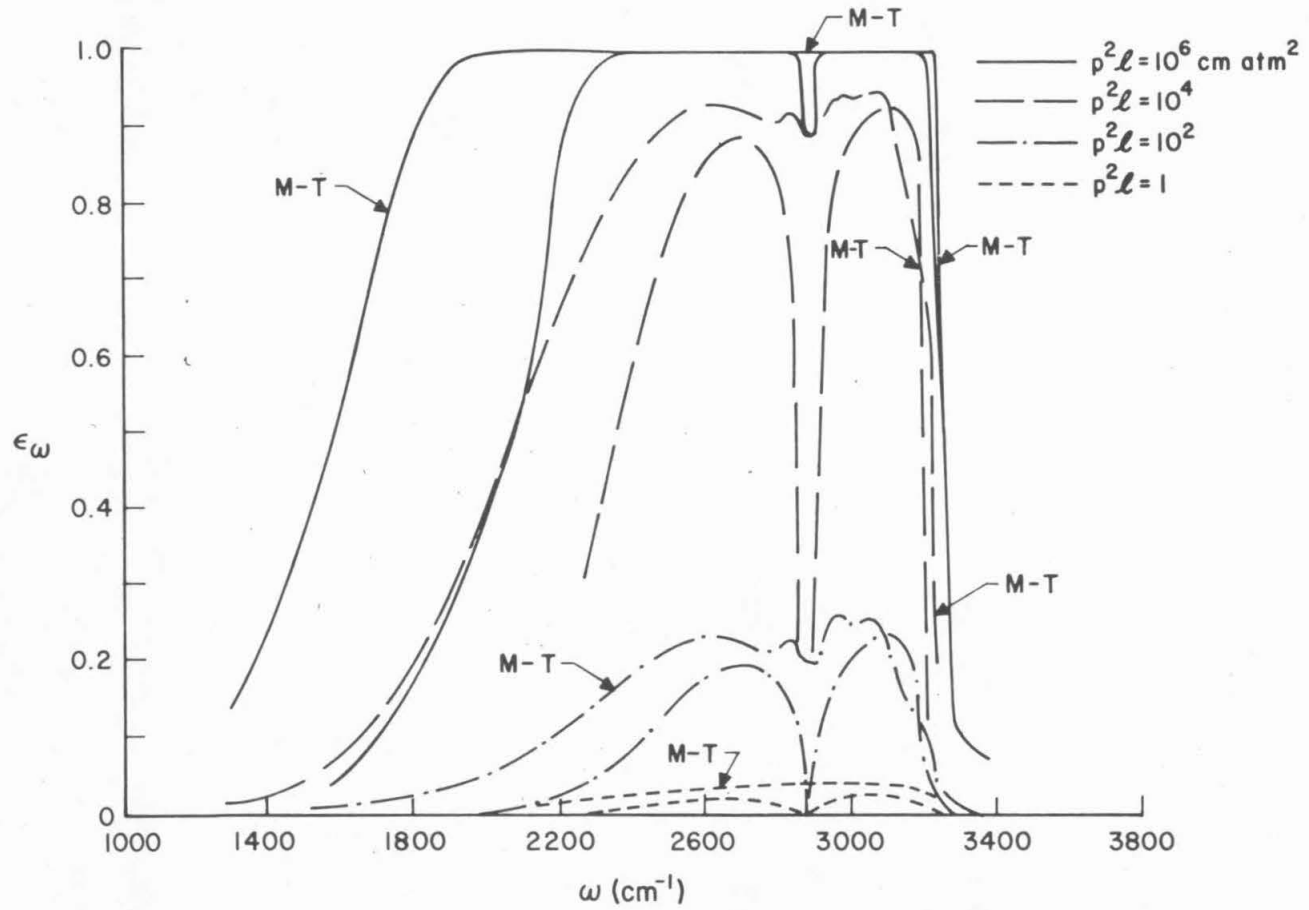

FIG. 15b. SPECTRAL EMISSIVITIES OF HCl AT 2400°K, CALCULATED TO THE HARMONIC OSCILLATOR APPROXIMATION, COMPARED WITH THE RESULTS OBTAINED BY MALKMUS AND THOMSON IN THE ANHARMONIC OSCILLATOR APPROXIMATION. THE CURVES COMPUTED BY MALKMUS AND THOMSON ARE IDENTIFIED BY THE NOTATION M-T.

600°K, the agreement is satisfactory but there is quite a large discrepancy, particularly in the P branch, at 2400°K. For the strong-line approximation, it appears that vibration-rotation interaction and anharmonicity terms should be included in the calculation of spectral absorption coefficients at elevated temperatures. However, for the weak-line approximation, the harmonic-oscillator rigid-rotator model gives reasonable agreement with the more elaborate numerical calculations as may be seen from Figs. 12 and 13.

Malkmus and Thomson[23] have recently made an improved calculation of spectral emissivity employing a digital computer. They chose for their model of a diatomic molecule an anharmonic oscillator with the first approximation to the vibration-rotation interaction; i.e., the energy levels are given by the expression

$$E(v, J) = \{\omega_e(v+\tfrac{1}{2}) - \omega_e x_e(v+\tfrac{1}{2})^2 + \omega_e y_e(v+\tfrac{1}{2})^3 + \omega_e z_e(v+\tfrac{1}{2})^4 + B_e J(J+1) - \alpha_e(v+\tfrac{1}{2})J(J+1)\}\,hc \ .$$

Malkmus and Thomson used the random Elsasser model[233], assumed a Lorentz line shape, but neglected line wing emission beyond the band head. For HCl, Malkmus and Thomson used the data of Benedict, et al.[228] for the fundamental band strength and line widths in order to make a direct comparison with the more elaborate calculations of Stull and Plass[16]. Their results are also shown in Figs. 12 to 15, and may be seen to be in better agreement with Stull and Plass than our calculations, as would be expected. However, our crude approximation yields a fair estimate of the spectral emissivity of a diatomic molecule without involving such lengthy computations as to necessitate the use of a digital computer.

III. APPROXIMATE SPECTRAL EMISSIVITY CALCULATIONS FOR WATER VAPOR AT ELEVATED TEMPERATURES

A. INTRODUCTION.

At the high temperatures encountered in combustion, an appreciable fraction of the energy transfer is by radiation. For this reason, a knowledge of the emissivities of the combustion products (e.g., HCℓ, CO_2, H_2O) is important. Until recently,[234] the basic spectroscopic constants for H_2O, required for an a priori emissivity calculation, were unknown. Since it is possible[6, 11] to correlate the total emissivity data of water vapor in terms of a just-overlapping line model and effective bandwidths, in the temperature range between 333 and 1666°K, by assuming "reasonable" values for the integrated intensities of the various bands, the choice of a just-overlapping line model for a spectral emissivity calculation appears justified. This model assumes that the individual spectral lines are sufficiently pressure-broadened that they overlap one another, smearing out the structure of the band. For water vapor, overlapping begins to occur at room temperature for a pressure of about 3 atm[235] and as the temperature is increased, the pressure required for overlapping should decrease.

An a priori spectral emissivity calculation at 1111°K has been performed for self-broadening water vapor at a pressure of 2 atm using a "harmonic oscillator"-symmetric top approximation.

B. THE INFRARED SPECTRUM OF WATER VAPOR.

The infrared spectrum of water vapor consists of spectral lines corresponding to transitions between various vibration-rotation energy levels. The wave number ω of a given line is given by the difference

in the sum of the vibrational and rotational energies of the final and initial states. The intensity of an individual line is given by the relation*

$$S_{\ell u} = \frac{8\pi^3 \omega_{\ell u}}{3hcp} \frac{N}{Q_T} |R_{\ell u}|^2 \exp(-E_\ell/kT)\left[1 - \exp\left(-\frac{hc\omega_{\ell u}}{kT}\right)\right] \qquad (186)$$

where N is the number of molecules per unit volume, Q_T is the total partition function, and $R_{\ell u}$ is the electric dipole matrix element corresponding to the transition; E_ℓ is the sum of the vibrational and rotational energies of the lower (initial) state.

Herzberg[37] gives the selection rules governing allowed transitions for a triatomic, asymmetric molecule such as H_2O. For the molecular species HHO, two types of rotational transitions are allowed: $\Delta K = 0$ and $\Delta K = \pm 1$ corresponding, respectively, to the parallel and perpendicular transitions of a symmetric top molecule. Here K is the component of angular momentum about the symmetry axis. It is related to the total angular momentum J in that J takes on the values K, K+1, ... Vibration-rotation bands of water vapor, composed of one of these types of transitions, will approach as limits the parallel or perpendicular bands of the equivalent symmetric top molecule, and they will have the same general structure. The structure of the band depends greatly on the relative values of the moments of inertia; only for the limiting cases of the symmetrical top or the linear molecule can any simple regularities be expected. For an asymmetric molecule such as HDO, a given vibrational band will contain rotational transitions of both types[236]. The corresponding band for HDO of the equivalent

---

* Reference (60), equation (7-125).

symmetric top molecule will be a hybrid band containing both $\Delta K = 0$ and $\Delta K = \pm 1$ transitions (for HHO molecules, this is not the case). The usual rotation selection rule $\Delta J = 0, \pm 1$ applies to all transitions.

Unfortunately, the matrix element $R_{\ell u}$ for an asymmetric top cannot be expressed explicitly in terms of "good" quantum numbers[36, 60, 81]. For a symmetric top, equation (186) becomes*

$$S_J \simeq \frac{8\pi^3 \omega}{3hc} \frac{N}{P} \frac{|R_{0v'}|^2}{Q_R} \sum_{K=0}^{J} g_{JK} \exp\left[-\frac{E(J,K)}{kT}\right] . \qquad (187)$$

Here we are assuming that practically all of the molecules are in the ground vibrational level. Furthermore, at infrared frequencies, the induced emission term $[1 - \exp(-hc\omega/kT)]$ has been approximated by unity.

For a symmetric top, the rotational energy is given by†

$$E(J,K) = hc\left[J(J+1)\sqrt{BC} + K^2(A - \sqrt{BC}\,)\right] \qquad (188)$$

where $A > B > C$. For the ground state of the water molecule, the following numerical values apply: $A = 27.8\ cm^{-1}$, $B = 14.5\ cm^{-1}$, and $C = 9.28\ cm^{-1}$. The degeneracies of the energy levels are

$$g_{JK} = 2(2J+1) \text{ for } K \neq 0, \text{ and } g_{JK} = 2J+1 \text{ for } K = 0. \qquad (189)$$

From equations (188) and (189) we find that

$$\sum_{K=0}^{J} g_{JK} \exp\left[-\frac{E(J,K)}{kT}\right] \simeq \left\{4J \exp\left[-\frac{hc\sqrt{BC}}{kT} J^2\right]\right\} \int_0^J \exp\left[-\frac{hc(A - \sqrt{BC})}{kT} K^2\right] dK \qquad (190)$$

---

* See Reference (6), equation (11-137).

† See Reference (60), equation (7-123).

where the summation has been replaced by an integral. Letting

$$\gamma = hc\sqrt{BC}/kT \ , \tag{191}$$

$$\beta = (A\sqrt{BC} - 1) \ , \tag{192}$$

and

$$u' = 2\gamma J \ , \tag{193}$$

equation (190) may be written as

$$\sum_{K=0}^{J} g_{JK} \exp\left[-\frac{E(J,K)}{kT}\right] \simeq \left\{\frac{2u'}{\gamma}\exp\left[-\frac{u'^2}{4\gamma}\right] \int_0^{u'/2\gamma} \exp[-\gamma\beta K^2]dK\right\} \tag{194}$$

or,*

$$\sum_{K=0}^{J} g_{JK} \exp\left[-\frac{E(J,K)}{kT}\right] \simeq \left\{u'\left(\frac{\pi}{\gamma^3\beta}\right)^{\frac{1}{2}}\exp[-\frac{u'^2}{4\gamma}]\mathrm{erf}[\frac{u'}{2}(\frac{\beta}{\gamma})^{\frac{1}{2}}]\right\}. \tag{195}$$

Substituting the rotational partition function[237]

$$Q_R \simeq \left(\frac{kT}{hc}\right)^{3/2}\left(\frac{\pi}{ABC}\right)^{1/2} = \left(\frac{\pi}{\gamma^3(1+\beta)}\right)^{1/2} \tag{196}$$

and equation (195) in equation (187), the integrated intensity of the J^{th} line in the vibration-rotation spectrum is given by

$$S_J \simeq \frac{1}{2}\alpha u'\left(\frac{1+\beta}{\beta}\right)^{1/2}\exp\left[-\frac{u'^2}{4\gamma}\right]\mathrm{erf}\left[\frac{u'}{2}\left(\frac{\beta}{\gamma}\right)^{1/2}\right] \tag{197}$$

where

$$\alpha \equiv \alpha_{0v'} = \frac{8\pi^3\omega_o}{3hc}\frac{N}{p}|R_{0v'}|^2 \ . \tag{198}$$

Equation (198) refers to each branch of a vibration-rotation band consisting of P and R branches, and the wavenumber ω has been approximated by the wavenumber ω_o at the band center. For a

---

* Here we use the definition

$$\mathrm{erf}(x) \equiv \frac{2}{\sqrt{\pi}}\int_0^x \exp[-\xi^2]d\xi \ .$$

vibration-rotation band,

$$u' = 2\gamma J = \frac{hc|\omega-\omega_o|}{kT} . \qquad (193a)$$

For the pure rotation spectrum, equation (187) becomes

$$S_J = \alpha' u'^2 \left(\frac{1+\beta}{\beta}\right)^{\frac{1}{2}} \exp\left[-\frac{u'^2}{4\gamma}\right] \operatorname{erf}\left[\frac{u'}{2}\left(\frac{\beta}{\gamma}\right)^{\frac{1}{2}}\right] \qquad (197a)$$

where

$$\alpha' \equiv \frac{8\pi^3}{3h^2c^2}\mu_o^2 . \qquad (198a)$$

The vibrational matrix element for this case is $|R_{oo}|^2 = \mu_o^2$ where μ_o is the permanent dipole moment of the molecule. For water vapor, $\mu_o \simeq 1.87$ Debyes. Equation (197a) has a different functional form than equation (197) because, for the pure rotation spectrum,

$$u' = 2\gamma J = \frac{hc\omega}{kT} . \qquad (193b)$$

In the just-overlapping line model, the average spectral absorption coefficient $\overline{P}_\omega$ is equal to S_J divided by the mean line spacing. For vibration-rotation bands, we have

$$\overline{P}_\omega = \frac{\alpha}{4\sqrt{BC}} u' \left(\frac{1+\beta}{\beta}\right)^{\frac{1}{2}} \exp\left[-\frac{u'^2}{4\gamma}\right] \operatorname{erf}\left[\frac{u'}{2}\left(\frac{\beta}{\gamma}\right)^{\frac{1}{2}}\right] , \qquad (199)$$

since the mean line spacing is $\delta^* = 2\sqrt{BC}$.

Measurements of the absolute intensities of all the individual bands in the water vapor spectrum have not been made. Goldstein[234] has recently obtained absolute intensity values for the bands in the 1.38 μ, 1.87 μ, and 2.7 μ regions using a high-pressure absorption cell. These spectral regions each contain several bands which overlap one another.

From a table similar* to Table X, the relative intensity of each of the various bands lying within a particular spectral region can be found. This allows the f-number for each transition to be determined, and hence, in principle, the intensity at any temperature. Benedict and Plyler[238] have given f-numbers for the transitions with the greatest intensity in the 1.1, 1.38, 1.87, 2.7, and 6.3 μ regions. These values differ somewhat from Goldstein's and were obtained from flame measurements which are inherently less accurate than cell measurements. Goldstein's values were used in this calculation for the 1.38, 1.87, and 2.7 μ spectral regions, and Benedict and Plyler's for the 1.1 μ and 6.3 μ regions.† Table XI presents a comparison of the integrated intensity measurements for various transitions. The 3.2 μ (020→000) band was assumed to have an integrated intensity of 2 cm^{-2} atm^{-1}.

C. APPROXIMATE SPECTRAL EMISSIVITY CALCULATIONS FOR WATER VAPOR.

From these integrated intensities and equations (1), (17), (197), and (197a), an a priori calculation of the spectral emissivity of water vapor was performed at a temperature of 1111°K, and an optical depth of 77.42 cm atm. Table X gives the relative intensities of all of the bands for the species HHO^{16} for T = 300°K. The relative intensities for the

---

* Table X gives the relative intensities of the bands falling within a given spectral region which are the principal contributors to the total intensity at 300°K. At higher temperatures, other transitions must be taken into account, and their relative intensities calculated at that temperature.

† The bands with wavelengths shorter than 1μ (e.g., 0.94 μ, 0.90μ) contribute very little to the total emissivity for the temperature range of interest here, and will be neglected in this calculation.

Table X. Vibrational Transitions of HHO^{16} at $T = 300^{o}K$ (236)

Group	Transition	ω^{*} (cm^{-1})	Relative Intensity	ΔK
6.3 μ	000→010	1595.0	1.00	± 1
	010→020	1556.4	9.6×10^{-4}	± 1
	010→100	2056.7	1.9×10^{-5}	± 1
	010→001	2160.6	9.6×10^{-5}	0
3.2 μ	000→020	3151.4	1.00	± 1
	010→030	3073.4	4.8×10^{-4}	± 1
2.7 μ	000→001	3755.8	1.00	0
	000→100	3651.7	.10	± 1
	010→011	3737.0	4.8×10^{-4}	0
	010→110	3630.0	4.8×10^{-5}	± 1
1.87 μ	000→011	5332.0	1.00	0
	000→110	5225	2.0×10^{-2}	± 1
	000→030	4668.4	6.7×10^{-3}	± 1
	010→021	5279.0	4.8×10^{-4}	0
	010→120	5166.0	9.6×10^{-6}	± 1
	010→040	4551.0	3.2×10^{-6}	± 1
	010→101	5656.6	4.8×10^{-4}	0
	010→200	5593.1	3.8×10^{-5}	± 1
	010→002	5847.2	5.8×10^{-5}	± 1
1.38 μ	000→101	7251.6	1.00	0
	000→021	6874	1.0×10^{-1}	0
	000→120	6761	1.3×10^{-2}	± 1

Group	Transition	ν^*	Relative Intensity	ΔK
	000→040	6146	4.3×10^{-3}	± 1
	000→200	7188.1	2.5×10^{-1}	± 1
	000→002	7442.2	2.5×10^{-1}	± 1
	010→111	7212.0	4.8×10^{-4}	0
	010→031	6769	4.8×10^{-5}	0
	010→130	6663	6.2×10^{-6}	± 1
	010→050	5990	2.1×10^{-6}	± 1
	010→210	7148.1	1.2×10^{-4}	± 1
	010→012	7402.6	1.2×10^{-4}	± 1
1.1 μ	000→111	8807.05	1.00	0
	000→031	8364.0	3.3×10^{-1}	0
	000→130	8258	6.0×10^{-2}	± 1
	000→050	7585	2.0×10^{-2}	± 1
	000→210	8743.1	8.0×10^{-2}	± 1
	000→012	8997.55	1.2×10^{-1}	± 1
	010→121	8727.12	4.8×10^{-4}	0
	010→041	8227.2	1.6×10^{-4}	0
	010→140	8121	2.9×10^{-5}	± 1
	010→060	7390	9.6×10^{-6}	± 1
	010→220	7050	3.8×10^{-5}	± 1
	010→022	7304	5.8×10^{-5}	± 1
	010→300	8994	3.2×10^{-6}	± 1
	010→003	9437	3.2×10^{-6}	0
	010→201	9018	6.4×10^{-6}	0
	010→102	9266	9.6×10^{-6}	± 1

Table X (continued)

* The wave numbers of the band centers were computed from equation (132) using the following vibrational constants of Darling and Dennison[59] (all in cm^{-1}):

$\omega_1 = 3825.32$, $\omega_2 = 1653.91$, $\omega_3 = 3935.59$,

$x_{11} = -43.89$, $x_{22} = -19.5$, $x_{33} = -46.37$,

$x_{12} = -20.02$, $x_{13} = -155.06$, $x_{23} = -19.81$,

$|\gamma| = 74.46$, where γ is the perturbation constant appearing in the matrix element:

$$\langle v_1, v_2, v_3 | W | v_1-2, v_2, v_3+2 \rangle = \frac{\gamma}{2}\sqrt{v_1(v_1-1)(v_3+1)(v_3+2)}$$

for H_2O. The constants of Darling and Dennison were obtained by fitting equation (132) to experimental data[239-241]. Slightly different constants have been given by Nielsen[242] and are based upon subsequent measurements[86]. For H_2O, the two vibrations $\nu_1 = 3652\ cm^{-1}$ and $\nu_3 = 3756\ cm^{-1}$ have a similar magnitude but can not perturb each other since they belong to different symmetry species. The two overtones $2\nu_1$ and $2\nu_3$, however, have the same species (A_1) and can perturb each other. In general, there is Fermi resonance between any state (v_1, v_2, v_3) with $v_1 > 2$ and the state (v_1-2, v_2, v_3+2). The perturbed energy levels are given by equation (130).

other isotopic species are obtained by multiplying the values in Table X by the relative abundances.+

At room temperatures, the absorption is due primarily to vibrational transitions from the ground state. As the temperature is raised, a number of higher vibrational states are excited with appreciable populations. Transitions with $\Delta v_2 = 2$ will lie in the 3.2 u region.

+ Water vapor contains the following isotopes: HHO^{16} (99.8 per cent), HHO^{18} (0.2 per cent), HHO^{17} (0.04 per cent), HDO (0.03 per cent).

Table XI. Integrated Intensities of Water Vapor Transitions

Spectral Region	ν_o (cm^{-1})	Transition	Integrated Intensity (cm^{-2} atm^{-1})		
			Benedict and Plyler[238]	Goldstein[234]	Jaffe and Benedict[243]
6.3 μ	1595	010→000	300		
2.7 μ	3755	001→000	100	180	192 ± 28
1.87 μ	5331	011→000	30	23.2	
1.38 μ	7250	101→000	20	8.7	
1.1 μ	8807	111→000	0.6		

It is apparent that many hundreds of vibrational transitions must be taken into account at temperatures of the order of 1200°K. An accurate calculation, including all transitions contributing significantly to the total absorption in any spectral region, would obviously require the use of a digital computer. Hence we shall make the approximation, valid only for diatomic molecules, that

$$\sum_{v_1', v_2', v_3} \alpha(v_1, v_2, v_3 \rightarrow v_1+\Delta v_1, v_2+\Delta v_2, v_3+\Delta v_3) \simeq \bar{\alpha}(0, 0, 0 \rightarrow \Delta v_1, \Delta v_2, \Delta v_3)$$

and furthermore, that the temperature variation of the integrated intensity is given by $\bar{\alpha}(T) = \left(\frac{300^\circ K}{T}\right)\bar{\alpha}(300^\circ K)$.

It should be noted that the intensity distribution within a group of vibrational transitions actually shifts to lower frequencies as the temperature is increased and transitions from higher vibrational initial states become important.* This shift obviously cannot be accounted for in our approximate calculation and, therefore, the computed spectral

* This shift follows from the fact that the vibrational constants x_{ij} appearing in equation (132) are negative.

absorption coefficients can be expected to differ noticeably from measured values as the temperature is increased.

Within a given group of transitions, the relative intensities appearing in Table X for transitions from the ground state have been used. The absolute intensities used in the calculations are shown in Table XI only for the strongest transitions. The intensities of the other transitions in the spectral regions were obtained from the tabulated relative intensities.

The values thus obtained were compared with Nelson's[244] observed values.* Nelson's measurements were made on self-broadened water vapor at temperatures from 555°K to 1111°K and total pressures of 1 and 2 atm. Table XII lists the spectral emissivity measurements on H_2O that have been made to date. Agreement between the calculated and measured values is expected to be poorest at the lowest pressure, since the rotational lines are insufficiently pressure-broadened. This expectation is verified by the data in Fig. 22 where a comparison is made for the 6.3 μ band at a total pressure of 1 atm. Nelson's measurements were made with low spectral resolution and necessarily include all of the weaker bands which occur in the same frequency interval with the most intense transitions. Figures 16 through 21 show the calculated spectral emissivities for the various spectral regions and Nelson's measured values. The spectral

* Of the many experimental measurements made of the water vapor spectra in the infrared[245-307], the majority have been concerned with the structure of the molecule. Most of the available data for the spectral absorption were obtained in connection with atmospheric transmission studies at low temperatures and low partial pressures of water vapor where the bands are not pressure-broadened.

Table XII. Measurements of Spectral Emissivities or of the Absorption by Individual Bands of Water Vapor

Spectral Region (cm^{-1})	Total Pressure (atm) and gas used for pressure broadening	Optical Depth (cm atm)	Temperature (^{o}K)	Reference and Method of Measurement
3929 3497	0.066-0.92 N_2	0.5-3.14	1273	(219) cell
2900-4300	.063-1.0 H_2O	.002-.032	900, 1200, 1500	(218) cell
2900-6000	0.58	0.40-0.80	1200-2400	(216) rocket exhaust
1100-2200	.0033-.98	12-1850		
2800-4400	.0028-.99	3-3000		
4900-6100	.0039-.97	15-4800	295	(3) cell
6500-8000	.0068-.97	32-660		
8000-9500	.013-.97 N_2	32-2300		
3100-4200	.92 N_2	1.67-4.18	1275	(204) cell
2900-4200	.13-.92 N_2	1.67-7.3	500-1273	(93) cell
2900-6200	1	1.5-2.7	1600-2400	(211) rocket exhaust

Table XII (continued)

400-10,000	1, 2 H_2O	38.7, 77.4	555-1111	(208) cell
400-10,000	1, 2 H_2O	38.7, 77.4	555-1111	(244) cell

agreement is fair in the majority of the spectral regions. Due to the low spectral resolution of Nelson's measurements, better spectral agreement is not to be expected. The band absorption

$$A_{band} = \int_{band} [1 - \exp(-P_\omega X)] d\omega = \int \epsilon_\omega d\omega \qquad (200)$$

is independent of the spectral slit width[2], and our calculated values of the band absorption are in good agreement with observed values.

The total emissivity of water vapor was obtained from the relation

$$\epsilon = \frac{1}{\sigma T^4} \int R_\omega^\circ \epsilon_\omega \, d\omega \qquad (201)$$

where R_ω° is the blackbody spectral radiancy. The calculated total emissivity was $\epsilon = 0.382$. Hottel[95] gives a value of $\epsilon = 0.340$ for $X = 3.54$ ft. atm. at $1111^\circ K$ with a total pressure of 1 atm and a zero partial pressure of water vapor. Hottel presents curves of a correction factor to be applied to the emissivity for other values of partial pressure and total pressure. He warns against extrapolating these curves beyond partial pressure of water vapor greater than 1 atm, where the correction factor is equal to 1.3 . This leads to a (corrected) emissivity value of $\epsilon = 0.442$. Due to the uncertainty in Hottel's correction

factor, it is felt that the agreement of this calculation is quite good.

Table XIII gives a comparison of the calculated and observed values of absorption in the various spectral regions. Goldstein[317] has recently made further integrated intensity measurements. Using his new values, $\alpha_{000\rightarrow101} = 7.3$ and $\alpha_{000\rightarrow011} = 20$, the spectral emissivity of the 1.38 μ and 1.87 μ regions was recalculated, and the results are shown in Figures 17 and 18. The new values of the absorption for these regions are given in parentheses in Table XIII, page 116.

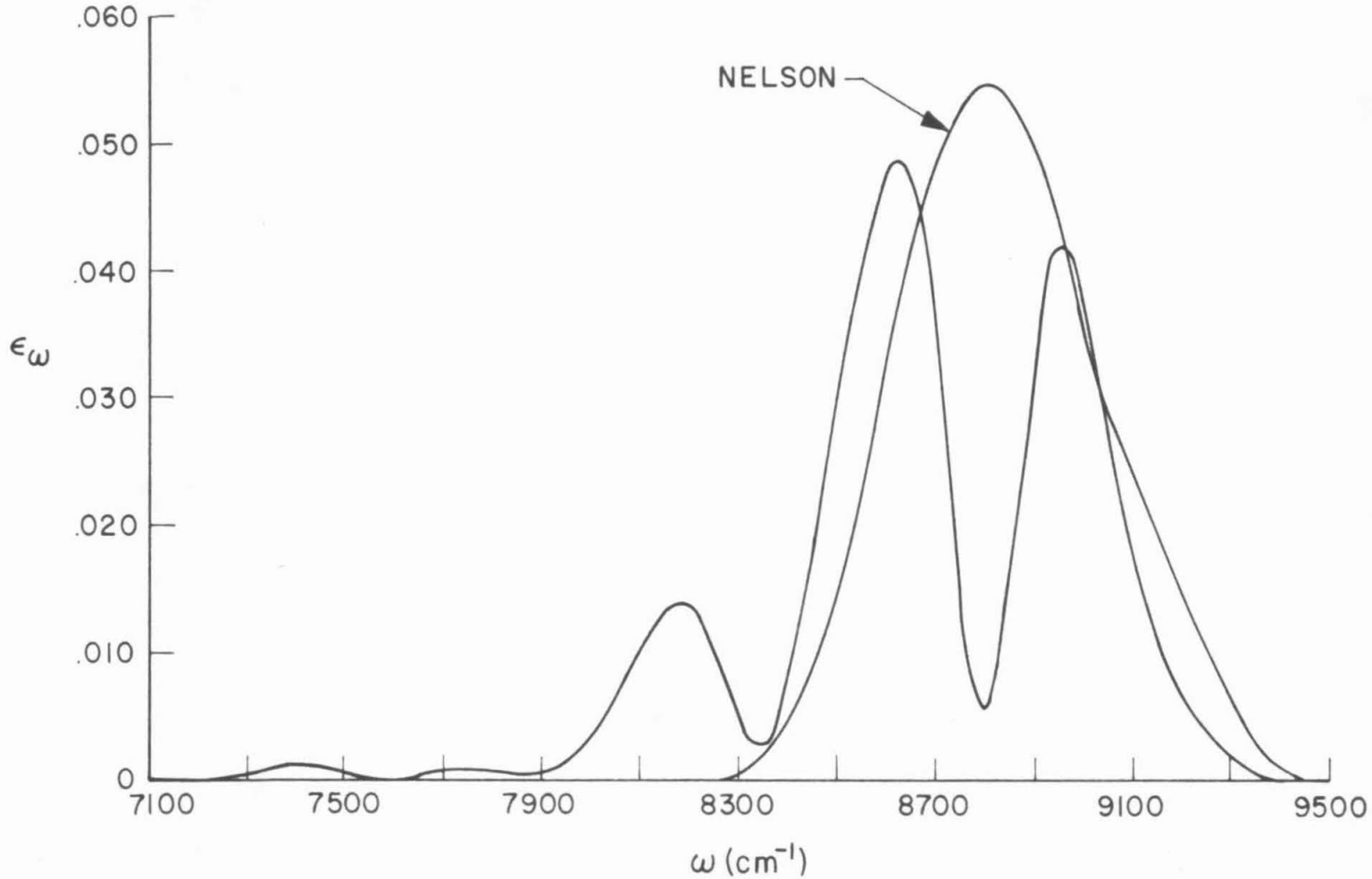

Figure 16. Spectral emissivity of the 1.1 u bands of H_2O at 1111°K for a pathlength of 1.27 ft. and a pressure of 2 atm.

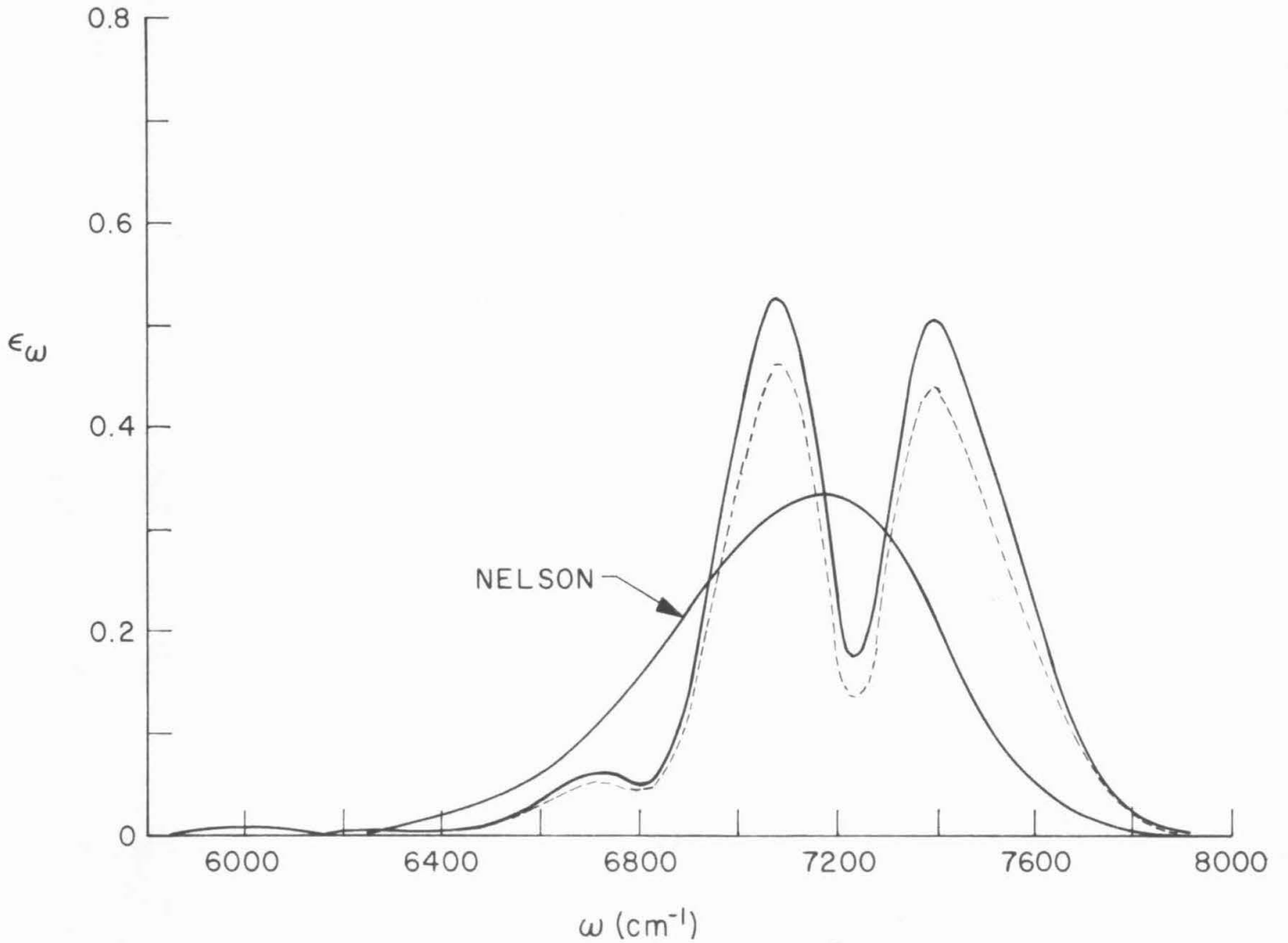

Figure 17. Spectral emissivity of the 1.38 μ bands of H_2O at 1111°K for a pathlength of 1.27 ft. and a pressure of 2 atm. The dashed lines were calculated using Goldstein's revised estimate for the integrated intensity of the 1.38 μ bands.

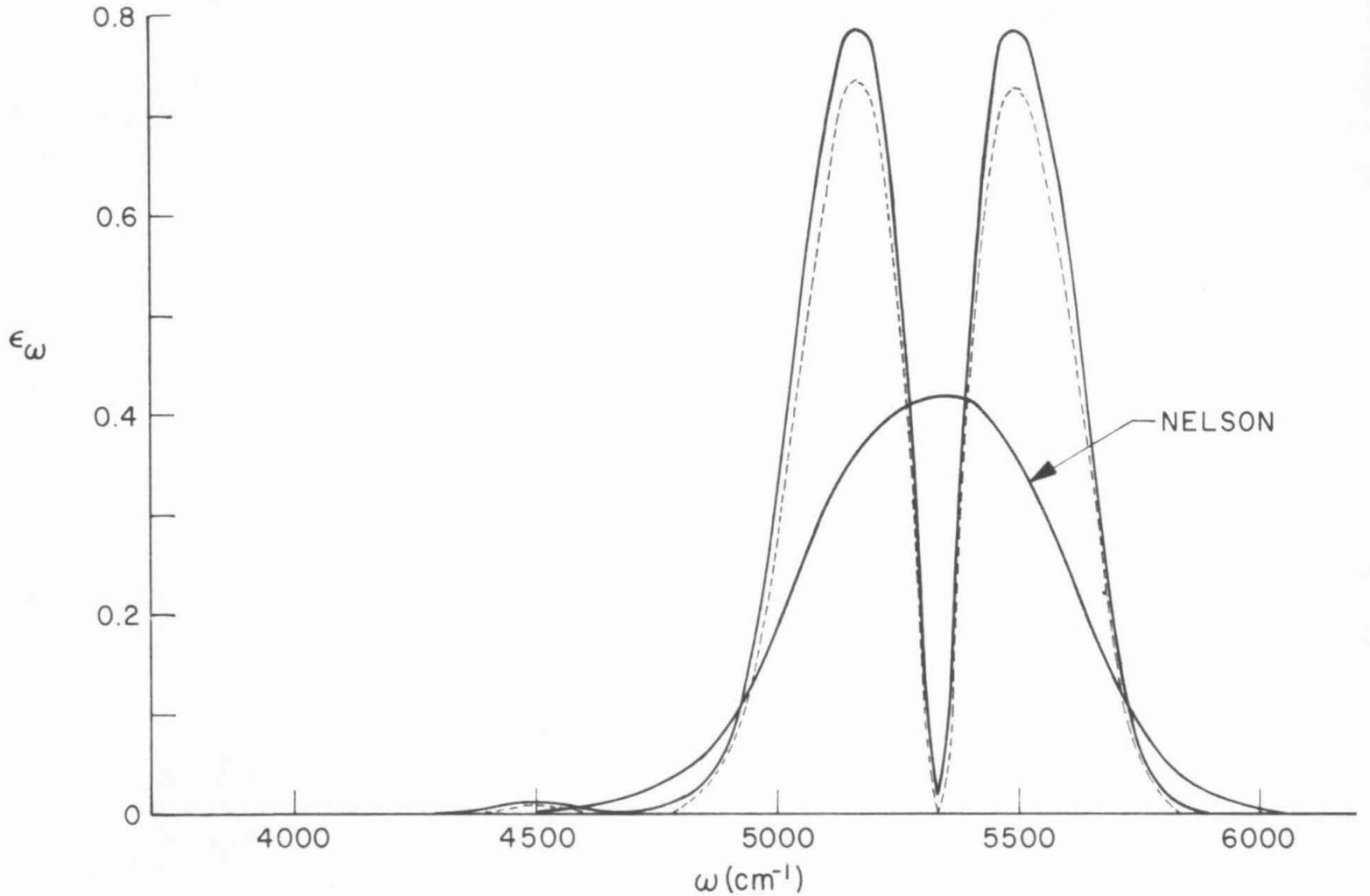

Figure 18. Spectral emissivity of the 1.87 μ bands of H_2O at 1111°K for a pathlength of 1.27 ft. and a pressure of 2 atm. The dashed lines were calculated using Goldstein's revised estimate for the integrated intensity of the 1.87 μ bands.

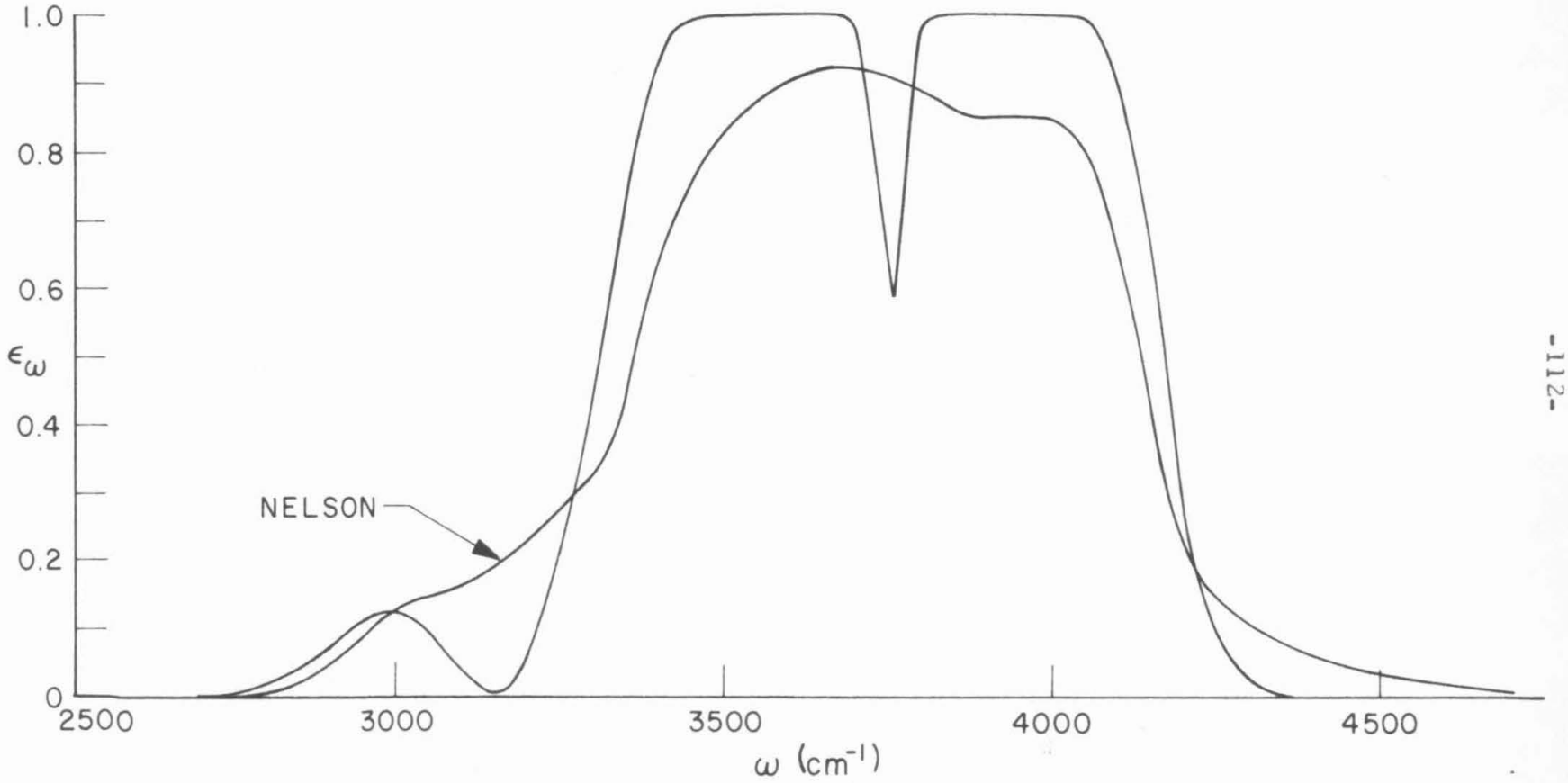

Figure 19. Spectral emissivity of the 2.7 and 3.2 μ bands of H_2O at 1111°K for a pathlength of 1.27 ft. and pressure of 2 atm.

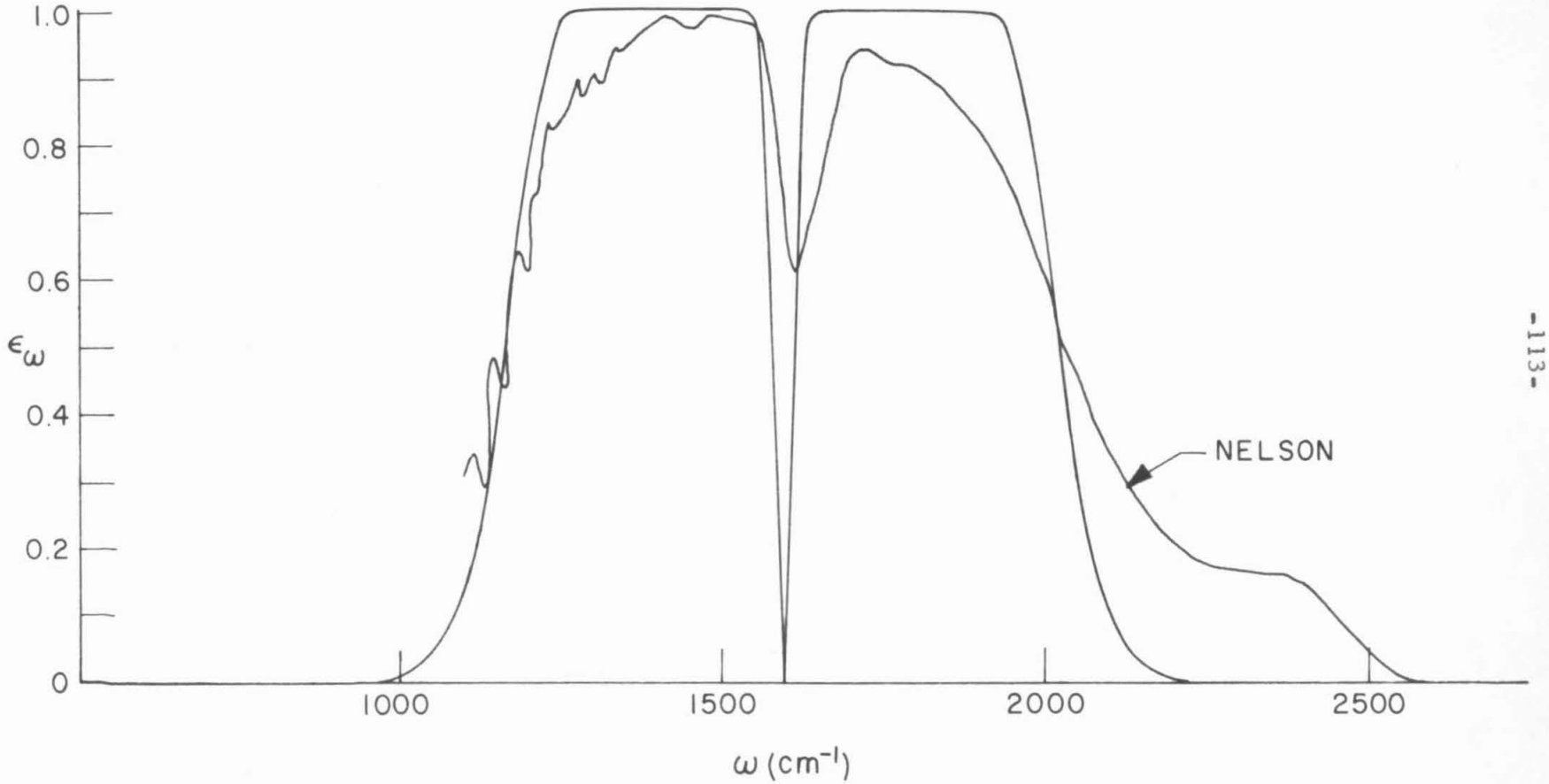

Figure 20. Spectral emissivity of the 6.3 μ bands of H_2O at 1111^{o}K for a pathlength of 1.27 ft. and a pressure of 2 atm.

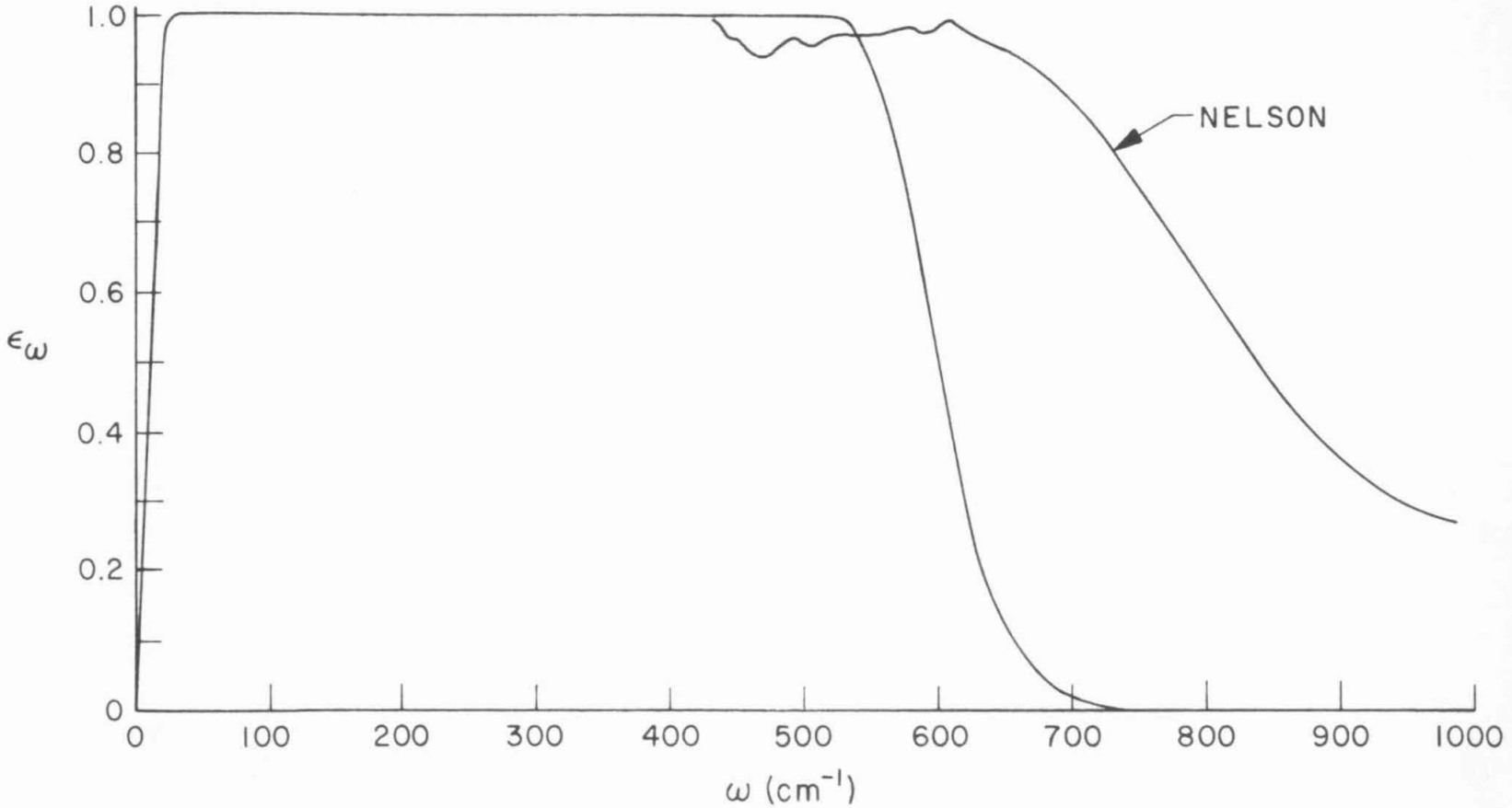

Figure 21. Spectral emissivity of the pure rotation spectrum of H_2O at 1111°K for a pathlength of 1.27 ft. and a pressure of 2 atm.

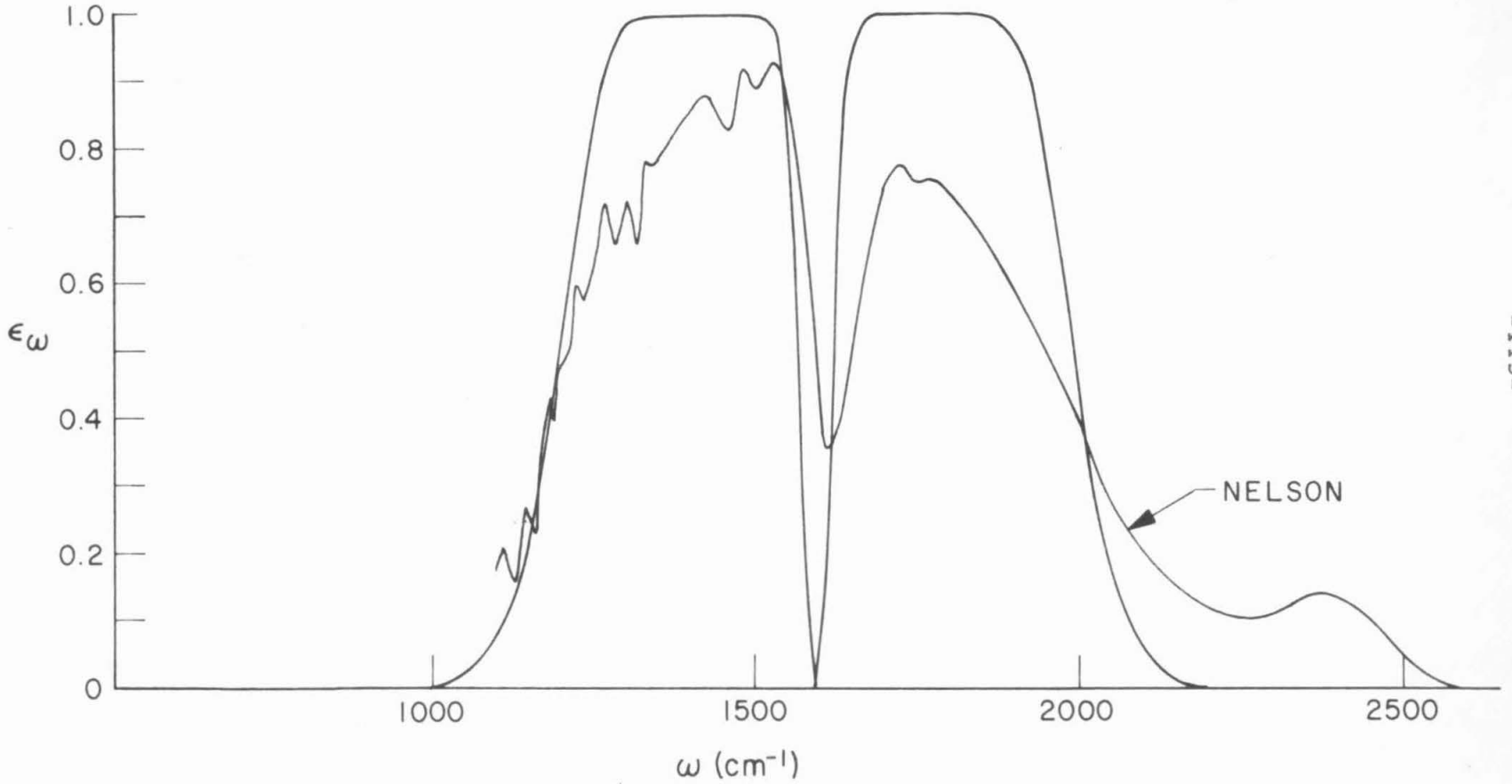

Figure 22. Spectral emissivity of the 6.3 u bands of H_2O at 1111°K for a pathlength of 1.27 ft. and a pressure of 1 atm.

Table XIII. Calculated Absorption of Water Vapor for Various Spectral Regions at a Temperature of 1111°K and a Path Length of 1.27 Ft.

Spectral Region (in μ)	Total Pressure (atm)	Absorption (cm^{-1}) Calculated	Observed	Percentage Difference
1.1	2	25.4	26	- 2
1.38	2	300 (256)	217	+ 38 (+18)
1.87	2	392 (368)	260	+ 50 (+41)
2.7 and 3.2	2	848	785	+ 8
6.3	2	815	857	- 5
6.3	1	726	654	+ 11
pure rotation	2	578	...	...

APPENDIX A

Radiation from Isolated Spectral Lines

The total emitted radiation of an isolated single spectral line with dispersion contour is described by the Landenburg and Reiche law[6, 7, 308, 309].

$$\frac{R_{L_j}}{R^{o}_{\omega_j}} \simeq A_j = \int_{j^{th}\ \text{line}} [1 - \exp(-P_{\omega_j} X)]\, d\omega \qquad (a\text{-}1)$$

$$A_j = \int_{-\infty}^{\infty} \left\{ 1 - \exp\left[\frac{- S_j b X/\pi}{(\omega-\omega_j)^2 + b^2} \right] \right\} d(\omega-\omega_j) \qquad (a\text{-}2)$$

$$A_j = 2\pi b f(x) = 2\pi b f\left(\frac{S_j X}{2\pi b}\right) \qquad (a\text{-}3)$$

where R_{L_j} is the radiancy of the j^{th} line whose integrated intensity is S_j, b is the halfwidth of the line, and $R^{o}_{\omega_j}$ is the average blackbody radiancy of the line centered at ω_j. The function f(x) is defined by

$$f(x) = x e^{-x} [I_o(x) + I_1(x)] \qquad (a\text{-}4)$$

where I_o and I_1 are Bessel functions of imaginary argument and $x = SX/2\pi b$.

This law reduces to a simpler form for the limiting cases of large or small x. For small values of x, $I_n(x)$ may be replaced by the series expansion[310]

$$I_n(x) = \sum_{r=0}^{\infty} \frac{(x/2)^{n+2r}}{r!\ (n+r)!}\ , \qquad (a\text{-}5)$$

and similarly, exp(-x) can be expanded in powers of x. Retaining only terms of order x^2, equation (a-4) becomes

$$f(x) = x[1 - (x/2) + \ldots] \quad . \tag{a-6}$$

Hence, for small values of x, the approximate relation

$$A_j \simeq 2\pi b x_j = S_j X \tag{a-7}$$

can be used. It is apparent from equation (a-6) that equation (a-7) is accurate to within q percent if[6, 7]

$$x < 0.02\, q \quad . \tag{a-8}$$

For large values of x, an asymptotic formula[310] for $I_n(x)$,

$$I_n(x) \simeq \frac{e^x}{(2\pi x)^{1/2}} \left\{ 1 + \frac{1-4n^2}{1!\ 8x} + \frac{(1-4n^2)(9-4n^2)}{2!\ (8x)^2} + \ldots \right\} \tag{a-9}$$

may be used in equation (a-4). Keeping only the first two terms yields

$$f(x) \simeq (2x/\pi)^{1/2}[1 - 1/(8x) + \ldots] \tag{a-10}$$

or, for large values of x,

$$A_j \simeq 2\pi b(2x/\pi)^{1/2} = 2\sqrt{S_j b X} \quad . \tag{a-11}$$

Equation (a-11) is accurate within q percent if[6, 7]

$$x > 12.5/q \quad , \tag{a-12}$$

i. e., it is accurate within 10 per cent when $x > 1.25$.

These two limiting forms for the absorption by a single line with dispersion contour are referred to as the linear approximation and the square root approximation.

If a line undergoes pure Doppler broadening, the absorption coefficient is given by[309]

$$P_\omega = S_j \left(\frac{mc^2}{2\pi k T \omega_j^2} \right)^{\frac{1}{2}} \exp\left[\frac{-mc^2(\omega-\omega_j)^2}{2kT\omega_j^2} \right] \tag{a-13}$$

where m is the mass per molecule.

In terms of the Doppler halfwidth[309],

$$b_D = \left(\frac{2kT\ell n2}{mc^2}\right)^{\frac{1}{2}} \omega_j \qquad \text{(a-14)}$$

and the absorption coefficient at the center line

$$P' = S_j\left(\frac{mc^2}{2\pi kT}\right)^{\frac{1}{2}} \frac{1}{\omega_j} \quad , \qquad \text{(a-15)}$$

the spectral absorption coefficient becomes

$$P_\omega = P' \exp - \left(\frac{\omega-\omega_j}{b_D}\right)^2 \ell n2 \ , \qquad \text{(a-16)}$$

and the line absorption A_L is given by

$$A_L = \int_{-\infty}^{\infty} \left\{1 - \exp\left[-P'_j X \exp(-\xi^2)\right]\right\} d\xi \qquad \text{(a-17)}$$

where

$$\xi = \frac{(\omega-\omega_j)(\ell n2)^{\frac{1}{2}}}{b_D} \quad . \qquad \text{(a-18)}$$

In general, both the Doppler effect and collision damping would be expected to contribute to line shape, and in this case, the line radiancy may be most easily obtained by reference to the curve of growth (see ref. 309, Fig. 4-8). An asymptotic expansion for line radiancy valid in the wings of a spectral line has been derived by Plass and Fivel[311]

$$A_L = 2(SbX)^{\frac{1}{2}}\left\{1 - \frac{\left[1 - \frac{3}{2a^2}\right]}{8x} + \ldots\right\} \qquad \text{(a-19)}$$

where

$$a = \frac{b_N + b_C}{b_D} (\ell n2)^{\frac{1}{2}} \qquad \text{(a-20)}$$

and b_N and b_C refer to natural and collision halfwidths, respectively. Equation (a-19) is obtained by expanding

$$P_\omega = P'\left(\frac{a}{\pi}\right) \int_{-\infty}^{\infty} \frac{\exp(-y^2)}{a^2 + (\xi - y)^2}\, dy \qquad \text{(a-21)}$$

for values of $|\omega-\omega_j| \gg a$ and $|\omega-\omega_j| \gg b_D$ to obtain

$$P_\omega = \frac{S_j(b_N+b_C)}{\pi(\omega-\omega_j)^2}\left\{1 + \left(\frac{3}{2} - a^2\right)\frac{1}{\xi^2} + \left(\frac{15}{4} - 5a^2 + a^4\right)\frac{1}{\xi^4} + \ldots\right\}, \qquad \text{(a-22)}$$

which is then substituted into equation (a-1) to obtain the line radiancy.

It should be noted that, even if the Doppler halfwidth is considerably greater than the Lorentz halfwidth, the square root approximation is still valid for sufficiently large x. Physically, this is because the absorption coefficient falls off exponentially in the wings of a Doppler line, while it only falls off as $(1/\omega)^2$ in the wings of the Lorentz line shape. Thus, at optical depths where a line is essentially black at its center, the variation in absorption with path length is determined by the wings of the lines where the $(1/\omega)^2$ term dominates.

The collision halfwidth, b_C, varies inversely as the square root of temperature and directly as the pressure of the broadening gas. Hence the square root approximation for the line absorption can be written as

$$A_L = 2(Ssp_a b_C^{\circ} p_t)^{\frac{1}{2}} \qquad \text{(a-23)}$$

where the subscripts p_a and p_t refer to the absorber and total pressures, respectively, and b_C° is the line halfwidth per unit pressure. Since the collision halfwidth b_C° depends upon whether the line is self-broadened, or broadened by a foreign gas[312-316] (and self-broadening is much more effective), one can write

$$b_C^{\circ} p_t = b_a^{\circ} p_a + b_b^{\circ} p_b \qquad \text{(a-24)}$$

where the subscript b refers to the foreign gas broadener.

Both limiting cases of the Landenburg and Reiche law may be written in the form[203]

$$A_L = K(s\,p_a)^m (p_t)^n \qquad \text{(a-25)}$$

where K is a proportionality factor which depends upon the temperature as well as the nature of the gases. For the limiting case of weak absorption, the exponent $m = 1$ and $n = 0$; while for the case of strong absorption, $m = \frac{1}{2}$ and $n = \frac{1}{2}$. The use of total pressure in equation (a-25) instead of a linear combination of p_a and p_b implies either that $p_a \ll p_b$ or that self-broadening and foreign gas broadening are equally effective.

REFERENCES TO PART I.

REFERENCES

1. G. Herzberg, Spectra of Diatomic Molecules, 2nd Edition, Van Nostrand, Princeton, 1950.

2. J. R. Nielsen, V. Thornton, and E. B. Dale, "The Absorption Laws for Gases in the Infra-Red," Rev. Mod. Phys., 16, 307-324, (1944).

3. J. N. Howard, D. L. Burch, and D. Williams, "Near-Infrared Transmission Through Synthetic Atmospheres," Geophysical Research Papers, No. 40, AFCRC-TR-55-213, Ohio State University, November 1955; see also J. Opt. Soc. Amer. 46, 186-190, 237-241, 242-245, 334-338, 452-455, (1956).

4. S. S. Penner, Quantitative Molecular Spectroscopy and Gas Emissivities, pp. 108, 248, Addison-Wesley, Reading, Mass., 1959; hereafter this book will be referred to as QMS.

5. D. M. Dennison, "The Infrared Spectra of Polyatomic Molecules, Part I," Rev. Mod. Phys. 3, 280-344, (1931).

6. QMS, Chapters 11 and 14.

7. G. N. Plass, "Models for Spectral Band Absorption," ASI Publication No. U-176, Aeronutronic Systems, Inc., Glendale, Calif., April 1958; see also J. Opt. Soc. Amer. 48, 690-703 (1958).

8. G. N. Plass, "Useful Representations for Laboratory Band Absorption Measurements," ASI Publication No. U-401, Aeronutronic Systems, Inc., Glendale, Calif., March 1959; see also J. Opt. Soc. Amer. 50, 868-875 (1960).

9. M. Lapp and S. S. Penner, "Equilibrium Emissivity Calculations (from Spectroscopic Data) for CO_2 at 300°K and at 600°K," Technical Report No. 32, Contract Nonr-220(03), NR 015 401, California Institute of Technology, Pasadena, June 1960.

10. M. Lapp, L. D. Gray, and S. S. Penner, "Equilibrium Emissivity Calculations for CO_2," International Developments in Heat Transfer, pp. 812-819, ASME, New York, 1961.

11. A. Thomson, "An Approximate Analytic Expression for the Engineering Emissivity of Water Vapor II," Technical Note No. 5, Contract AF 04(645)-24, Gruen Applied Science Labs., Inc., Pasadena, 1957.

12. S.S. Penner and A. Thomson, "Infrared Emissivities and Absorptivities of Gases," J. Appl. Phys. 28, 614-623 (1957).

13. S.S. Penner, "Approximate Emissivity Calculations for Polyatomic Molecules. I. CO_2," J. Appl. Phys. 25, 660-667 (1954).

14. H. Mayer, "Methods of Opacity Calculations," Los Alamos Scientific Laboratory Report LA-647, October 31, 1947.

15. R. M. Goody, "A Statistical Model for Water-Vapour Absorption," Quart. J Roy. Met. Soc., 78, 165-169 (1952).

16. V. R. Stull and G. N. Plass, "Spectral Emissivity of Hydrogen Chloride from 1000-3400 cm^{-1}," Publication No. U461, Scientific Report No. 5, Aeronutronic, Newport Beach, May 15, 1959; see also J. Opt. Soc. Amer. 50, 1279-1285 (1960).

17. QMS, Chapter 8.

18. W. M. Elsasser, "Mean Absorption and Equivalent Absorption Coefficient of a Band Spectrum," Phys. Rev. 54, 126-129 (1938).

19. W. M. Elsasser, "The Far Infrared Water Bands and Heat Transfer in the Atmosphere," Phys. Rev. 56, 855-856 (1939).

20. W. M. Elsasser, "Heat Transfer by Infrared Radiation in the Atmosphere," Harvard Meteor. Studies No. 6, Harvard Univ., Cambridge, 1942.

21. G. N. Plass, "Spectral Emissivity of Carbon Dioxide from 1800-2500 cm^{-1}," Publication U-238 Aeronutronic Systems, Inc., Glendale, California, 1958; see also J. Opt. Soc. Amer. 49, 821-828 (1959).

22. W. Malkmus, "Infrared Emissivity of Carbon Dioxide," Space Science Laboratory Report AE62-0204, General Dynamics-Astronautics, February 1962.

23. W. Malkmus and A. Thomson, "Infrared Emissivity of Diatomic Gases for the Anharmonic Vibrating-Rotator Model," J. Quant. Spectrosc. Radiat. Transfer 2, 17-39 (1962); see also Convair Report ZPh-095, May 5, 1961.

24. M. Lapp, Ph. D. Thesis, California Institute of Technology, Pasadena, June 1960.

25. L. D. Gray, "Semi-Empirical Fit of CO_2 Emissivities," Technical Report No. 34, Contract Nonr-220(03), NR 015 401, California Institute of Technology, Pasadena, October 1960.

26. L. Pauling and E. B. Wilson, Jr., Introduction to Quantum Mechanics, McGraw-Hill, New York 1935.

27. M. Born and R. Oppenheimer, "Zur Quantentheorie der Molekeln," Ann. d. Phys. 84, 457-484 (1927).

28. H. Goldstein, Classical Mechanics, Addison-Wesley, Reading, Mass., 1950.

29. E. T. Whittaker, A Treatise on the Analytical Dynamics of Particles and Rigid Bodies, 4th Edition, Chapter VII, Cambridge Univ. Press, 1959.

30. A. G. Webster, The Dynamics of Particles and of Rigid Elastic and Fluid Bodies, 2nd Edition, Chapters 5 and 6, Dover, New York, 1959.

31. B. Friedman, Principles and Techniques of Applied Mathematics, pp. 107-109, John Wiley, New York 1956.

32. H. Eyring, J. Walter and G. E. Kimball, Quantum Chemistry, John Wiley, New York 1944.

33. V. Heine, Group Theory in Quantum Mechanics, Pergamon Press, New York 1960.

34. L. D. Landau and E. M. Lifshitz, Quantum Mechanics, Non-Relativistic Theory, Addison-Wesley, Reading, Mass. 1958.

35. J. Rosenthal and G. M. Murphy, "Group Theory and the Vibrations of Polyatomic Molecules," Rev. Mod. Phys. 8, 317-346 (1936).

36. E. B. Wilson, Jr., J. C. Decius, and P. C. Cross, Molecular Vibrations, McGraw-Hill, New York, 1955.

37. G. Herzberg, Infrared and Raman Spectra of Polyatomic Molecules, Van Nostrand, New York, 1945.

38. H. Margenau and G. M. Murphy, The Mathematics of Physics and Chemistry, Van Nostrand, New York, 1943.

39. H. Lass, Elements of Pure and Applied Mathematics, McGraw-Hill, New York, 1957.

40. F. Seitz, "A Matrix-Algebra Development of the Crystallographic Groups. I," Z. Kristallographie A88, 433-459 (1934).

41. E. Wigner, Gruppentheorie und ihre Anwendung auf die Quantenmechanik der Atomspektren, Viewig, Brunswick, 1931; see also E. P. Wigner, Group Theory and its Application to the Quantum Mechanics of Atomic Spectra, Academic Press, New York, 1959.

42. H. Weyl, Theory of Groups and Quantum Mechanics, Methuen, London, 1931.

43. B. L. Van der Waerden, Die Gruppentheoretische Methode in der Quantenmechanik, J. Springer, Berlin, 1932.

44. H. A. Bethe, "Termaufspaltung in Kristallen," Ann. Physik 3, 133-208 (1929).

45. R. S. Mulliken, "Electronic Structures of Polyatomic Molecules and Valence, IV. Electronic States, Quantum Theory of the Double Bond," Phys. Rev. 43, 279-302 (1933).

46. L. Tisza, "Zur Deutung der Spektren Mehratomiger Molekule," Z. Physik, 82, 48-72 (1933).

47. E. B. Wilson, Jr., "Degeneracy, Selection Rules and Other Properties of the Normal Vibrations of Certain Polyatomic Molecules," J. Chem. Phys. 2, 432-439 (1934).

48. G. Placzek, Marx Handbuch der Radiologie, Vol. VI, Part II, p. 209, Akademische Verlagsgesellschaft, Leipzig, 1934.

49. E. P. Wigner, "Über die elastischen Eigenschwingungen symmetrischer Systeme, "Nachrichten von der Gesellschaft der Wissenschaften zu Göttingen aus dem Jahre 1930, pp. 133-146, Weidmannsche Buchhandlung, Berlin, 1931.

50. J. B. Howard and E. B. Wilson, Jr., "The Normal Frequencies of Vibration of Symmetrical Pyramidal Molecules AB_3 with Application to the Raman Spectra of Trihalides," J. Chem. Phys. 2, 630-634 (1934).

51. E. B. Wilson, Jr., "The Normal Modes and Frequencies of Vibration of the Regular Plane Hexagon Model of the Benzene Molecule," Phys. Rev. 45, 706-714 (1934).

52. E. B. Wilson, Jr., "Normal Frequencies of Vibration of the Plane Square Molecule AB_4 with Reference to the Structure of Nickel Carbonyl," J. Chem. Phys. 3, 59 (1935).

53. S. Bhagavantam and T. Venkatarayudu, Theory of Groups and its Application to Physical Problems, Andhra Univ., Waltair, 1948.

54. P. C. Cross and J. H. Van Vleck, "Molecular Vibrations of Three Particle Systems with Special Applications to the Ethyl Halides and Ethyl Alcohol," J. Chem. Phys. 1, 350-356 (1933).

55. J. H. Van Vleck and P. C. Cross, "A Calculation of the Vibration Frequencies and other Constants of the H_2O Molecule," J. Chem. Phys. 1, 357-361 (1933).

56. N. Davidson, Statistical Mechanics, Chapter 11, McGraw-Hill, New York, 1962.

57. L. G. Bonner, "The Vibrational Spectrum of Water Vapor," Phys. Rev. 46, 458-464 (1934).

58. H. M. Randall, D. M. Dennison, H. Ginsburg, and L.R. Weber, "The Far Infrared Spectrum of Water Vapor," Phys. Rev. 52, 160-174 (1937).

59. B. T. Darling and D. M. Dennison, "The Water Vapor Molecule," Phys. Rev. 57, 128-139 (1940).

60. QMS, Chapter 7.

61. A. H. Nielsen, "Recent Advances in Infrared Spectroscopy," Office of Ordnance Research, Technical Memo 53-2, December 1953.

62. E. Fermi, "Über den Ramaneffekt des Kohlendioxydes," Z. Physik 71, 250-259 (1931).

63. A. Adel and D. M. Dennison, "The Infrared Spectrum of Carbon Dioxide. Part I," Phys. Rev. 43, 716-723 (1933).

64. D. M. Dennison, "The Infra-Red Spectra of Polyatomic Molecules, Part II," Rev. Mod. Phys. 12, 175-214 (1940).

65. E. Teller, "Theorie der langwelligen Molekülspektren," Hand- und Jahrbuch der chemischen physik, 9, II, 43-160, Akademische Verlagsgesellschaft, Leipzig, (1934).

66. C. Eckart, "Some Studies Concerning Rotating Axes and Polyatomic Molecules," Phys. Rev. 47, 552-558 (1935).

67. E. B. Wilson, Jr., "The Effect of Rotational Distortion on the Thermodynamic Properties of Water and Other Polyatomic Molecules," J. Chem. Phys. 4, 526-528 (1936).

68. M. L. Eidinoff and J. G. Aston, "The Rotational Entropy of Non-Rigid Polyatomic Molecules," J. Chem. Phys. 3, 379-383 (1935).

69. J. H. Van Vleck, "The Rotational Energy of Polyatomic Molecules," Phys. Rev. 47, 487-494 (1935).

70. D. M. Dennison and M. Johnson, "The Interaction Between Vibration and Rotation for Symmetrical Molecules," Phys. Rev. 47, 93-94 (1935).

71. E. E. Witmer, "The Quantization of the Rotational Motion of the Polyatomic Molecule by the New Wave Mechanics," Proc. Nat. Acad. Sci. 13, 60-65 (1927).

72. H. A. Kramers and G. P. Ittman, "Zur Quantelung des asymmetrischen Kreisels," Zeit. f. Physik 53, 553-565 (1929).

73. H. A. Kramers and G. P. Ittman, "Zur Quantelung des asymmetrischen Kreisels, II," Zeit. f. Physik 58, 217-231 (1929).

74. H. A. Kramers and G. P. Ittman, "Zur Quantelung des asymmetrischen Kreisels, III," Zeit. f. Physik 60, 663-681 (1930).

75. S. C. Wang, "On the Asymmetrical Top in Quantum Mechanics," Phys. Rev. 34, 243-252 (1929).

76. O. Klein, "Zur Frage der Quantelung des asymmetrischen Kreisels," Zeit. f. Physik 58, 730-734 (1929).

77. H. B. G. Casimir, "Zur quantenmechanischen Behandlung des Kreiselproblems," Zeit. f. Physik 59, 623-624 (1929).

78. H. B. G. Casimir, Rotation of a Rigid Body in Quantum Mechanics, J. B. Wolthers, The Hague, 1931.

79. B. S. Ray, "Über die Eigenwerte des asymmetrischen Kreisels," Zeit. f. Physik 78, 74-91 (1932).

80. G. W. King, R. M. Hainer, and P. C. Cross, "The Asymmetric Rotor, I. Calculation and Symmetry Classification of Energy Levels," J. Chem. Phys. 11, 27-42 (1943).

81. P. C. Cross, R. M. Hainer, and G. W. King, "The Asymmetric Rotor, II. Calculation of Dipole Intensities and Line Classification," J. Chem. Phys. 12, 210-243 (1944).

82. G. W. King, "Calculation of the Higher Energy Levels of the Asymmetric Rotor by Means of the Correspondence Principle," Phys. Rev. 70, 108 (1946); see also, G. W. King, "The Asymmetric Rotor, VI. Calculation of Higher Energy Levels by Means of the Correspondence Principle," J. Chem. Phys. 15, 820-830 (1947).

83. S. Golden, "An Asymptotic Expression for the Energy Levels of the Rigid Asymmetric Rotor," J. Chem. Phys. 16, 78-86 (1948).

84. S. Golden, "An Asymptotic Expression for the Energy Levels of the Asymmetric Rotor, II. Centrifugal Distortion Correction," J. Chem. Phys. 16, 250-253 (1948).

85. W. H. Shaffer and H. H. Nielsen, "The Vibration-Rotation Energies of the Nonlinear Triatomic XY_2 Type of Molecule," Phys. Rev. 56, 188-202 (1939).

86. H. H. Nielsen, "The Near Infra-Red Spectrum of Water Vapor. I. The Perpendicular Bands ν_2 and $2\nu_2$," Phys. Rev. 59, 565-575 (1941).

87. B. L. Crawford and P. C. Cross, "Elements of the Factored Secular Equation for the Semi-Rigid Water Type Rotator, with Application to the Hydrogen Sulfide Band at 10,100 A," J. Chem. Phys. 5, 621 (1937).

88. H. A. Jahn and E. Teller, "Stability of Polyatomic Molecules in Degenerate Electronic States. I. Orbital Degeneracy," Proc. Roy. Soc. London 161, 220-235 (1937).

89. E. B. Wilson, Jr. and J. B. Howard, "The Vibration-Rotation Energy Levels of Polyatomic Molecules. I. Mathematical Theory of Semi-Rigid Asymmetrical Top Molecules," J. Chem. Phys. 4, 260-268 (1936).

90. E. B. Wilson, Jr., "The Vibration-Rotation Energy Levels of Polyatomic Molecules. III. Effect of Centrifugal Distortion," J. Chem. Phys. 5, 617-620 (1937).

91. E. B. Wilson, Jr., "The Present Status of the Statistical Method of Calculating Thermodynamic Functions," Chem. Rev. 27, 17-38 (1940).

92. C. C. Ferriso, "The Temperature, Spectrum, and Emissivity of Exhaust Gases from a Small Rocket," Report No. AZR-014, Vol. III, Convair Astronautics, San Diego, California, 1960.

93. R. H. Tourin and P. M. Henry, "Infrared Spectral Emissivities and Internal Energy Distributions of Carbon Dioxide and Water Vapor at High Temperatures," The Warner and Swasey Co., Control Instrument Division, New York, AFCRC-TR60-203(1959).

94. An excellent discussion of the problems and errors involved in extrapolation of line profile data for CO_2 obtained at moderate temperatures was presented by W. S. Benedict at the Symposium on Quantitative Spectroscopy and Selected Military Applications, California Institute of Technology, Pasadena, California, March, 1960.

95. H. C. Hottel, Chapter 4 in Heat Transmission, by W. H. McAdams, McGraw-Hill Book Co., New York, New York, 1954.

96. D. K. Edwards, "Absorption by Infrared Bands of Carbon Dioxide Gas at Elevated Pressures and Temperatures," J. Opt. Soc. Amer. 50, 617-626 (1960); see also, D. K. Edwards, Ph. D. Thesis, Mechanical Engineering, University of California, Berkeley, California, March 1959.

97. K. Ångström, "Über die Wärmeabsorption von atmosphärischen Gasen," Ann. d. Phys. 39, 267-293 (1890).

98. F. Paschen, "Über die Emission der Gase," Ann. d. Phys. 51, 1-39 (1894).

99. H. Rubens and E. Aschkinass, "Beobachtungen über Absorption und Emission von Wasserdampf und Kohlensäure im Ultrarothen Spectrum," Ann. d. Physik 64, 584-601 (1898).

100. K. Ångström, "Über die Abhangigkeit der Absorption der Gase, besonders der Kohlensäure von der Dichte," Ann. d. Phys. 6, 163-173 (1901).

101. C. Schaefer, "Über das ultrarote Absorptionsspektrum der Kohlensäure in seiner Abhangigkeit vom Druck," Ann. Physik 16, 93-105 (1905).

102. H. Rubens and E. Ladenburg, "Über das langwellig Absorptionsspektrum der Kohlensäure," Ver. deut. phys. Ges. 7, 170-182 (1905).

103. E. von Bahr, "Über die Einwirkung des Druckes auf die Absorption ultraroter Strahlung durch Gase," Ann. d. Phys. 29, 780-796 (1909).

104. E. von Bahr, "Über die Einwirkung des Druckes auf die Absorption ultraroter Strahlung durch Gase," Ann. d. Phys. 33, 585-606 (1910).

105. G. Hertz, "Über das ultrarote Absorptionsspektrum der Kohlensäure in seiner Abhängigkeit von Druck und Partialdruck," Ver. deut. phys. Ges. 13, 617-644 (1911).

106. E. von Bahr, "Über den Einfluss der Temperatur auf die ultrarote Absorption der Gase," Ann. d. Phys. 38, 206-222 (1912).

107. W. Burmeister, "Untersuchungen über die ultraroten Absorptionsspektra einiger Gase," Ver. deut. phys. Ges. 15, 589-611 (1913).

108. E. von Bahr, "Über die ultrarote Absorption der Gase," Ver. deut. phys. Ges. 15, 710-730 (1913).

109. E. von Bahr, "Über die ultrarote Absorption der Gase, "Ver. deut. phys. Ges. 15, 1150-1158 (1913).

110. H. Schmidt, "Über Emission und Absorption erhitzer Kohlensäure," Ann. d. Phys. 42, 415-459 (1913).

111. K. Hof, "Study of the spectra of carbon monoxide and carbon dioxide," Z. wiss. Phot. 14, 39-55, 69-88 (1914).

112. N. Bjerrum, "Über die ultraroten Spektren der Gase. III. Die Konfiguration des Kohlendioxydmoleküls und die Gesetze der intramolekularen Kräfte," Verh. d. phys. Ges. 16, 737-753 (1914).

113. W. Gerlach, "Über die Absorption der schwarzen Strahlung in Wasserdampf- und Kohlensäuregehalt der Luft," Ann. d. Phys. 50, 233-244 (1916).

114. E. F. Barker, "Cardon Dioxide Absorption in the Near Infrared," Astrophys. J. 55, 391-400 (1922).

115. A. Eucken, "Die Tragheitsmomente und die Gestalt der Kohlensäuremolekel," Zeit. f. phys. Chem. 100, 159-170 (1922).

116. C. Schaefer, "The Regularities of Infrared Spectra and a Contradiction of the Classical Theory of Dispersion," Ann. phys. 67, 407-419 (1922).

117. J. Ôkubo, "The Absorption of Near Infra-Red Radiation by Carbon Dioxide," Sci. Repts. Tohoku Imp. U. 12, 39-43 (1923).

118. H. M. Randall, "Report on the Fine Structure of Near Infrared Absorption Bands," J. Opt. Soc. Amer. 7, 45-57 (1923).

119. A. Schack, "Über die Strahlung der Feuergase und ihre praktische Berechnung," Zeit. f. techn. Physik 5, 267-278 (1924).

120. H. Deslandres, "Complementary investigations on the structure and distribution of band spectra," Compt. rend. 181, 387-392 (1925).

121. J. W. Ellis, "Emission and absorption bands of carbon dioxide in the infrared," Phys. Rev. 26, 469-474 (1925).

122. C. Schaefer and B. Philipps, "Das Absorptionsspektrum der Kohlensäure und die Gestalt der CO_2 Molekel," Zeit. f. Phys. 36, 641-670 (1926).

123. J. W. Ellis, "The molecular spectrum of carbon dioxide," Nature 118, 82-83 (1926).

124. A. Euchen, "Zur Frage nach der Gestalt der Kohlensäuremolekel," Zeit. f. Phys. 37, 714-721 (1926).

125. C. T. Zahn, "The Electric Moment of CO_2, NH_3 and SO_2," Phys. Rev. 27, 455-459 (1926).

126. A. Schack, "Die Gasstrahlung vom physikalischen und technischen Standpunkt," Zeit. f. techn. Physik 7, 556-563 (1926).

127. K. L. Wolk, "Die Gestalt der Kohlensäuremolekel," Zeit. f. phys. Chem. 131, 90-96 (1927).

128. H. C. Hottel, "Heat Transmission by Radiation from Non-Luminous Gases," Ind. Eng. Chem. 19, 888-894 (1927).

129. H. A. Stuart, "Über die Temperaturabhangigkeit der Dielectrizitätskonstanten von Gasen und Dämpfen. I. Methode und Ergebnisse fur Kohlensäure und Luft," Zeit. f. Phys. 47, 457-478 (1928).

130. C. R. Bailey, "The Raman and Infra-Red Spectra of Carbon Dioxide," Nature 123, 410 (1929).

131. P. N. Ghosh and P. C. Mahanti, "Über die Molekularstruktur driatomiger Gase," Phys. Zeit. 30, 531-537 (1929).

132. A. Angström, "Variation of atmospheric radiation temperature and its dependence on the composition of the atmosphere," Gerlands Beitr. Geophys. 21, 2-3, 145-161 (1929); Science Abstracts 32A, 966.

133. J. H. Van Vleck, "On the Vibrational Selection Principles in the Raman Effect," Proc. Nat. Acad. of Sciences 15, 754-764 (1929).

134. C. Schaefer and F. Matossi, Das Ultrarote Spektrum, J. Springer, Berlin, 1930.

135. H. D. Smyth and T. C. Chow, "Regularities in the emission spectrum of CO_2," Phys. Rev. 37, 1023 (1930).

136. P. E. Martin and E. F. Barker, "The fundamental vibration bands of carbon dioxide," Phys. Rev. 37, 1708-1709 (1930).

137. S. Bhagavantam, "Raman effect and molecular structure," Ind. J. Phys. 5, 73-95 (1930).

138. P. E. Martin and E. F. Barker, "The infrared absorption spectrum of carbon dioxide," Phys. Rev. 41, 291-303 (1932).

139. R. S. Mulliken, "Interpretation of the rotational structure of the CO_2 emission bands," Phys. Rev. 42, 364-372 (1932).

140. A. B. D. Cassie and C. R. Bailey, "Infrared and Raman bands of CO_2, carbon oxysulfide and carbon disulfide molecules," Z. Physik 79, 35-41 (1932).

141. A. Langseth and J. R. Nielsen, "Raman and infrared spectra of carbon dioxide," Z. physik Chem. 19, 35-46 (1932).

142. E. F. Barker and A. Adel, "Resolution of the Two Difference Bands of CO_2 Near 10μ," Phys. Rev. 44, 185-187 (1933).

143. C. Tingwaldt, "Die Absorption der Kohlensäure im Gebiet der Bande $\lambda = 2.7\mu$ zwischen 300° und 1100° abs.," Physik Zeit. 35, 715-720 (1934).

144. A. Adel, V. M. Slipher, and E. F. Barker, "The Absorption of Sunlight by the Earth's Atmosphere in the Remote Infrared Region of the Spectrum," Phys. Rev. 47, 580-584 (1935).

145. H. C. Hottel and V. C. Smith, "Radiation from Nonluminous Flames," Trans. ASME 57, 463-470 (1935).

146. H. C. Hottel and H. G. Mangelsdorf, "Heat transmission by radiation from non-luminous gases," Trans. Amer. Inst. Chem. Engrs. 31, 517-549 (1935).

147. E. Eckert, "Messung der Gesamtstrahlung von Wasserdampf und Kohlensäure in Mischung mit nichtstrahlenden Gasen bei Temperaturen bis zu 1300°C," VDI-Forchungs-Heft 387, Beilage zu Forsch. Ing. Wes. 8 (1937).

148. D. M. Cameron and H. H. Nielsen, "The 4.3μ fundamental band in the spectrum of CO_2," Phys. Rev. 53, 246-247 (1938).

149. A. H. Nielsen, "Infrared absorption by $C^{13}O_2^{16}$ at 4.375μ," Phys. Rev. 53, 983-985 (1938).

150. C. Tingwaldt, "Die Absorption der Kohlensäure im Gebiet der Bande λ = 4.3 μ zwischen 300° und 1000° absolut," Physik Zeit. 39, 1-6 (1938).

151. O. Bronder, "Bemerkung zu einer Arbeit von C. Tingwaldt: 'Die Absorption der Kohlensäure im Gebiete der Bande λ = 4.3μ zwischen 300° and 1000°abs.,' sowie zu einer Arbeit von A. Schack, 'Uber die Strahlung der Feuergase und ihre praktische Berechnung,' " Physik. Zeit. 39, 620-621 (1938).

152. F. Schnaidt, "The absorption of water vapor and carbon dioxide with reference to pressure and temperature dependence," Gerlands. Beitr. Geophys. 54, 203-234 (1939).

153. A. Schack, "Zur Extrapolation der Messungen der ultraroten Strahlung von Kohlensäure und Wasserdampf," Z. tech. Physik 22, 50-56 (1941).

154. H. Schwiedenssen, "Bemerkung zu A. Schack, Düsseldorf: 'Zur Extrapolation der Messungen der ultraroten Strahlung von Kohlensäure und Wasserdampf,'" Z. tech. Physik 22, 201-202 (1941).

155. A. Schack, "Entgegnung zur Zuschrift von H. Schwiedessen," Z. tech. Physik. 22, 202-203 (1941).

156. W. C. Price, "Absorption spectra and absorption coefficients of atmospheric gases," Repts. Progress Physics 9, 10-17 (1942-43).

157. G. B. B. M. Sutherland and G. S. Callendar, "The infrared spectra of atmospheric gases other than water vapor," Repts. Progress Physics 9, 18-28 (1942-43).

158. A. H. Nielsen and Y. T. Yao, "The Analysis of the Vibration-Rotation Band ω_2 for $C^{12}O_2^{16}$ and $C^{13}O_2^{16}$," Phys. Rev. 68, 173-180 (1945); erratum Phys. Rev. 71, 825 (1947).

159. L. D. Kaplan, "The absorption spectrum of carbon dioxide from 14 to 16 microns," J. Chem. Phys. 15, 809-815 (1947).

160. A. M. Thorndike, "The experimental determination of the intensities of infrared absorption bands. III. Carbon dioxide, methane, and ethane," J. Chem. Phys. 15, 868-874 (1947).

161. C. W. Peters, "Infrared Absorption of Carbon Dioxide at 15 Microns," ONR-Johns Hopkins Report, Feb. 2, 1949.

162. R. Jones and E. E. Bell, "The 2.7μ bands of carbon dioxide," Phys. Rev. 79, 1004 (1950).

163. S. I. Evans, "Radiation from non-luminous gases," Bull. Brit. Coal Utilization Research Assoc. 14, 369-381 (1950).

164. E. K. Plyler and C. W. Peters, "Wave lengths for calibration of prism spectrometers," J. Res. NBS 45, 462-468 (1950).

165. W. S. Benedict and E. K. Plyler, "Absorption spectra of water vapor and carbon dioxide in the region of 2.7 microns," J. Res. NBS 46, 246-265 (1951).

166. D. F. Eggers, Jr. and B. L. Crawford, Jr., "Vibrational intensities. III. Carbon dioxide and nitrous oxide," J. Chem. Phys. 19, 1554-1561 (1951).

167. J. H. Taylor, W. S. Benedict, and J. Strong, "Atmospheric Transmission at High Temperatures," J. Chem. Phys. 20, 528-529 (1952).

168. E. K. Plyler and J. J. Ball, "Infrared Emission Spectra of Hydroxyl Radical Carbon Monoxide, and Carbon Dioxide from 3μ to 5.5μ," J. Chem. Phys. 20, 1178-1179 (1952).

169. R. H. Tourin, "Infrared emission and absorption of thermally excited carbon dioxide," J. Chem. Phys. 20, 1651 (1952).

170. D. Weber, R. J. Holm, and S. S. Penner, "Integrated Absorption for Vibration-Rotation Bands of Carbon Dioxide," J. Chem. Phys. 20, 1820 (1952).

171. J. H. Taylor, W. S. Benedict, and J. Strong, "Infrared spectra of water and carbon dioxide at 500°," J. Chem. Phys. 20, 1884-1898 (1952).

172. G. N. Plass, "A Method for the Determination of Atmospheric Transmission Functions from Laboratory Absorption Measurements," J. Opt. Soc. Amer. 42, 677-683 (1952).

173. J. N. Howard and R. M. Chapman, "Near infrared absorption by entire bands of carbon dioxide," J. Opt. Soc. Amer. 42, 856 (1952).

174. W. H. Cloud, "The 15 Micron Band of CO_2 Broadened by Nitrogen and Helium," ONR-Johns Hopkins Report, Jan. 1, 1952.

175. N. M. Gailer and E. K. Plyler, "The $3\nu_3$ Bands of Carbon Disulfide and Carbon Dioxide," J. Res. NBS 48, 392-393 (1952).

176. R. J. Holm, D. Weber, and S. S. Penner, "Emissivity for carbon dioxide at elevated pressures," J. Appl. Phys. 23, 1283 (1952).

177. W. M. Elsasser and J. I. King, "Stratospheric Radiation," Tech. Rept. No. 9, University of Utah (1953).

178. G. Herzberg and L. Herzberg, "Rotation-vibration spectra of diatomic and simple polyatomic molecules with long absorbing paths. XI. The spectrum of carbon dioxide below 1.25μ," J. Opt. Soc. Amer. 43, 1037-1044 (1953).

179. G. J. Gollin, "Radiation and furnace design," J. Inst. Fuel 26, 151-162 (1953).

180. A. Adel, "Absorption line width in the infrared spectrum of atmospheric carbon dioxide," Phys. Rev. 90, 1024-1025 (1953).

181. J. Fahrenfort, "The infrared spectrum of CO_2 under pressure," Chem. Weekblad. 50, 501-505 (1954).

182. J. Fahrenfort, H. de Kluiver, and T. P. J. H. Babeliowsky, "Infrared absorption induced in CO_2 under pressure," J. phys. radium 15, 614 (1954).

183. A. Langseth, "Infrared and Raman spectra of simple linear molecules," J. phys. radium 15, 614 (1954).

184. R. Tourin, "Infrared Emission and Absorption of CO_2 at High Temperatures," Report No. 258, Warner and Swasey Research Corp., New York, New York (1954).

185. R. H. Tourin, "Infrared spectra of thermally excited gases," NBS Circular 523, 87-91 (1954).

186. R. Sloan, J. H. Shaw, and D. Williams, "Infrared emission spectrum of the atmosphere," J. Opt. Soc. Amer. 45, 455-460 (1955).

187. W. L. France and F. P. Dickey, "Fine structure of the 2.7μ carbon dioxide rotation-vibration band," J. Chem. Phys. 23, 471-474 (1955).

188. N. Ya. Dodonova and V. V. Sobolev, "Carbon dioxide radiation in the 15μ region in a gas discharge," Zhur. Eksptl. i. Teoret. Fiz. 28, 764-766 (1955).

189. K. Rossmann, K. N. Rao, and H. H. Nielsen, "Infrared spectrum and molecular constants of carbon dioxide. I. ν_2 of $C^{12}O_2^{16}$ at 15μ," J. Chem. Phys. 24, 103-105 (1956).

190. K. Rossmann, W. L. France, and K. N. Rao, "Infrared spectrum and molecular constants of CO_2. II. Levels 10^00 and 02^00; 10^01 and 02^01 coupled by Fermi resonance," J. Chem. Phys. 24, 1007-1008 (1956).

191. L. D. Kaplan and D. F. Eggers, Jr., "Intensity and line width of the 15μ CO_2 band determined by a curve of growth method," J. Chem. Phys. 25, 876-883 (1956).

192. A. Kh. Khalilov, "Rotation-vibration spectra of molecules in the infrared region," Trudy Inst. Fiz. i Mat., Akad. Nauk. Azerbaidzhan SSR, Ser. Fiz. 8, 55-62 (1956).

193. G. N. Plass, "Infrared radiation in the atmosphere," Amer. J. Physics 24, 303-321 (1956).

194. K. P. Vasilevskii, "The vibration-rotational absorption and emission spectra of CO_2," Optika i Spektroskopiya 1, 587-589 (1956).

195. H. J. Kostkowski and L. D. Kaplan, "Absolute intensities of the 721 and 742 cm^{-1} bands of CO_2," J. Chem. Phys. 26, 1252-1253 (1957).

196. D. F. Eggers, Jr. and C. B. Arends, "Infrared intensities and band moments of $CO^{16}O^{18}$," J. Chem. Phys. 27, 1405-1410 (1957).

197. G. Yamamoto and T. Sasamori, "Calculation of the Absorption of the 15μ Carbon-Dioxide Band," Sci. Rep. Tohuku Univ. Geophysics Series 5, 10, 37-57 (1958).

198. D. F. Eggers, Jr., "Infrared intensities and bond moments of $CO^{16}O^{18}$," J. Chem. Phys. 28, 512 (1958).

199. J. Overend, M. J. Youngquist, E. C. Curtis, and B. Crawford, Jr., "Vibrational Intensities. XI. CO_2 and the Wilson-Wells Method," J. Chem. Phys. 30, 532-537 (1959).

200. J. T. Bevans, "Correlation of the Total Emissivity of Carbon Dioxide," ASME Paper Number 60-WA-175, presented at the Winter Annual Meeting, New York, 1960.

201. L. W. Megill and P. M. Jamnik, "Technique for Calculating Infrared Absorptance by a Regular Band," J. Opt. Soc. Amer. 51, 1294-1297 (1961).

202. W. T. Roach, "The absorption of solar radiation by watervapour and carbon dioxide in a cloudless atmosphere," Quart. J. Roy. Meteorol. Soc. 87, 364 (1961).

203. H. J. Babrov, P. M. Henry, and R. H. Tourin, "Methods for Predicting Infrared Radiance of Flames by Extrapolation from Laboratory Measurements," Sci. Rept. No. 2, Warner and Swasey, Flushing, New York, Oct. 1961.

204. R. H. Tourin, "Spectral Emissivities of Hot CO_2-H_2O Mixtures in the 2.7μ Region," J. Opt. Soc. Amer. 51, 799-800 (1961).

205. K. Watanabe, M. Zelikoff, and E. C. Y. Inn, "Absorption Coefficients of Several Atmospheric Gases," Geophysical Research Papers, No. 21, Geophysics Research Directorate, Air Force Cambridge Research Center, June 1953.

206. R. O'B. Carpenter, "Emission and Absorption in the 4.3 Micron CO_2 Band," Contract No. AF 19(604)-2405, Baird-Atomic, Inc., Cambridge 38, Massachusetts, 1959.

207. D. G. Murcray, J. N. Brooks, F. H. Murcray, and W. J. Williams, "Atmospheric Absorptions in the Near Infrared at High Altitudes," J. Opt. Soc. Amer. 50, 107-112 (1960).

208. R. V. Dunkle, D. K. Edwards, J. T. Gier, and K. E. Nelson, "Gaseous Radiation Studies," Final Report NSF G 7007, Department of Engineering, University of California, Los Angeles, February 1960.

209. M. Steinberg and W. O. Davis, "High Temperature Absorption of Carbon Dioxide at 4.40 μ," J. Chem. Phys. 34, 1373-1377 (1961).

210. R. H. Tourin, "Measurements of Infrared Spectral Emissivities of Hot Carbon Dioxide in the 4.3 μ Region," J. Opt. Soc. Amer. 51, 175-183 (1961).

211. C. C. Ferriso, "High Temperature Infrared Emission and Absorption Studies," Space Physics Report AE61-0910, General Dynamics/Astronautics, 14 September 1961.

212. V. R. Stull, P. J. Wyatt, and G. N. Plass, "Final Report on Theoretical Study of the Infrared Radiative Behavior of Flames. Volume II. The Infrared Absorption of Carbon Dioxide," Publication No. U-1505, Aeronutronic Division Ford Motor Company, Newport Beach, California, 30 December 1961.

213. R. H. Tourin and H. J. Babrov, "Absorption Coefficients of Hot CO_2 at 4.40 μ," J. Chem. Phys. 37, 581-582 (1962).

214. G. J. Penzias and R. H. Tourin, "Methods for Infrared Analysis of Rocket Flames in Situ," Combustion and Flame 6, 147-152 (1962).

215. E. K. Plyler, E. D. Tidwell, and W. S. Benedict, "Absorption Bands of Carbon Dioxide from 2.8 - 4.2 μ," J. Opt. Soc. Amer. 52, 1017-1022 (1962).

216. C. C. Ferriso, "The Emission of Hot CO_2 and H_2O in Small Rocket-Exit Exhaust Gases," Eighth Symposium (International) on Combustion, 275-287, Williams and Wilkins, Baltimore, 1962.

217. G. N. Plass and V. R. Stull, "Carbon Dioxide Absorption for Path Lengths Applicable to the Atmosphere of Venus," Publication No. U-1844, Aeronutronic Division Ford Motor Company, Newport Beach, California, 24 September 1962.

218. D. E. Burch and D. A. Gryvnak, "Infrared Radiation Emitted by Hot Gases and its Transmission through Synthetic Atmospheres," Publication No. U-1929, Aeronutronic Division Ford Motor Company, Newport Beach, California, 31 October 1962.

219. G. J. Penzias, G. J. Maclay, and H. J. Babrov, "Infrared Analysis of High Temperature Gases in Situ," NASA CR 1, October 15, 1962.

220. U. P. Oppenheim and Y. Ben-Aryeh, "Statistical Model Applied to the Region of the ν_3 Fundamental of CO_2 at 1200°K," J. Opt. Soc. Amer. 53, 344-350 (1963).

221. E. R. G. Eckert and R. M. Drake, Jr., Heat and Mass Transfer, Chapters 13 and 14, McGraw-Hill, New York, 1959.

222. S. S. Penner and L. D. Gray, "Approximate Infrared Emissivity Calculations for HCℓ at Elevated Temperatures," J. Opt. Soc. Amer. 51, 460-462 (1961).

223. B. Kivel, H. Mayer, and H. A. Bethe, "Radiation from Hot Air. Part I. Theory of Nitric Oxide Absorption," Annals of Physics 2, 57-80 (1957).

224. J. C. Keck, J. C. Camm, B. Kivel, and T. Wentink, Jr., "Radiation from Hot Air. Part II. Shock Tube Study of Absolute Intensities," Annals of Physics 7, 1-38 (1959).

225. R. W. Patch, W. L. Shackleford, and S. S. Penner, "Approximate Spectral Absorption Coefficient Calculations for Electronic Band Systems Belonging to Diatomic Molecules," J. Quant. Spectrosc. Radiat. Transfer 2, 263-271 (1962).

226. S. A. Golden, "Approximate Spectral Absorption Coefficients for Pure Rotational Transitions in Diatomic Molecules," J. Quant. Spectrosc. Radiat. Transfer 2, 201-214 (1962).

227. S. S. Penner, K. G. P. Sulzmann, and C. B. Ludwig, "Approximate Infrared Emissivity Calculations for NO at Elevated Temperatures," J. Quant. Spectrosc. Radiat. Transfer 1, 96-103 (1961); see also Convair Report ZPh-079, November 29, 1960.

228. W. S. Benedict, R. C. Herman, G. E. Moore, and S. Silverman, "The Strengths, Widths, and Shapes of Infrared Lines. II. The HCℓ Fundamental," Can. J. Phys. 34, 850-875 (1956); see also W. S. Benedict, R. C. Herman, G. E. Moore, and S. Silverman, "Infrared Line and Band Strengths and Dipole Moment Function in HCℓ and DCℓ," J. Chem. Phys. 26, 1671-1677 (1957).

229. H. Babrov, G. Ameer, and W. Benesch, "Line Strengths and Widths in the HCℓ Fundamental Band," J. Mol. Spectroscopy 3, 185-200 (1959).

230. D. Weber and S. S. Penner, "Rotational Line-Width Measurements on NO, HCℓ, HBr," J. Chem. Phys. 21, 1503-1506 (1953).

231. L. D. Gray, "Approximate Calculations of Spectral Emissivities in the Infrared for HCℓ in the Strong-Line Approximation," Technical Report No. 37, Contract Nonr-220(03), NR 015 401, California Institute of Technology, Pasadena, May 1961.

232. QMS, p. 371.

233. P. J. Wyatt, V. R. Stull, and G. N. Plass, "Quasi-Random Model of Band Absorption," J. Opt. Soc. Amer. 52, 1209-1217 (1962).

234. R. Goldstein, "Preliminary Absolute Intensity Measurements for the 1.38, 1.87, and 2.8 μ Bands of Water Vapor Between 125 and 200°C," to be published in J. Quant. Spectrosc. Radiat. Transfer; see also Technical Report No. 42, Contract Nonr-220(45), NR 015 401, California Institute of Technology, Pasadena, August 1962.

235. QMS, p. 246.

236. P. J. Wyatt, V. R. Stull, and G. N. Plass, "Infrared Transmission Studies, Volume II. The Infrared Absorption of Water Vapor," SSD-TDR-62-127-Volume II, Aeronutronic Division of Ford Motor Company, Newport Beach, California, Sept. 20, 1962.

237. S. S. Penner, Chemistry Problems in Jet Propulsion, p. 208, Pergamon Press, London, 1957.

238. W. S. Benedict and E. K. Plyler, "High-Resolution Spectra of Hydrocarbon Flames in the Infrared," Energy Transfer in Hot Gases, NBS Circular 523, 1954.

239. E. K. Plyler and W. W. Sleator, "Further Study of the Absorption of Infrared Radiation by Water Vapor," Phys. Rev. 37, 1493-1507 (1931).

240. D. H. Rank, K. D. Larsen, and E. B. Bordner, "The Raman Spectrum of Heavy Water Vapor," J. Chem. Phys. 2, 464-467 (1934).

241. D. Bender, "The Raman Effect of Water Vapor," Phys. Rev. 47, 252 (1935).

242. H. H. Nielsen, "The Near Infrared Spectrum of Water Vapor. II. The Parallel Bands ν_3, $\nu_1+\nu_2$, $\nu_2+\nu_3$ and the Perpendicular Band ν_1," Phys. Rev. 62, 422-433 (1942).

243. J. H. Jaffe and W. S. Benedict, "The Strength of the ν_3 Vibration of H_2O," to be published in J. Quant. Spectrosc. Radiat. Transfer.

244. K. E. Nelson, M. S. Thesis, University of California, Berkeley, California, 1959.

245. E. Von Bahr, "Das Absorptionsspektrum des Wasserdampfes," Ver. deut. phys. Ges. 15, 731-737 (1913).

246. H. Rubens, "Absorption of water vapor and new "rest-ray" groups in the region of long wave lengths," Sitzb. kgl. preuss. Akad. 1913, 513-49; 1910, 45; Ann. Physik 26, 619 (1908).

247. H. Rubens and G. Hettner, "Das Rotationsspektrum des Wasserdampfes," Ver. deut. phys. Ges. 18, 154-167 (1916).

248. H. Rubens and G. Hettner, "Das langwellige Wasserdampfsspektrum und seine Deutung durch die Quantentheorie," Sitzber. kgl. preuss Akad., Part I. 167-183 (1916).

249. W. W. Sleator, "The Absorption of Near Infra-red Radiation by Water-Vapor," Ap. J. 48, 124-143 (1918).

250. G. Hettner, "Über das ultrarote Absorptionsspektrum des Wasserdampfes," Ann. Phys. 55, 476-496 (1918).

251. H. Rubens, "Grating measurements in the long-wave spectrum," Sitzb. kgl. preuss. Akad. 1921, 8-27 (1921).

252. H. Witt, "Prüfung einer spektrometrischen Methode im langwelligen Spektrum," Zeit. f. Phys. 28, 236-248 (1924).

253. H. Witt, "Über Serien im Absorptionsspektrum des Wasserdampfes," Zeit. f. Phys. 28, 249-255 (1924).

254. W. W. Sleator and E. R. Phelps, "The fine structure of the near infrared absorption bands of water vapor," Ap. J. 62, 28-48 (1925).

255. E. Fermi, "Relation between the constants of the infrared bands of triatomic molecules," Atti accad. Lincei (VI) 1, 386-387 (1925).

256. R. Mecke, "Über die Absorptionsspektren des Wasserdampfes und des Ammoniaks," Phys. Zeit. 30, 907-910 (1929).

257. E. D. McAlister and H. J. Unger, "Water vapor absorption spectrum in the near infrared," Phys. Rev. 37, 1012 (1930).

258. C. R. Bailey, "The infra-red spectrum of water vapor," Trans. Faraday Soc. 26, 203-211, 213-215 (1930).

259. B. Stansfeld, "The behavior of the water spectrum in the temperature interval from 20 to 220° and in the spectral range 1 to 3.2 μ," Z. physik 74, 460-465 (1932).

260. P. Lueg and K. Hedfeld, "Die Rotationsschwingungsbanden des Wasserdampfes zwischen 0.9 und 6.5 μ," Z. Physik 75, 512-520 (1932).

261. E. K. Plyler, "The Infrared Absorption Bands of Water Vapor," Phys. Rev. 39, 77-82 (1932).

262. R. Mecke, "Intensitätswechsel im Rotationsschwingungsspektrum des Wasserdampfes, (Ortho- und Para-Wasser), Naturwissenschaften 20, 657 (1932).

263. H. L. Johnston and M. K. Walker, "Raman Effect in Water Vapor," Phys. Rev. 39, 535 (1932).

264. L. R. Weber and H. M. Randall, "The absorption spectrum of water vapor beyond 10 μ," Phys. Rev. 40, 837-847 (1932).

265. E. Schmidt, "Messung der Gesamtstrahlung des Wasserdampfes bei Temperaturen bis 1000°C," Forsch. Geb. Ing. Wes. 3, 57-70 (1932).

266. R. Mecke, "Das Rotationsschwingungsspektrum des Wasserdampfes, I.," Zeit. f. Phys. 81, 313-331 (1933).

267. W. Baumann and R. Mecke, "Das Rotationsschwingungsspektrum des Wasserdampfes, II.," Z. Physik 81, 445-464 (1933).

268. K. Freudenberg and R. Mecke, "Das Rotationsschwingungsspektrum des Wasserdampfes, III.," Z. Physik 81, 465-481 (1933).

269. J. H. Hsu, "Fine structure of the absorption band of water vapor at 0.94 μ," Chinese J. Phys. 1, 59-67 (1935).

270. J. E. Eberhardt, Sc. D. Thesis, Massachusetts Institute of Technology, "Measurements on Watervapor for Temperatures up to 2000°F," 1936.

271. C. H. Palmer, Jr., "Long-path water vapor spectra with pressure broadening. I. 20 μ to 31.7 μ. II. 29 μ to 40 μ," J. Opt. Soc. Amer. 47, 1024-1031 (1937).

272. R. B. Barnes, W. S. Benedict, and C. M. Lewis, " The Far Infrared Spectrum of H_2O," Phys. Rev. 47, 918-921 (1935).

273. W. M. Elsasser, "Far Infrared Absorption of Atmospheric Water Vapor," Astrophys. J. 87, 497 (1938).

274. D. M. Dennison, "The infrared spectrum of watervapor," Astrophys. J. 89, 292-294 (1939).

275. J. J. Fox and A. E. Martin, "Investigations of infrared spectra 2.5 - 7.5 μ, Absorption of water," Proc. Roy. Soc. London A174, 234-262 (1940).

276. H. H. Nielsen, "New Measurements on the Vibration-rotation Bands of Water Vapor," Phys. Rev. 57, 346 (1940).

277. H. Hopf, "Water vapor absorption lines in the spectral region from 0.15 to 0.50 mm wavelength," Z. Physik 116, 310-316 (1940).

278. H. C. Hottel and R. B. Egbert, "Radiant Heat Transmission from Water Vapor," Trans. Amer. Inst. Chem. Engrs. 38, 531-568 (1942).

279. C. C. Haworth, Jr. and F. C. Todd, "Near infrared absorption by water vapor," Phys. Rev. 62, 298 (1942).

280. T. G. Cowling, "The absorption of water vapor in the far infrared," Repts. Progress Physics 9, 29-41 (1942-43).

281. T. G. Cowling, "Hitherto unidentified absorption bands of water vapor," Nature 152, 694 (1943).

282. O. C. Mohler and W. S. Benedict, "Atmospheric Absorption of Water Vapor between 1.42 μ and 2.50 μ," Phys. Rev. 74, 702-703 (1948).

283. R. C. Nelson and W. S. Benedict, "Absorption of Water Vapor between 1.3 μ and 1.97 μ," Phys. Rev. 74, 703-704 (1948).

284. W. S. Benedict, "New Bands in the Vibration-Rotation Spectrum of Water Vapor," Phys. Rev. 74, 1246-1247 (1948).

285. L. F. Drummeter, Jr., "Infrared Absorption of Water Vapor at 1.8 Microns," ONR-Johns Hopkins Report, June 2, 1949.

286. W. S. Benedict, H. H. Claassen, and J. H. Shaw, "The absorption spectrum of water vapor between 4.5 μ and 13 μ," Scientific Report 1A-3, The Ohio State University Research Foundation; see also J. Res. Nat. Bur. Stand. 49, 91-133 (1951).

287. T. K. McCubbin, Jr., "The spectra of HCl, NH_3, H_2O, and H_2S from 100 to 700 microns," J. Chem. Phys. 20, 668-671 (1952).

288. C. C. Kiess, "Wavelengths of Rotational Lines in the Water Vapor Bands at 0.93 and 1.13 Microns," J. Res. Nat. Bur. Stand. 48, 377-380 (1952).

289. A. M. Brounshtein, "Absorption of radiation by water vapor at different densities and temperatures," Trudy Glov. Geofiz. Observatorii, No. 42, 5-31 (1953); Referat Zhur. Fiz. No. 10452 (1955).

290. J. Lecomte and C. Duval, "The infrared spectrum and the study of water in solids," J. Chim. Phys. 50, C53-C71 (1953).

291. L. Genzel and W. Eckhardt, "Spectraluntersuchungen im Gebiet um 1 mm Wellenlänge," Zeit. f. Physik 139, 578-591 (1954).

292. F. W. Dalby, H. H. Nielsen, and F. P. Deckey, "The absorption spectra of water vapor in the 2.7 μ and 6.0 μ regions," Phys. Rev. 94, 1423 (1954).

293. D. E. Burch, J. N. Howard, and D. Williams, "The effect of foreign gas broadening on the total absorption by the 6.3 μ band of water vapor," Phys. Rev. 94, 1424 (1954).

294. V. Roberts, "Calibration of infrared spectrometers in the wavelength region 15 - 25 μ," J. Sci. Instrum. 31, 226 (1954).

295. E. K. Plyler and N. Acquista, "Small grating spectrometer for the far infrared region," J. Chem. Phys. 23, 752-753 (1955).

296. W. S. Benedict, N. Gailer, and E. K. Plyler, "Rotation-Vibration Spectra of Deuterated Water Vapor," J. Chem. Phys. 24, 1139-1165 (1956).

297. H. C. Jones, "Determination of Accurate Water Vapor Calibration Points for Prism Spectrophotometers in the Region 1330 - 2100 cm^{-1}," J. Chem. Phys. 24, 1250-1252 (1956).

298. F. W. Dalby and H. H. Nielsen, "Infrared spectrum of water vapor. I. The 6.26 μ region," J. Chem. Phys. 25, 934-940 (1956).

299. H. A. Daw, "Transmission of radiation through watervapor subject to pressure broadening in the region of 4.2 μ to 23 μ," Thesis, University of Utah, Salt Lake City (1956). [Univ. microfilm publ. no. 16452]

300. H. A. Gebbie and G. A. Vanasse, "Interferometric Spectroscopy in the Far Infra-Red," Nature (London) 178, 432-433 (1956).

301. F. W. Dalby, "Infrared spectrum of water vapor," Dissertation abstract 16, 769-770 (1956); Univ. microfilms publ. no. 16066, 108 pp.

302. Giichi Yamamoto and T. Sasamori, "Numerical study of water vapor transmission," Sci. Repts. Tohoku U. (5th series) 8, 36-45 (1957).

303. K. P. Vasilevskiĭ and B. S. Neporent, "The absorption of infrared radiation by water vapor as the function of its concentration and the path length for a single line and for a group of lines in the band 2.7 μ," Optika i Spektroskopiya 4, 474-480 (1958).

304. "Emittance and Reflectance in the Infrared: An Annotated Bibliography," Report 2389-15-S, Univ. of Michigan, Willow Run Laboratories, April 1959.

305. J. T. Houghton and J. S. Seeley, "Spectroscopic observations of the water-vapour content of the stratosphere," Quart. J. Roy. Met. Soc. 86, 358-370 (1960).

306. P. J. Wyatt, V. R. Stull, and G. N. Plass, "Final Report on Theoretical Study of the Infrared Radiative Behavior of Flames. Volume I. The Infrared Absorption of Water Vapor," Publication No. U-1504, Aeronutronic Division Ford Motor Company, Newport Beach, California, December 30, 1961.

307. R. H. Tourin, "Some Spectral Emissivities of Water Vapor in the 2.7 μ region," J. Opt. Soc. Amer. 51, 1225-1228 (1961).

308. R. Landenburg and F. Reiche, "Über selektive Absorption," Ann. Physik 42, 181-209 (1911).

309. QMS, Chapters 3 and 4.

310. H. and B. S. Jeffreys, Methods of Mathematical Physics, pp. 574, 584, Cambridge University Press, 1956.

311. G. N. Plass and D. I. Fivel, "Influence of Doppler Effect and Damping in Line-Absorption Coefficient and Atmospheric Radiation Transfer," Astrophys. J. 117, 225-233 (1953).

312. H. Margenau and W. W. Watson, "Pressure Effects on Spectral Lines," Rev. Mod. Phys. 8, 22-53 (1936).

313. S. Ch'en and M. Takeo, "Broadening and Shift of Spectral Lines Due to the Presence of Froeign Gases," Rev. Mod. Phys. 29, 20-73 (1957).

314. R. G. Breene, Jr., "Line Shape," Rev. Mod. Phys. 29, 94-143 (1957); see also R. G. Breene, The Shift and Shape of Spectral Lines, Pergamon Press, New York, 1961.

315. C. J. Tsao and B. Curnutte, "Line-Widths of Pressure-Broadened Spectral Lines," J. Quant. Spectrosc. Radiat. Transfer 2, 41-91 (1962).

316. O. H. von Roos, "General Theory of Collision-Broadening of Spectral Lines," JPL Technical Report 32-100, Jet Propulsion Laboratory, Pasadena, California, 1961.

317. R. Goldstein, personal communication.

PART II: REPRESENTATIVE RADIATIVE ENERGY TRANSFER CALCULATIONS FOR TRANSPARENT AND OPTICALLY DENSE MEDIA

I. INTRODUCTION

Radiant energy transfer in two-phase media may be significantly greater than for the case of pure gases because of the much higher emissivities of condensed phases. However, when the local absorption coefficient becomes very large, the radiation becomes "trapped" locally, in which case it must "diffuse" to the walls. In the diffusion approximation, the medium is assumed to be optically dense and the distribution of radiant energy is nearly isotropic.

For the case of a medium at constant temperature and pressure, radiant energy transfer is dependent on geometrical interchange factors. These have been evaluated for various conical configurations, and a representative calculation has been carried out of the radiant energy transfer to a centrally located area element at the plane of intersection between two truncated cones.

Finally, an estimate of the Rosseland mean absorption coefficient is made for dispersed carbon particles at 1000 and 2000°K.

II. GENERAL EQUATIONS OF RADIATIVE ENERGY TRANSFER[1-7]

A. Fundamental Quantities and Definitions

Consider a small volume element with radiant energy density ρ_ν, i.e.

$$\rho_\nu = \frac{de_\nu}{dV} \tag{1}$$

is the radiant energy in unit volume in the frequency range between ν and $\nu + d\nu$.

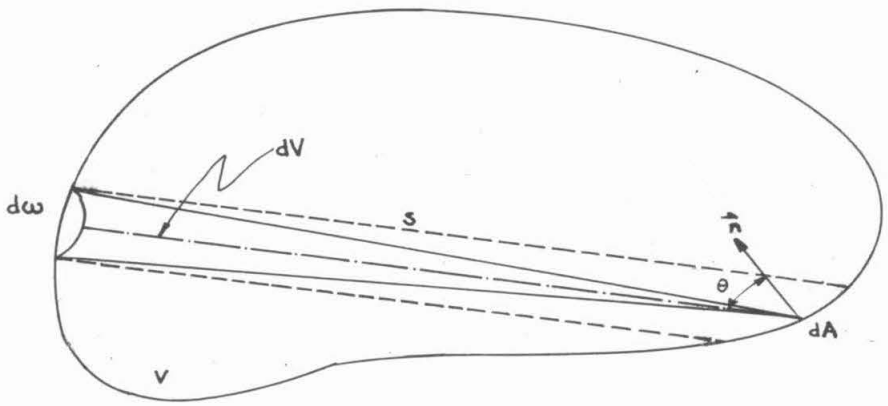

Fig. 1. Schematic diagram showing the geometric configuration discussed in the text.

The energy ϵ_ν in the frequency interval ν to $\nu + d\nu$ passing through an element of area dA, in a direction θ with respect to the normal, into the solid angle $d\omega$ in time dt is

$$de_\nu = I_\nu \cos\theta \, dA \, d\omega \, d\nu \, dt \, . \tag{2}$$

Equation (2) is the defining relation for I_ν, the radiant flux in the

frequency interval between ν and $\nu + d\nu$ per unit projected area per unit solid angle; I_ν is termed the (spectral) intensity of radiation. The spectral radiant energy passing through the cone subtended by the solid angle $d\omega$ in time $t = s/c$ (s is the distance traveled; c is the velocity of light) is

$$\rho_\nu dV = I_\nu \cos\theta \, d\omega (s/c) dA .$$

The total radiant energy contained in the volume V is

$$V\rho_\nu = \int_\omega \int_A I_\nu \cos\theta \, d\omega (s/c) dA$$

or, since $dV = dA \, s \cos\theta$,

$$\rho_\nu = \frac{1}{c} \int_\omega I_\nu \, d\omega . \tag{3}$$

In terms of the mean intensity, J_ν, defined as the value of the monochromatic intensity of radiation averaged over all directions around a point, viz.,

$$J_\nu \equiv \int_\omega I_\nu \frac{d\omega}{4\pi} , \tag{4}$$

we find that

$$\rho_\nu = \frac{4\pi}{c} J_\nu . \tag{5}$$

Equation (2) gives the radiant energy in the frequency interval ν to $\nu + d\nu$ which passes across an element of area dA in a direction inclined at an angle θ with respect to the outward normal into the solid angle $d\omega$. The net flux in all directions passing unit area in the frequency interval between ν and $\nu + d\nu$ in unit time is, therefore,

$$\pi F_\nu = \int_\omega I_\nu \cos\theta \, d\omega . \tag{6}$$

The net flux, πF_ν, depends on the choice of direction of the normal with respect to the reference area. For later convenience*, we define a quantity H_ν by the relation

$$H_\nu \equiv \int_\omega I_\nu \cos\theta \, \frac{d\omega}{4\pi} \tag{7}$$

whence $F_\nu = 4H_\nu$. (8)

The pressure exerted by the radiation field in the frequency interval ν to $\nu + d\nu$ on the element of area dA is

$$p = \int_\omega \frac{I_\nu \cos^2\theta}{c} \, d\omega . \tag{9}$$

Equation (9) represents the rate of change of the momentum ϵ_ν/c in the direction normal to dA. It is now convenient to define

$$K_\nu \equiv \int_\omega I_\nu \cos^2\theta \, \frac{d\omega}{4\pi} \tag{10}$$

so that

$$p = \frac{4\pi}{c} K_\nu . \tag{11}$$

For isotropic radiation, it is apparent that

$$p = \frac{4\pi}{c} J_\nu \overline{\cos^2\theta} = \frac{1}{3} \rho_\nu ; \tag{12}$$

equation (12) is a well-known result and shows that the radiation pressure equals one-third of the energy density.

---

* The quantities H_ν and K_ν were first introduced into radiative transfer theory by Eddington.

B. Continuity Equation for Radiant Energy

Consider a small cylindrical volume element within a radiating medium (see Fig. 2). The height of the cylinder is ds and the base has an area dA.

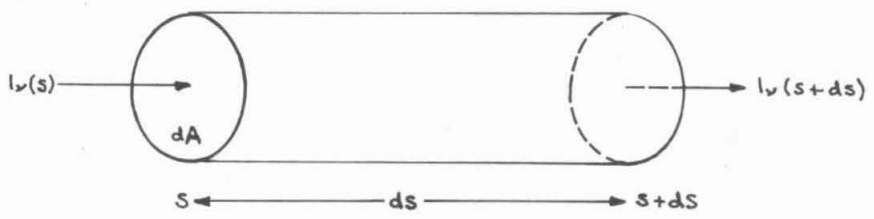

Fig. 2. Schematic diagram of an infinitesimal cylinder which constitutes a useful concept for a derivation of the continuity equation for radiative energy transfer.

The radiant energy, in the frequency interval ν to $\nu + d\nu$, passing through the surface at the plane s is

$$d\varepsilon_\nu(s) = I_\nu(s)\, dA\, d\omega\, d\nu\, dt ,$$

whereas the amount passing through the surface at $s + ds$ is

$$d\varepsilon_\nu(s+ds) = I_\nu(s+ds)\, dA\, d\omega\, d\nu\, dt .$$

In traveling a distance ds, the radiant intensity will be diminished by $\varkappa_\nu I_\nu(s)\, ds\, dA\, d\omega\, d\nu\, dt$ where $\varkappa_\nu$ is the absorption coefficient at the frequency ν. On the other hand, the intensity $j_\nu(s)\, dA\, ds\, d\omega\, d\nu\, dt$ will be emitted by the material within the cylinder, where j_ν is the emission coefficient at the frequency ν. If we allow for the energy within the cylinder to vary with time, then the amount of energy stored within the volume is $\frac{1}{c}\frac{\partial}{\partial t} I_\nu(s)\, dA\, d\omega\, ds\, d\nu$. Dividing the resulting equation by

ds dA dω dν dt , we find that

$$\frac{1}{c}\frac{\partial I_\nu(s)}{\partial t} + \frac{\partial I_\nu(s)}{\partial s} = -\varkappa_\nu I_\nu(s) + j_\nu(s) . \qquad (13)$$

Equation (13) is the Schwarzschild-Milne equation of transfer and is of great generality since it clearly applies even if radiant energy transfer is not the only mode of energy transfer.[5]

C. The Source Function S_ν

For the case of thermodynamic equilibrium, it follows from Kirchhoff's law, that

$$j_\nu = \varkappa_\nu B_\nu$$

where B_ν is the Kirchhoff-Planck function. However, following Unsöld[1], we prefer to define a source function, S_ν , by the expression

$$j_\nu = \varkappa_\nu S_\nu . \qquad (14)$$

In order to calculate the source function S_ν as a function of frequency ν and geometrical depth s , we must look more closely at the physical mechanisms of radiant energy emission. The following special cases are of interest:

1) Local thermodynamic equilibrium. For this case, the source function is given by the Kirchhoff-Planck function

$$S_\nu = B_\nu = \frac{2h\nu^3}{c^2}\frac{1}{[\exp(h\nu/kT)-1]} \qquad (15)$$

where T is the local temperature.

2) Pure scattering. The energy absorbed in unit volume in unit time is $\sigma_\nu \int_\omega I_\nu \, d\omega$ where σ_ν is the scattering coefficient at the frequency ν . The source function becomes now

$$S_\nu = \frac{\sigma_\nu}{\kappa_\nu} \int_\omega I_\nu \frac{d\omega}{4\pi} \cdot \tag{16}$$

3) Both absorption and scattering occur. For this case, equation (13) becomes

$$\frac{1}{c}\frac{\partial I_\nu}{\partial t} + \frac{\partial I_\nu}{\partial s} = -(\kappa_\nu + \sigma_\nu)I_\nu + \kappa_\nu B_\nu + \sigma_\nu \int I_\nu \frac{d\omega}{4\pi} \cdot \tag{17}$$

III. THE DIFFUSION APPROXIMATION

When the absorption coefficients and/or the gas volume are sufficiently large, radiant transfer calculations are made by utilizing the diffusion approximation. The diffusion approximation is applicable when the radiation mean free path is small compared with the characteristic dimensions of the problem for the wavelengths of interest. Before presenting a derivation of this approximation, it is of interest to note that there have, in fact, been two different approaches which led to a diffusion equation for radiative energy transfer.

Early experiments on resonance radiation suggested that when a photon is emitted by an individual atom, it does not travel directly to the walls of the enclosure, but after traversing a short distance it may be absorbed by another atom raising the latter to an excited state. This process of emission and reabsorption results in the transfer of excitation energy from atom to atom, and the eventual escape of the radiation to the boundary of the enclosure requires a large number of such transfers. The radiation in such cases is termed "imprisoned".[8] K. T. Compton[9, 10] regarded the passage of the quanta of resonance radiation through a gas as analogous to the diffusion of foreign gas molecules and obtained a "diffusion" equation for the number density of excited atoms, n, in the form

$$\frac{\partial n}{\partial t} = \left(\frac{\bar{\lambda}^2}{3\tau} \right) \nabla^2 n \qquad (18)$$

where τ is the lifetime of an individual atom in an excited state and $\bar{\lambda}$ is a mean free path.

Milne[11] later arrived at an equation for the diffusion of radiation without recourse to the analogy with molecular diffusion. Milne's

result is

$$\frac{\partial^2}{\partial x^2}\left(n + \tau \frac{\partial n}{\partial t}\right) = 4\left(\frac{N}{\bar{\lambda}}\right)^2 \tau \frac{\partial n}{\partial t} \qquad (19)$$

where N is the total concentration of atoms.

Difficulty in defining a "correct" value of $\bar{\lambda}$, which would be valid over a range of frequencies, led Holstein to the conclusion that the description of radiative transport by a diffusion equation was logically impossible, although Kentry[12] had earlier included the frequency spectrum for a single line in computing $\bar{\lambda}$.*

The second approach, and the one which we shall follow here, was suggested by Eddington[7] who introduced a method involving spherical harmonics for reducing the exact integro-differential transfer equation to an approximate differential equation which could be more readily solved. This technique has become a standard procedure** for solving the equation of neutron transport[14, 15].

A. Equation of Transfer for Plane Geometries[1-7]

It is convenient to rewrite the equation of transfer, equation (17), in terms of the geometrical depth x measured from the surface. Reference to Fig. 3 shows that

$$dx = -ds \cos\theta . \qquad (20)$$

Setting $\mu = \cos\theta$ and using equation (4), equation (17) becomes

---

* See also ref. 13.

** The equation for radiative transfer, equation (17), for a grey atmosphere and unpolarized light is identical with the equation of neutron transport for the case of constant collision cross section.

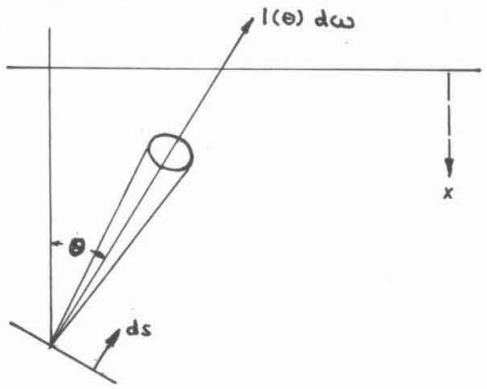

Fig. 3. Schematic diagram showing the geometric arrangement discussed in the text.

$$\frac{1}{c}\frac{\partial I_\nu(x,\mu)}{\partial t} - \mu\frac{\partial I_\nu(x,\mu)}{\partial x} = -(\kappa_\nu+\sigma_\nu)I_\nu + \kappa_\nu B_\nu + \sigma_\nu J_\nu . \tag{21}$$

In terms of the dimensionless variables

$$t^* = (\kappa_\nu + \sigma_\nu)ct \tag{22}$$

and

$$\tau_\nu = \int_{-\infty}^{x} (\kappa_\nu + \sigma_\nu)\,dx , \tag{23}$$

where τ_ν is the optical depth, equation (21) becomes

$$\frac{\partial I_\nu(\tau_\nu,\mu)}{\partial t^*} - \mu\frac{\partial I_\nu(\tau_\nu,\mu)}{\partial \tau_\nu} = -I_\nu(\tau_\nu,\mu) + \eta B_\nu + (1-\eta)J_\nu \tag{24}$$

and

$$\eta = \kappa_\nu/(\kappa_\nu + \sigma_\nu) . \tag{25}$$

B. The Spherical Harmonic Method[1, 3, 14, 15, 16]

The angular dependence of the intensity, I_ν, may be expressed conveniently in terms of Legendre polynomials. Thus we set

$$I_\nu(\tau_\nu,\mu) = \sum_{\ell=0}^{\infty} \frac{2\ell+1}{2} I_\nu^{(\ell)}(\tau_\nu) P_\ell(\mu) \tag{26}$$

where

$$I_\nu^{(\ell)}(\tau_\nu) = \int_{-1}^{1} I_\nu(\tau_\nu, \mu) P_\ell(\mu) d\mu . \tag{27}$$

From equations (4), (7), (10), and (27) it is now apparent that

$$I_\nu^{(0)} = 2 J_\nu , \tag{28a}$$

$$I_\nu^{(1)} = 2 H_\nu , \tag{28b}$$

$$I_\nu^{(2)} = 3 K_\nu - J_\nu . \tag{28c}$$

If $I_\nu(\tau_\nu, \mu)$ is replaced by the first three terms of the expansion given in equation (26) we obtain Chandrasekhar's[16] first approximation, viz.,

$$I_\nu(\tau_\nu, \mu) \simeq \frac{1}{2} I_\nu^{(0)} P_o + \frac{3}{2} I_\nu^{(1)} P_1 + \frac{5}{2} I_\nu^{(2)} P_2$$

$$= J_\nu P_o + 3 H_\nu P_1 + \frac{15}{2} (K_\nu - \frac{1}{3} J_\nu) P_2 .$$

The equation of transfer now reduces to

$$\left[P_o \frac{\partial J_\nu}{\partial t^*} + 3 P_1 \frac{\partial H_\nu}{\partial t^*} + \frac{15}{2} P_2 \frac{\partial}{\partial t^*} (K_\nu - \frac{1}{3} J_\nu) \right.$$

$$\left. - \mu P_o \frac{\partial J_\nu}{\partial \tau_\nu} - 3 \mu P_1 \frac{\partial H_\nu}{\partial \tau_\nu} - \frac{15}{2} \mu P_2 \frac{\partial}{\partial \tau_\nu} (K_\nu - \frac{1}{3} J_\nu) \right]$$

$$= - 3 P_1 H_\nu - \frac{15}{2} P_2 (K_\nu - \frac{1}{3} J_\nu) + \eta P_o (B_\nu - J_\nu) . \tag{29}$$

Using the recursion formula[17]

$$(2\ell+1) \mu P_\ell(\mu) = (\ell+1) P_{\ell+1}(\mu) + \ell P_{\ell-1}(\mu) , \quad \mu P_o = P_1 ,$$

and equating the coefficients of the Legendre polynomials, equation (29) leads to the following set of equations:

$$\frac{\partial J_\nu}{\partial t^*} - \frac{\partial H_\nu}{\partial \tau_\nu} = \eta(B_\nu - J_\nu), \tag{30a}$$

$$\frac{\partial H_\nu}{\partial t^*} - \frac{1}{3}\frac{\partial J_\nu}{\partial \tau_\nu} - \frac{\partial}{\partial \tau_\nu}(K_\nu - \frac{1}{3} J_\nu) = - H_\nu, \tag{30b}$$

$$\frac{15}{2}\frac{\partial}{\partial t^*}(K_\nu - \frac{1}{3} J_\nu) - 2\frac{\partial H_\nu}{\partial \tau_\nu} = \frac{-15}{2}(K_\nu - \frac{1}{3} J_\nu), \tag{30c}$$

$$\frac{\partial}{\partial \tau_\nu}(K_\nu - \frac{1}{3} J_\nu) = 0. \tag{30d}$$

Eddington* assumed that the anisotropy of radiation is sufficiently small to permit replacement of $\cos^2\theta$ in equation (10) by its mean value, i.e.,

$$K_\nu \simeq \frac{1}{3} J_\nu . \tag{31}$$

Equations (30a) to (30d) are now simplified to the following expressions:

$$\frac{\partial J_\nu}{\partial t^*} - \frac{\partial H_\nu}{\partial \tau_\nu} = \eta(B_\nu - J_\nu) , \tag{32a}$$

$$\frac{\partial H_\nu}{\partial t^*} - \frac{1}{3}\frac{\partial J_\nu}{\partial \tau_\nu} = - H_\nu , \tag{32b}$$

$$\frac{\partial H_\nu}{\partial \tau_\nu} = 0 . \tag{32c}$$

Equation (32c) shows that the net flux is constant [see equations (6) to (8)]. If $|\partial H_\nu/\partial t^*| \ll |H_\nu|$, i.e., if the radiation mean free path $(\kappa_\nu + \sigma_\nu)^{-1}$ is small compared to a characteristic dimension of the container, then equation (32b) becomes

---

* Eddington's approximation was originally applied to the interior of a star, and physical reasoning leads to the conjecture that, in strict radiative equilibrium, the radiation becomes nearly isotropic at a great depth below the surface of the star.[5]

$$H_\nu \simeq \frac{1}{3}\frac{\partial J_\nu}{\partial \tau_\nu} \tag{33}$$

whereas equation (32a) takes the form

$$\frac{\partial J_\nu}{\partial t^*} \simeq \frac{1}{3}\frac{\partial^2 J_\nu}{\partial \tau_\nu^2} + \eta(B_\nu - J_\nu) . \tag{34}$$

Equation (34) is known as the "diffusion approximation" to the equation of radiative transfer.

Lehner and Wing[18, 19] attacked directly the time-dependent transport equation, equation (17). Their method of solution involves advanced-function theory and the theory of semigroups of operators. A simpler version is needed for practical work and, for this reason, solutions of the diffusion approximation are of interest.

C. Boundary Conditions

A physically meaningful solution of equation (34) requires imposition of appropriate boundary conditions. However, since the diffusion approximation cannot apply in the immediate neighborhood of the boundary of the system, considerable caution is necessary in using the diffusion approximation[20].

The boundary conditions for a medium radiating to a black enclosing surface at temperature $T = 0$, which corresponds to maximum heat transfer from the medium to the surface, are the same as for the problem of radiative equilibrium of a stellar atmosphere, i.e.,

$$I_\nu(0, \mu) \equiv 0 \qquad \text{for} \qquad -1 < \mu < 0 . \tag{35}$$

As was noted by Chandrasekhar[16], this boundary condition is equivalent to an infinite set of linear relations as $\tau_\nu \to 0$ among the quantities

$I_\nu^{(\ell)}$ defined in equation (27), which clearly cannot all be satisfied by retaining only a finite number of terms in the expansion given in equation (26). Nevertheless, the use of equation (35) should give a reasonable approximation to the actual radiative transfer.

Equation (32c) leads at once to the integral

$$H_\nu = \text{constant} \equiv \frac{F_\nu}{4} , \tag{36}$$

which clearly insures the constancy of the net integrated flux. Since H_ν is constant, equation (33) can be integrated with the result

$$J_\nu = \frac{3}{4} F_\nu \tau_\nu + \underline{a} \tag{37}$$

where $\underline{a}$ is an arbitrary constant. As the optical depth $\tau_\nu \to \infty$, equation (37) shows that

$$J_\nu \to \frac{3}{4} F_\nu \tau_\nu . \tag{38}$$

In order to determine the constant $\underline{a}$, Chandrasekhar requires the flux incident on the surface as $\tau_\nu \to 0$ to be equal to the constant net flux $J_\nu = 2H_\nu = F_\nu/2$ in the interior of the radiating gases. Thus[16]

$$J_\nu(\tau) = \frac{3}{4} F_\nu(\tau_\nu + \frac{2}{3}) . \tag{39}$$

Unsöld[1] has discussed the exact solution to the Schwarzschild-Milne [see equation (13)] integral equation by numerical methods. He replaces equation (39) by the relation

$$J_\nu(\tau) = \frac{3}{4} F_\nu [\tau_\nu + q(\tau_\nu)] \tag{40}$$

where $q(0) = 0.5774$ and $q(\infty) = 0.7104$. According to equation (40), at a plane boundary between a radiating medium and a completely absorbing surface, the asymptotic distribution of the radiation intensity

should extrapolate to zero at an "extrapolation length" corresponding to the distance $0.5774\,(\kappa_\nu + \sigma_\nu)^{-1}$ beyond the surface. Mazur[20] and Kadanoff[21, 22], however, have ignored this extrapolation length in formulating the boundary conditions in their treatment of radiative transfer by the diffusion approximation.

IV. RADIATIVE ENERGY TRANSFER TO CENTRALLY LOCATED AREAS IN CYLINDRICAL AND CONICAL CHAMBERS CONTAINING ISOTHERMAL, GREY EMITTERS

In the special case where scattering may be neglected, and the temperature and pressure are constant, the transfer relation given in equation (13) may be integrated for a particular direction with the result

$$I_\nu = B_\nu [1 - \exp(-\varkappa_\nu s)] . \tag{41}$$

Substituting equation (41) into equation (7), the net radiant flux is found to be

$$Q_\nu = \pi F_\nu = 2\pi \int_0^{\pi/2} B_\nu [1 - \exp(-\varkappa_\nu s)] \cos\theta' \sin\theta' \, d\theta' \tag{42}$$

where s is in general a function of θ', and $\pi B_\nu = R_\nu^o$ is the black-body radiancy in the frequency range between ν and $\nu + d\nu$.

Consider the axisymmetric geometric arrangement sketched in Fig. 4. The path length for the region labeled 1 is

$$s_1 = H/\cos\theta' \tag{43a}$$

and the path length in the region labeled 2 is

$$s_2 = \frac{r_1}{[\sin\theta' - (\frac{r_2 - r_1}{H})\cos\theta']} . \tag{43b}$$

The total radiant flux, Q, incident in unit time on unit area dA is found by substituting equations (43a) and (43b) into equation (42) and integrating over frequency.[23] The result is

$$Q = 2 \int_0^\infty R_\nu^o(T_m) d\nu \left\{ \int_0^{\theta_o} [1 - \exp(-\frac{\varkappa_\nu H}{\cos\theta'})] \cos\theta' \sin\theta' \, d\theta' \right.$$

$$+ \int_{\theta_o}^{\pi/2} \left[1 - \exp\left(- \frac{\kappa_\nu r_1}{\sin\theta' - (\frac{r_2 - r_1}{H})\cos\theta'} \right) \right] \cos\theta' \sin\theta' \, d\theta' \Bigg\} \quad (44)$$

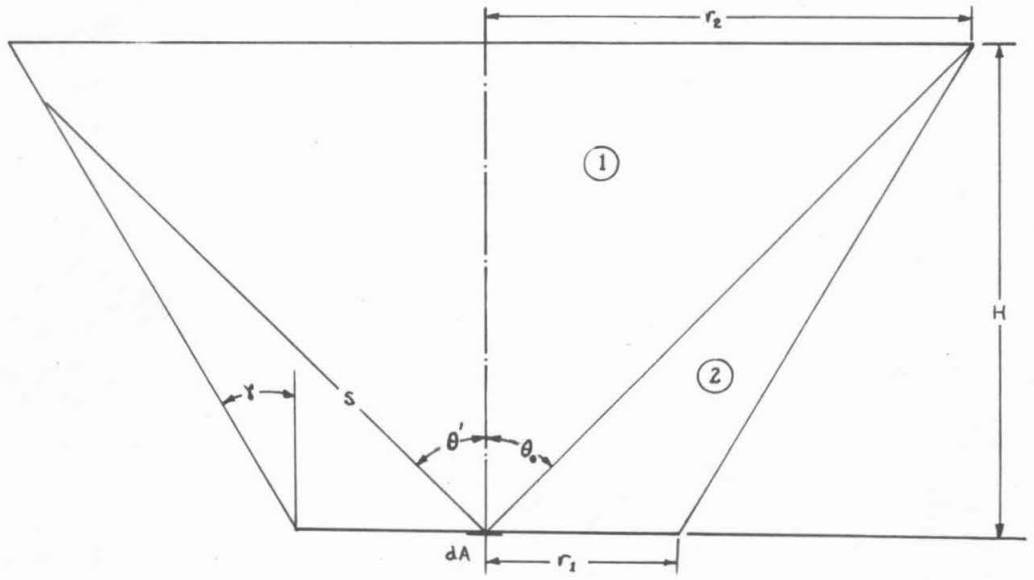

Fig. 4. Schematic diagram of an axisymmetric radiating region in the shape of a truncated cone.

where T_m is the assumed constant temperature of the medium. If a constant value $\bar{\kappa}_L$ is used for the linear absorption coefficient (i.e., the emitter is assumed to be grey), then equation (44) may be written as

$$Q = \sigma T_m^4 (\varepsilon_1 + \varepsilon_2) \quad (45)$$

where

$$\varepsilon_1 = 2 \int_0^{\theta_o} \left[1 - \exp\left(- \frac{\bar{\kappa}_L H}{\cos\theta'} \right) \right] \cos\theta' \sin\theta' \, d\theta' \quad (46)$$

and

and

$$\epsilon_2 = 2\int_{\theta_o}^{\pi/2}\left[1 - \exp\left(-\frac{\bar{k}_L r_1}{\sin\theta' - \left(\frac{r_2 - r_1}{H}\right)\cos\theta'}\right)\right]\cos\theta'\sin\theta'\,d\theta' \quad (47)$$

By making the substitution[2] $\mu = 1/\cos\theta'$, equation (46) is reduced to the form

$$\epsilon_1 = \sin^2\theta - 2\int_1^{1/\cos\theta_o}\frac{\exp(-\bar{k}_L H\mu)}{\mu^3}\,d\mu \quad (48)$$

and carrying out the integration gives[24]

$$\epsilon_1 = \sin^2\theta - 2E_3(\bar{k}_L H) + 2\cos^2\theta_o E_3\left(\frac{\bar{k}_L H}{\cos\theta_o}\right). \quad (49)$$

The functions $E_n(\tau) = \int_1^{\infty}\frac{\exp(-\tau z)}{z^n}\,dz$ are tabulated by Kourganoff[3]. It should be noted that $E_3(\tau) = \frac{1}{2}\Phi(\tau)$ where $\Phi(\tau)$ is the function defined by Schmidt.[23, 24]

The integral appearing in equation (47) can be easily evaluated only for the case $r_1 = r_2 = r$. Thus, for the cylinder, we find (compare Ref. 23) that

$$\epsilon_2 = \cos^2\theta_o - 2E_3(\bar{k}_L r) + 2\sin^2\theta_o E_3\left(\frac{\bar{k}_L r}{\sin\theta_o}\right). \quad (50)$$

For the more general case of a truncated cone, the integral in equation (47) has been evaluated numerically using the WDPC IBM 7090 computer.* The results of these numerical calculations are presented in Figs. 5, 6, and 7, where

$$I \equiv I(\alpha, \beta, \theta_o) = \int_{\theta_o}^{\pi/2}\left[1 - \exp\left(\frac{-\alpha}{\sin\theta' - \beta\cos\theta'}\right)\right]\sin\theta'\cos\theta'\,d\theta' \quad (51)$$

is plotted as a function of $\beta = (r_2 - r_1)/H$ for fixed values of $\alpha = \bar{k}_L r_1$

* The aid of Mr. B. E. Gray in programming the problem is gratefully acknowledged.

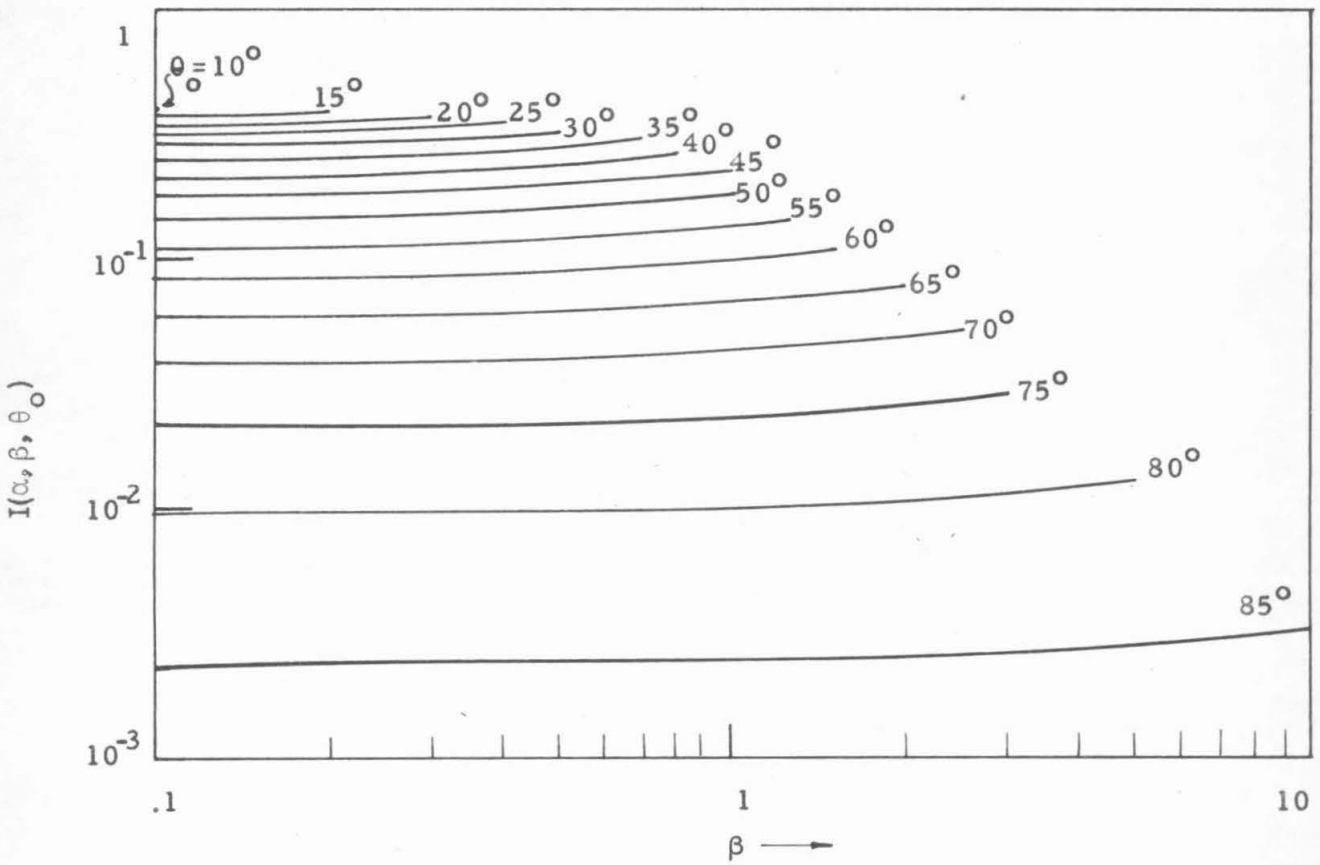

Fig. 5 The quantity $I(\alpha, \beta, \theta_o)$, defined in equation (51), as a function of β for $10^o \leq \theta_o \leq 85^o$ and $\alpha = \bar{k}_L r_1 = 1$.

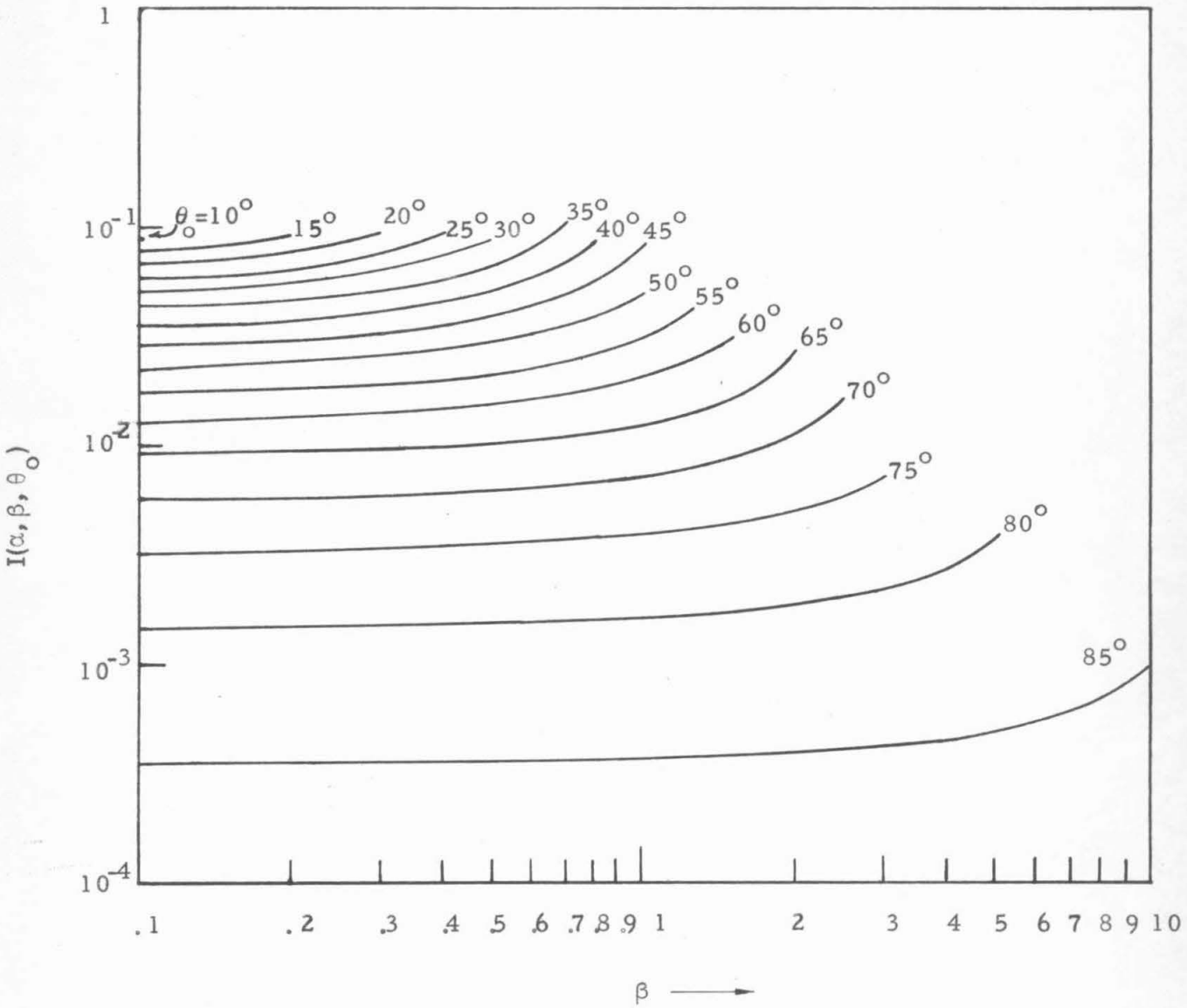

Fig. 6 The quantity $I(\alpha, \beta, \theta_o)$, defined in equation (51), as a function of β for $10^\circ \leq \theta_o \leq 85^\circ$ and $\alpha = \bar{k}_L r_1 = 1 \times 10^{-1}$.

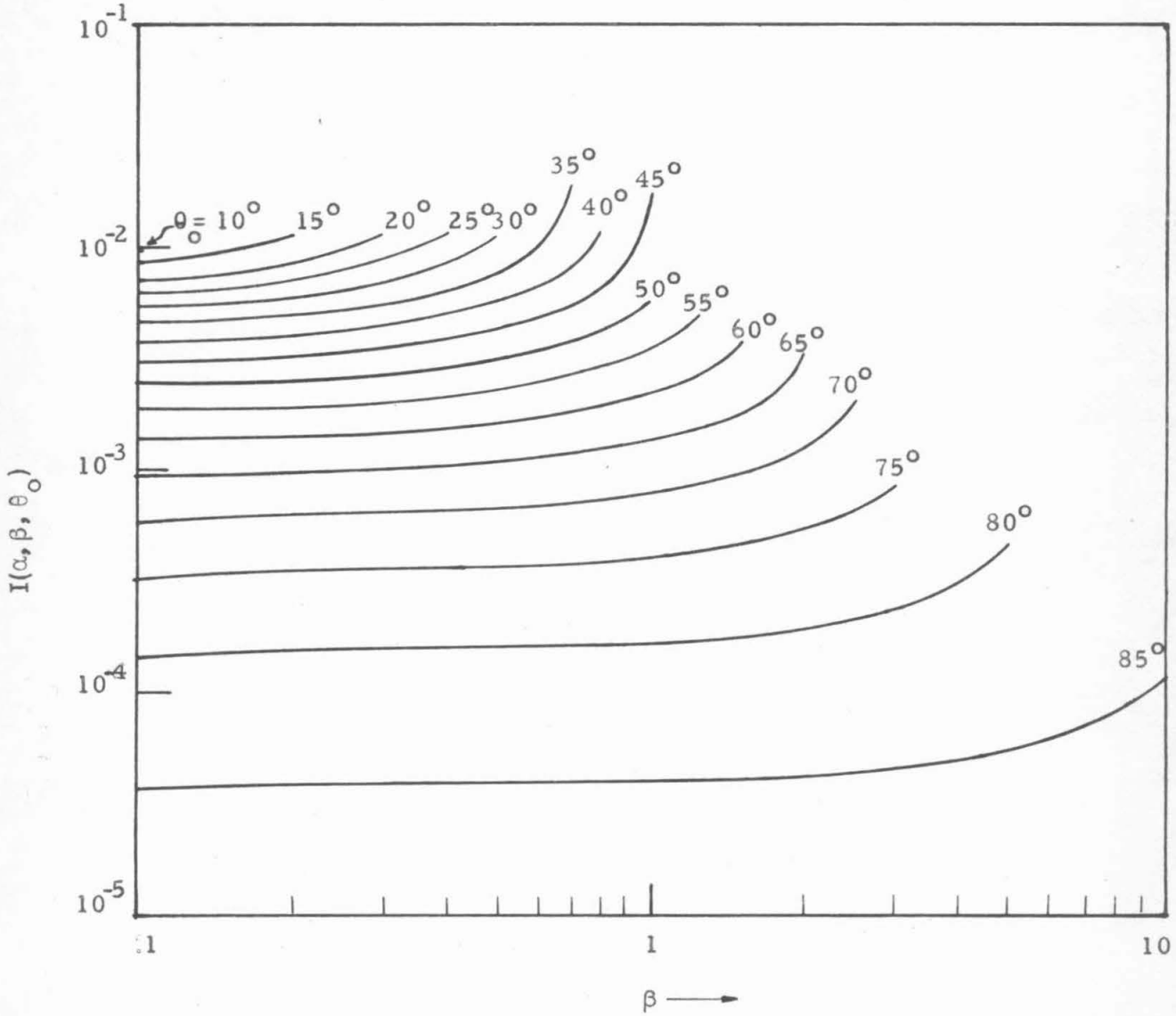

Fig. 7 The quantity $I(\alpha, \beta, \theta_o)$, defined in equation (51), as a function of β for $10^\circ \leq \theta_o \leq 85^\circ$ and $\alpha = \bar{k}_L r_1 = 1 \times 10^{-2}$.

with θ_o as a variable parameter.

For $\alpha < 10^{-2}$, it is readily shown that the quantities $I(\alpha, \beta, \theta_o)/\alpha$ are essentially constant for fixed values of β and θ_o. The exponent varies from $-\alpha/\beta$ at $\theta_o = 0$ to α at $\theta_o = \pi/2$; hence for $.1 \leq \beta \leq 10$ and $\alpha = 10^{-2}$, the maximum value of the exponent is 10^{-1}. For small values of α, the exponential in equation (47) may be expanded and

$$I \simeq \alpha \int_{\theta_o}^{\pi/2} \frac{\cos\theta' \sin\theta' \, d\theta'}{\sin\theta' - \beta\cos\theta'} \qquad \text{(for small values of } \alpha\text{).} \tag{52}$$

If $\theta' = \zeta + \gamma$ where $\tan\gamma = \beta$, then equation (52) becomes

$$I \simeq \frac{\alpha \cos\gamma}{2} \int_{\theta_o - \gamma}^{(\pi/2)-\gamma} \left[\frac{\sin 2\zeta \cos 2\gamma + \cos 2\zeta \sin 2\gamma}{\sin\zeta} \right] d\zeta \tag{53}$$

and

$$I \simeq \alpha \cos\gamma \left\{ \cos\gamma(1-\sin\theta_o) - \sin\gamma \cos\theta_o + \sin\gamma \cos\gamma \, \ell n \left[\left(\frac{\cos\gamma}{1+\sin\gamma} \right) \left(\frac{1+\cos(\theta_o - \gamma)}{\sin(\theta_o - \gamma)} \right) \right] \right\} . \tag{54}$$

Therefore, in terms of $\beta = \tan\gamma$, equation (54) can be written as

$$I \simeq \frac{\alpha}{\sqrt{1+\beta^2}} \left\{ \frac{1-\sin\theta_o - \beta\cos\theta_o}{\sqrt{1+\beta^2}} - \frac{\beta}{1+\beta^2} \ell n \left(\beta + \sqrt{1+\beta^2} \right) + \frac{\beta}{1+\beta^2} \ell n \left(\frac{\cos\theta_o + \beta\sin\theta_o + \sqrt{1+\beta^2}}{\sin\theta_o - \beta\cos\theta_o} \right) \right\} \quad \text{(for small } \alpha\text{).} \tag{55}$$

For $\alpha = 10^{-4}$, $\beta = 0.5$, $\theta_o = 45^o$, the exact result is $I = 0.429839$ whereas equation (55) leads to the value $I = 0.429895$.

For large values of α, the exponential term is negligibly small and

$$I \simeq \int_{\theta_o}^{\pi/2} \sin\theta' \cos\theta' \, d\theta' \qquad \text{(for } \alpha \text{ large)}, \qquad (56)$$

or

$$I \simeq \tfrac{1}{2} \cos^2\theta_o \qquad \text{(for } \alpha \text{ large)}. \qquad (57)$$

For $\alpha = 10$, $\theta_o = 45^o$, the exact value of I varies from I = .249996 at $\beta = 0$ to I = .250000 at $\beta = 1.0$.

To summarize, for $\alpha \geq 10$, $I(\alpha, \beta, \theta_o)$ is well approximated by equation (57) and, for $\alpha \leq 10^{-3}$, by equation (55). For intermediate values of α, the desired results may be obtained from Figs. 5, 6, and 7. Thus the problem of radiant heat transfer to a centrally located area in cylindrical and conical enclosures has been completely solved subject to the assumptions that the emitting system is at the constant temperature T_m and the linear absorption coefficient has the constant value $\bar{K}_L$. For convenience, the function $E_3(\tau_\nu)$ is listed in Table I for representative values of τ_ν.

As an example, the radiant heat transfer has been calculated to an area element at the throat of two intersecting cones for the geometrical configuration indicated in Fig. 8 and for $\bar{K}_L = 1.2 \times 10^{-3}$ cm^{-1}.

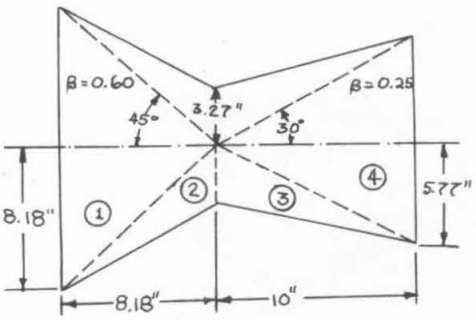

Fig. 8. Diagram showing the geometric configuration used in the text for the computation of radiant heat transfer to a centrally located area at the intersection of two cones.

TABLE I. Values of $E_3(\tau_\nu)$ [3]

τ_ν	$E_3(\tau_\nu)$	τ_ν	$E_3(\tau_\nu)$
0	.5000000000	0.60	.1915506378
0.01	.4902765642	0.70	.1660611621
0.02	.4809682915	0.80	.1443238017
0.03	.4719976872	0.90	.1257029783
0.04	.4633239418	1.00	.1096919670
0.05	.4549188498	1.25	.0785723481
0.06	.4467608833	1.50	.0567394897
0.07	.4388326798	1.75	.0412393202
0.08	.4311197306	2.00	.0301333804
0.09	.4236096057	2.25	.0221169820
0.10	.4162914579	2.50	.0162953698
0.20	.3519453121	2.75	.0120459808
0.30	.3000418266	3.00	.0089306461
0.40	.2572864233	3.25	.0066380708
0.50	.2216043643	3.50	.0049453783

The total radiant heat transfer from the fluid to unit area at the center of the plane located at the intersection between the two cones is

$$Q = \sigma T_m^4 (\epsilon_1 + \epsilon_2 + \epsilon_3 + \epsilon_4) = 0.0447\, \sigma T_m^4 ,$$

since

$$\epsilon_1 = 0.0141 , \quad \epsilon_2 = 0.0095 , \quad \epsilon_3 = 0.0131 , \text{ and } \quad \epsilon_4 = 0.0080$$

for the assumed configuration.

V. ROSSELAND MEAN ABSORPTION COEFFICIENTS IN TWO-PHASE SYSTEMS

A. Definition of Rosseland Mean Absorption Coefficient

The equations of transfer in the diffusion approximation given in equations (32a) to (32c) refer to monochromatic radiation. To obtain the total radiant energy transfer, these expressions must be integrated over all frequencies. To each monochromatic quantity, C_ν (e. g., intensity I_ν, mean intensity J_ν, etc.), there corresponds an integral

$$C = \int_0^\infty C_\nu \, d\nu \tag{58}$$

and the equation of transfer for the integrated quantities will have the same form as for the monochromatic quantities if a mean absorption coefficient, $\bar{\kappa}_L$, is defined as[25]

$$\frac{1}{\bar{\kappa}_{L,\,Ro}} = \frac{\int \frac{1}{\kappa_\nu} \frac{\partial B_\nu}{\partial T} \, d\nu}{\int \frac{\partial B_\nu}{\partial T} \, d\nu} \, . \tag{59}$$

The quantity $\bar{\kappa}_{L,\,Ro}$ is the Rosseland mean absorption coefficient.[1, 2, 7, 26] Substituting for the Kirchhoff-Planck function B_ν in equation (59) leads to the expression

$$\frac{1}{\bar{\kappa}_{L,\,Ro}} = \frac{15}{4\pi^4} \int \frac{x^4 e^x}{\kappa_\nu (e^x - 1)^2} \, dx = \frac{15}{4\pi^4} \int \frac{G(x)dx}{\kappa_\nu} \tag{60}$$

where $x = h\nu/kT$, and $G(x) = x^4 e^x (e^x - 1)^{-2}$ is the "Rosseland weighting function."

If induced emission is included, κ_ν in equation (60) should be

replaced by

$$\kappa_\nu' = \kappa_\nu(1-e^{-x}), \tag{61}$$

a correction which is important only when $x < 1$.

B. Mean Absorption Coefficients for Dispersed Carbon Particles

In a two-phase system consisting of particles dispersed in a gas, the particles may be treated as molecules if they are sufficiently small for the wavelengths of interest and scattering is unimportant.* In this case,

$$\kappa_\nu = pP_\nu + N\sigma_a \tag{62}$$

where P_ν is the spectral absorption coefficient of the gas in appropriate units, p the pressure of the gas, N the number of solid particles per unit volume, and σ_a the absorption cross section of the particle.

If the gas radiation is negligible compared to that of the particles at a given wavelength, then $\kappa_\nu \simeq N\sigma_a$. (63)

Theoretical estimates of σ_a may be made, in principle, for all particles by using the Mie theory[29,30] provided the optical constants are available for the particle system. Usually they are not. Hence it is customary to assume that low-temperature measurements of bulk properties may be extrapolated to high temperatures and apply to particles. Stull and Plass[28] have performed extension calculations of scattering and total cross sections and of spectral emissivities for carbon using (extrapolated) bulk properties measured by Halpern and Hall[31].

---

* The case where scattering cannot be neglected has been discussed by Bartky;[27] however, the calculations of Stull and Plass[28] show that the scattering cross section for finely divided carbon particles is usually much smaller than the total cross section.

Their results have been used to estimate the Rosseland mean absorption coefficient for carbon particles of 200A and 987A radius for a number density of 10^{12} particles per cm^3. From equations (60) and (62) it is apparent that the Rosseland mean absorption coefficient is directly proportional to the number density and, therefore, $\bar{K}_{L,Ro}$ may be calculated for any concentration of carbon particles having the specified radii.

The total cross section is plotted as a function of wavelength in Fig. 9 for carbon particles with 200A and 987A radius using the results of Stull and Plass[28]. For these carbon particles, the scattering cross section is negligibly small compared with the absorption cross section, and hence the latter is practically identical with the total cross section.

The dashed portions of the curve were extrapolated by using the relation[32]

$$\lambda \kappa_{\lambda} = \text{constant} . \tag{64}$$

Equation (64) follows directly from the expressions[28, 29, 30] for the total cross section, σ_t, and scattering cross section, σ_s, given by the Mie theory:

$$\sigma_t = 2\pi \left(\frac{a}{\rho}\right)^2 \mathrm{Re} \sum_{\ell=1}^{\infty} (2\ell+1)(a_\ell^r + b_\ell^r) , \tag{65a}$$

$$\sigma_s = 2\pi \left(\frac{a}{\rho}\right)^2 \sum_{\ell=1}^{\infty} (2\ell+1)(|a_\ell^r| + |b_\ell^r|^2) , \tag{65b}$$

where Re denotes the real part of the summation, the parameter ρ is equal to $2\pi a/\lambda$, $\underline{a}$ is the radius of the sphere, and the complex coefficients a_ℓ^r and b_ℓ^r can be expressed in terms of ρ and $N \equiv n - ix'$, the ratio of the propagation constant of the sphere to that of the medium.

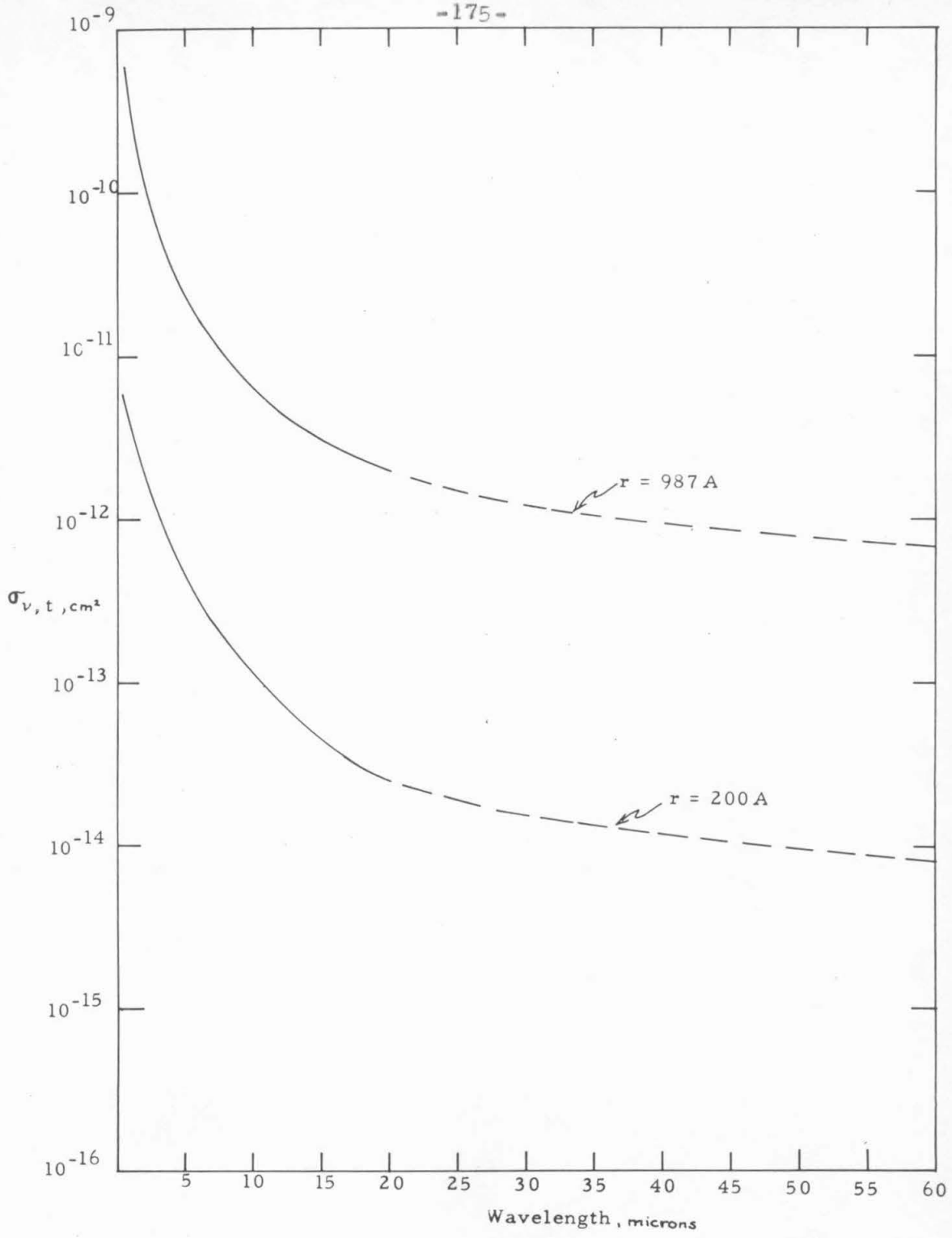

Fig. 9 The total absorption cross section $\sigma_{\nu,t}$ for spherical carbon particles with radius 200A and 987 A as a function of wavelength (from ref. 28). The dashed part of the curve is extrapolated.

Here $\underline{n}$ is the refractive index of the particle and κ' is the absorption index of the particle.

When the ratio of radius $\underline{a}$ to the wavelength λ is so small that ρ^5 can be neglected in comparison with ρ^3, all the coefficients are negligibly small except for[29]

$$b_1^r \simeq \frac{-2i}{3}\frac{N^2-1}{N^2+2}\rho^3 = \frac{-2i}{3}\left\{\frac{(n^2-\kappa'^2-1)-i(2n\kappa')}{(n^2-\kappa'^2+2)-i(2n\kappa')}\right\}\rho^3 . \qquad (66)$$

In this case, the absorption cross section, σ_a, becomes simply

$$\sigma_a = \sigma_t - \sigma_s \simeq 6\pi(a/\rho)^2 \,\mathrm{Re}\,(b_1^r) .$$

It now follows that

$$\sigma_a \simeq \left\{\frac{48\pi a^3 n\kappa'}{(n^2-\kappa'^2+2)+(2n\kappa')^2}\right\}\frac{1}{\lambda} . \qquad (67)$$

In Figure 10 the quantity $G(x)/\kappa'_\nu$ is plotted as a function of $x = h\nu/kT$ for 200A-radius carbon particles with a number density of 10^{12} particles per cm^3, at temperatures of 1000 and 2000°K. The Rosseland mean absorption coefficients are seen to be 0.318 and 0.937 cm^{-1}, respectively. Similarly, in Fig. 11, the results are plotted for 987A-radius carbon particles with a number density of 10^{12} particles per cm^3; the corresponding Rosseland mean absorption coefficients are 20.6 and 65.5 cm^{-1} at 1000 and 2000°K, respectively. Thus, the expected result is found that the mean absorption coefficient for carbon particles increases with temperature and particle size, for a fixed number density.

C. A Comparison of Radiative and Conductive Heat Transfer[26]

For a system in which the local temperature is defined, it is interesting to compare the relative magnitudes of conductive and

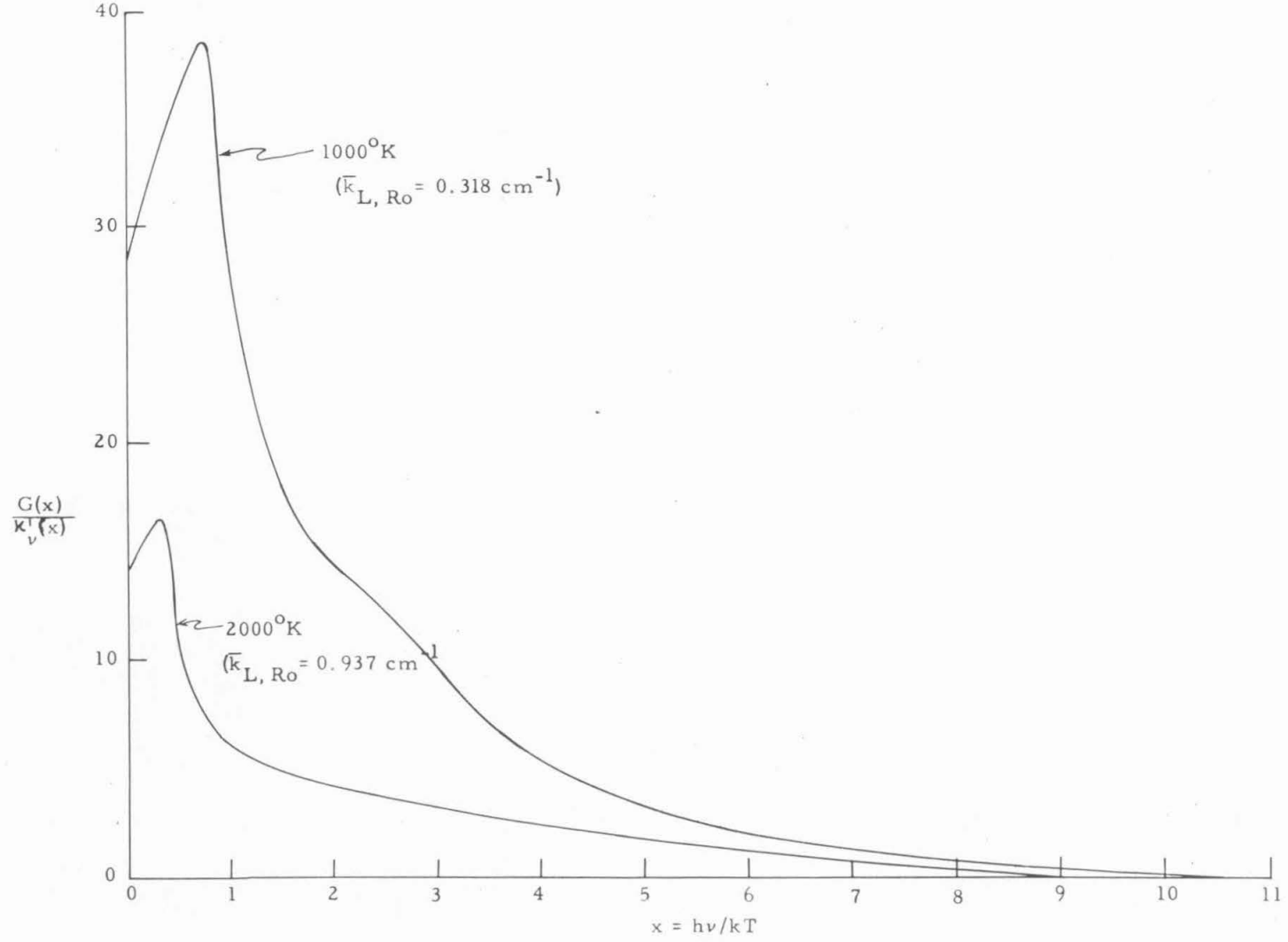

Fig. 10 The quantity $G(x)/\kappa'_\nu(x)$ as a function of $x = h\nu/kT$ for carbon particles with radius 200 A at 1000 and 2000 K for a number density of 10^{12} particles/cm^3.

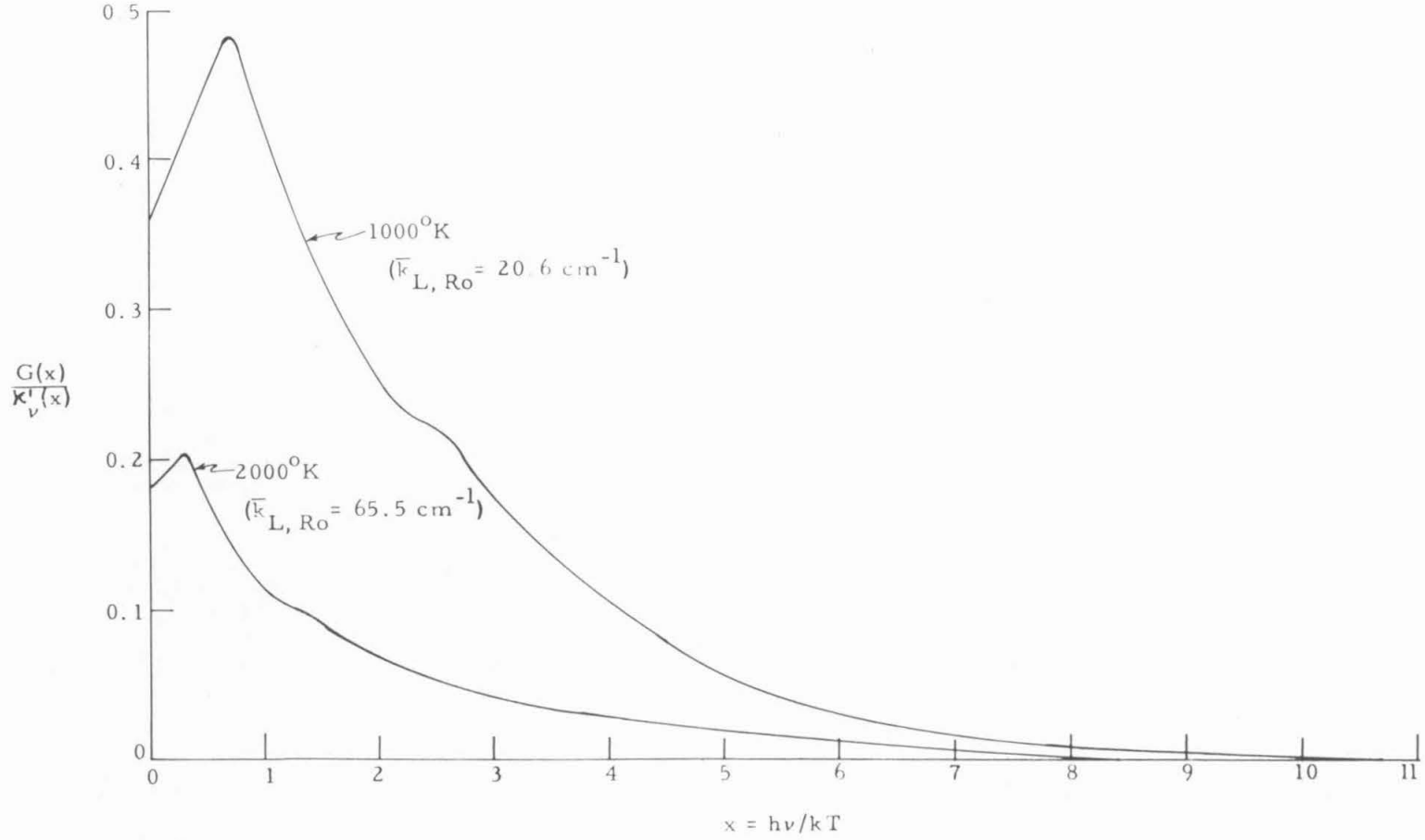

Fig. 11 The quantity $G(x)/\kappa'_\nu(x)$ as a function of $x = h\nu/kT$ for carbon particles with radius 987A at 1000 and 2000 K for a number density of 10^{12} particles/cm^3.

radiative heat transfer. For the one-dimensional case, Fourier's equation of heat conduction is

$$Q_c = -\lambda_c \frac{dT}{dx'}, \tag{68}$$

where λ_c is the thermal conductivity [cal/sec cm $^{\circ}$K] and Q is the heat energy flowing through a unit area in unit time. From equations (8) and (42), we find for the radiant energy flux

$$Q_r = 4\pi \int_0^{\infty} H_\nu \, d\nu. \tag{69}$$

If the diffusion approximation, equation (33), is used, equation (69) becomes

$$Q_r \simeq \frac{4\pi}{3} \int_0^{\infty} \frac{dJ_\nu}{d\tau_\nu} \, d\nu = \frac{-4\pi}{3} \int_0^{\infty} \frac{1}{\kappa_\nu} \frac{dJ_\nu}{dx'} \, d\nu \tag{70}$$

where scattering has been neglected, and the x'-direction has now been chosen to be in the direction of increasing temperature [compare equation (20)]. Rosseland[25] has shown that for large optical depths the spectral radiant intensity, $I_\nu(\theta)$, becomes essentially isotropic, and approaches the local spectral steradiancy, $B_\nu(T)$. Hence J_ν in equation (70) can be replaced by B_ν, and

$$Q_r \simeq \frac{-4\pi}{3} \int_0^{\infty} \frac{1}{\kappa_\nu} \frac{dB_\nu}{dx'} \, d\nu = \frac{-4\pi}{3} \frac{dT}{dx'} \int_0^{\infty} \frac{1}{\kappa_\nu} \frac{dB_\nu}{dT} \, d\nu. \tag{71}$$

Using equation (60), equation (71) reduces to

$$Q_r \simeq \frac{-4\pi}{3} \left(\frac{dT}{dx'}\right) \frac{1}{k_{L,Ro}} \int_0^{\infty} \frac{dB_\nu}{dT} \, d\nu = \frac{-16\sigma T^3}{3k_{L,Ro}} \left(\frac{dT}{dx'}\right) = -\lambda_r \frac{dT}{dx'}. \tag{72}$$

Comparing equations (68) and (72), it is apparent that radiative energy transfer will dominate if

$$\lambda_r = \frac{16\sigma T^3}{3\bar{K}_{L,R_o}} > \lambda_c \tag{73}$$

Consider, for example, a two-phase system consisting of spherical carbon particles dispersed in a gas whose average molecular weight is 36. Assuming the carbon particles to have a radius of 200A, the volume per particle is approximately 3×10^{-17} cm^3. Thus, for particle densities less than 10^{15} per cm^3, the thermal conductivity, λ_c, will be essentially that of the gas alone.[33]

Assuming, for simplicity, that the gas is monatomic, then the thermal conductivity is given by[34]

$$\lambda_c = \frac{1.99 \times 10^{-4} \sqrt{T/W}}{\tilde{\sigma}^2 \Omega^{(2,2)*}} \tag{74}$$

where λ_c is in cal/(cm sec $^\circ$K), W is the molecular weight in gm/mole, T is the absolute temperature in $^\circ$K, $\tilde{\sigma}$ represents the collision diameter in A, and $\Omega^{(2,2)*}$ is a collision integral. Setting $\Omega^{(2,2)*} = 1$ and $\tilde{\sigma} = 3.5$A, we obtain $\lambda_c = 0.86 \times 10^{-4}$ cal/(cm sec $^\circ$K) at 1000°K, and $\lambda_c = 1.21 \times 10^{-4}$ cal/(cm sec $^\circ$K) at 2000°K.

The Stefan-Boltzmann constant[1], $\sigma = 1.355 \times 10^{-12}$ cal/(cm^2 sec $^\circ$K^4). Hence, for a temperature of 1000°K, we have $(16/3)\sigma T^3 = 7.227 \times 10^{-3}$ cal/(cm^2 sec $^\circ$K), and the energy transport will be dominated by radiation if $\bar{K}_{L,R_o} < 84$ cm^{-1} at 1000°K. Reference to Figs. 10 and 11 shows that this condition corresponds, for carbon particles, to number densities of less than 2.5×10^{14} particles/cm^3 with 200A radius particles or 4×10^{12} particles/cm^3 for particles of 987A radius.

Similarly, at 2000°K, we must have $\bar{K}_{L,Ro} < 475\ cm^{-1}$ for radiative transfer to exceed the energy transport by conduction, which would require, for carbon particles, number densities of less than 5×10^{14} particles/cm^3 for particles of 200A radius or 7×10^{12} particles/cm^3 for particles with 987A radius.

The concept of a "radiation conductivity," λ_r, has also been used in calculations of the heat transfer in molten glass[35-40], the heat flux being given by

$$Q = -\lambda_{eff} \frac{dT}{dx'} = -(\lambda_r + \lambda_c) \frac{dT}{dx'} . \qquad (75)$$

REFERENCES TO PART II.

REFERENCES

1. A. Unsöld, Physik der Sternatmosphären, Zweite Auflage, Julius Springer, Berlin, 1955.

2. S. Chandrasekhar, Radiative Transfer, Dover Press, New York, 1960, and Oxford University Press, 1950.

3. V. Kourganoff, Basic Methods in Transfer Problems, Oxford University Press, 1952.

4. E. A. Milne, "Thermodynamics of the Stars," Handbuch der Astrophysik, Bd. III, Teil 3, 1. Halfte. pp. 65-255, Julius Springer, Berlin, 1930.

5. E. Hopf, Mathematical Problems of Radiative Equilibrium, Cambridge University Press, 1934.

6. I. W. Busbridge, The Mathematics of Radiative Transfer, Cambridge University Press, 1960.

7. A. S. Eddington, The Internal Constitution of the Stars, Chapter V, Dover Press, New York, 1959, and Cambridge University Press, 1930.

8. T. Holstein, "Imprisonment of Resonance Radiation in Gases," Phys. Rev. 72, 1212-1233, (1947).

9. K. T. Compton, "Theory of Ionization by Cumulative Action and the Low Voltage Arc," Phys. Rev. 20, 283-299 (1922).

10. K. T. Compton, "Some Properties of Resonance Radiation and Excited Atoms," Phil. Mag. 45, 750-760 (1923).

11. E. A. Milne, "The Diffusion of Imprisoned Radiation through a Gas," J. London Math. Soc. 1, 40-51 (1926).

12. C. Kentry, "On Radiation Diffusion and the Rapidity of Escape of Resonance Radiation from a Gas," Phys. Rev. 42, 823-842 (1932).

13. P. M. Morse and H. Feshback, Methods of Theoretical Physics, Part 1, pp. 171-200, McGraw-Hill Book Co., New York, 1953.

14. B. Davison, Neutron Transport Theory, Chapters VIII and X, Oxford University Press, 1957.

15. S. Glasstone and M. C. Edlund, The Elements of Nuclear Reactor Theory, Chapter XIV, D. Van Nostrand, New York, 1952.

16. S. Chandrasekhar, "On the Radiative Equilibrium of a Stellar Atmosphere," Astrophys. J. 99, 180-190 (1944).

17. R. Courant and D. Hilbert, Methods of Mathematical Physics, Vol. I, pp. 82-87, 501-521, Interscience Publishers, New York, 1953.

18. J. Lehner and G. M. Wing, "Solution of the Linearized Boltzmann Equation for Slab Geometry," Duke Math. J. 23, 125 (1956).

19. J. Lehner and G. M. Wing, "On the Spectrum of an Unsymmetric Operator Arising in the Transport Theory of Neutrons," Commun. Pure Appl. Math. 8, 217 (1955).

20. P. Mazur, "Radiant Interchange Between a Gas-Particle Mixture and a Rocket Nozzle Wall," AVCO Tech. Rept. RAD-TR-7-60-24, Oct. 31, 1960.

21. L. P. Kadanoff, "Radiative Transport within an Ablating Body," AVCO Research Rept. 37, Oct. 1958, and AVCO Research Rept. 61, July 1959.

22. L. P. Kadanoff, "Radiative Transport within an Ablating Body," J. Heat Transfer C83, 215 (1961).

23. S. S. Penner, Quantitative Molecular Spectroscopy and Gas Emissivities, Chapter 19, Addison Wesley, New York, 1959.

24. E. Schmidt, "Zur Berechnung der Strahlung von Gasvolumen," Z. Ver. deut. Ingr. 77, 1162 (1933). See also M. Jakob, Heat Transfer, Vol. II, pp. 106-110, John Wiley and Sons, New York, 1957.

25. S. Rosseland, "Note on the Absorption of Radiation within a Star," Monthly Notices 84, 525-528 (1924).

26. S. S. Penner and R. W. Patch, "Radiative Transfer Studies and Opacity Calculations for Heated Gases," Von Kármán Laboratory, GALCIT, Division of Engineering, California Institute of Technology, Technical Report No. 6, January 1962.

27. C. E. Bartky, "Radiation from Systems of Molecular and Particulate Emitters, Absorbers, and Scatterers," The University of Chicago, Laboratories for Applied Sciences, Report LAS-TN-199-24, October 1961.

28. V. R. Stull and G. N. Plass, "Emissivity of Dispersed Carbon Particles," J. Opt. Soc. Am. 50, 121-129 (1960).

29. J. A. Stratton, Electromagnetic Theory, pp. 563-573, McGraw-Hill Book Co., New York, 1941.

30. H. E. Van der Hulst, Light Scattering by Small Spheres, John Wiley, New York, 1957.

31. O. Halpern and H. Hall, "The Ionization Loss of Energy of Fast Charged Particles in Gases and Condensed Bodies," Phys. Rev. 73, 477-486 (1948).

32. S. Yagi and H. Iino, "Radiation from Soot Particles in Luminous Flames," Eighth Symposium (International) on Combustion, pp. 288-293, Williams and Wilkins, Baltimore, 1962.

33. M. Jakob, Heat Transfer, Vol. I, pp. 83-91, John Wiley, New York, 1949.

34. S. S. Penner, Chemistry Problems in Jet Propulsion, p. 249, Pergamon Press, London, 1957.

35. M. Czerny and L. Genzel, "Energiefluss und Termperaturverlauf in Glasbad von Schmelzwannen als Folge von Wärmeleitung und Wärmestrahlung," Glastech. Ber. 25, 387-392 (1952).

36. W. Geffcken, "Zur Fortleitung der Wärme in Glas bei hohen Temperaturen, I," Glastech. Ber. 25, 392-396 (1952).

37. B. S. Kellett, "Steady Flow of Heat Through Hot Glass," J. Opt. Soc. Am. 42, 339-343 (1952).

38. L. Genzel, "Der Anteil der Wärmenstrahlung bei Wärmeleitungsvorgängen," Z. Physik 135, 177-195 (1953).

39. L. Genzel, "Zur Berechnung der Strahlungsleitfähigkeit der Gläser," Glastech Ber. 26, 69-71 (1953).

40. R. Gardon, "A Review of Radiant Heat Transfer in Glass," J. Amer. Ceram. Soc. 44, 305-312 (1961).